Streamlining Upstream Processing of Complex Biopharmaceuticals

Marcos F. Q. de Sousa

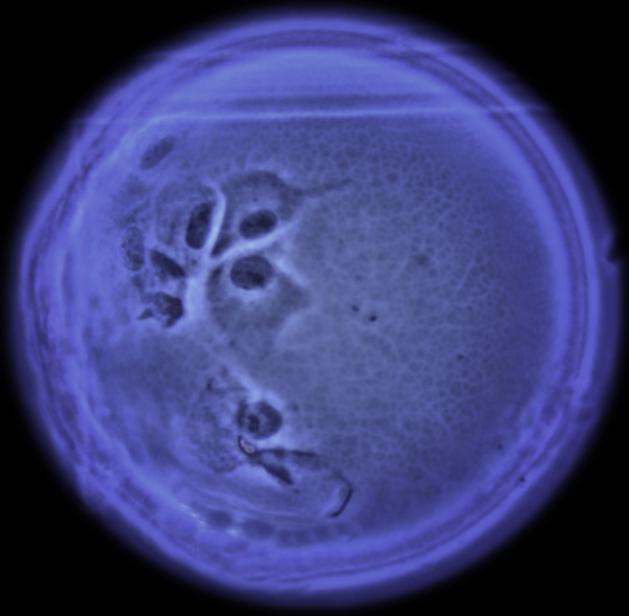

Dissertation presented to obtain the PhD degree in
Molecular Biosciences – Engineering Sciences and Technology

Instituto de Tecnologia Química e Biológica António Xavier | Universidade Nova de Lisboa

Oeiras,
October, 2020

UNIVERSIDADE NOVA DE LISBOA

Streamlining Upstream Processing of Complex Biopharmaceuticals

Marcos F. Q. de Sousa

Dissertation presented to obtain the PhD degree in the PhD program in Molecular Biosciences – Engineering Sciences and Technology

Instituto de Tecnologia Química e Biológica António Xavier
Universidade Nova de Lisboa

Supervisor: Dr. António Manuel Missionário Roldão

Co-Supervisor: Professor Manuel José Teixeira Carrondo

Streamlining Upstream Processing of Complex Biopharmaceuticals

by Marcos F. Q. de Sousa

First Edition: Oeiras, August 2020
Second Edition: Oeiras, October 2020

Cover: Vero cells on microcarrier stained with crystal violet dye. Cover was prepared by Marcos F. Q. de Sousa. Picture was prepared by Marcos F. Q. de Sousa and Pau Garriga.

ITQB, Instituto de Tecnologia Química e Biológica António Xavier
Avenida da República, 2780-157 Oeiras, Portugal
www.itqb.unl.pt

iBET, Instituto de Biologia Experimental e Tecnológica
Apartado 12, 2781-901 Oeiras, Portugal
www.ibet.pt

Financial support of:

PBS Biotech, Inc.

Sartorius GmbH

iNOVA4Health Research Unit (LISBOA-01-0145-FEDER-007344), cofunded by Fundação para a Ciência e a Tecnologia (FCT) / Ministério da Ciência e do Ensino Superior, through national funds, and by FEDER, under the PT2020 Partnership Agreement.

Aos meus Pais

Ao meu Irmão

Follow your dreams

TABLE OF CONTENTS

FOREWORD

I declare that the work presented in this doctoral thesis, except where otherwise stated, is based on my own research.

This PhD dissertation represents the research work conducted at the Animal Cell Technology Unit and Late Stage and Bioproduction Unit, in ITQB António Xavier (UNL) and iBET under the supervision of Dr António Manuel Missionário Roldão and Professor Manuel José Teixeira Carrondo.

The work presented here aim at creating new bioprocesses improving the upstream processing of a recombinant protein, virus vaccine, oncolytic vector, and human mesenchymal stem cells, selected based on their historical and growing importance. Bioengineering tools such as bioreactor and microcarriers technologies, perfusion and process integration were explored towards the developed of new upstream processing solutions.

Marcos F. Q. de Sousa
Oeiras, Portugal

ACKNOWLEDGEMENTS

I would like to express my gratitude to all the people that directly or indirectly was involved in this thesis and to iBET and ITQB António Xavier NOVA as the hosting institutions and for the excellent working conditions.

To my supervisor, Dr António Roldão, “the boss”, I owe most of this thesis to you. Thank you for bringing me to the exciting field of bioprocess engineering, for your guidance, support, trust, encouragement, energy, and for being a demanding boss when necessary. Thank you for all the opportunities that allowed me to grow both personally and as a scientist, which made total difference in the person I am today. To me, you are a role model of a successful scientist and leader.

To my co-supervisor Professor Manuel Carrondo, “the one of a kind”, I can never thank you enough for the endless support, encouragement and example of leadership, and for transmitting that excellence, rigor, hard work and pro-activity are fundamental for success in science. For your enthusiasm, inspiration, and for his sharp view of science and technology.

The “chefita”, Dr Paula M. Alves, I consider you a role model. Thank you for giving me the opportunity to work at the Animal Cell Technology Unit, confidence from the very first day and valuable suggestions and guidance throughout these years.

To Dr Margarida Serra, thank you for always being there for me, for your friendship, companionship, support, for your guidance, and for being so demanding when we wrote the paper together. My thesis would have never been possible without your excellent skills and mentoring.

Dr Marta Silva and Bárbara Sousa, thank you for the opportunity to embracing this challenge with me. There are no other persons I would have trusted my work with. Seeing you grow both professionally and personally

was a true reward. You taught me a lot. Without your commitment and hard work, part of this thesis would not have been possible as it was.

A special acknowledgment to Professor Carlos Augusto. To his memory, for the enthusiasm and support to my thesis. Thank you.

I'm grateful to BMX team. To Dr Pedro Matias to establishing the 3-way collaboration between ITQB-iMM-iBET. To Dr José Brito to support on protein structure. To iMM team for the opportunity and unique collaboration: thank you Bárbara Sousa, Dr Marta Marques, Dr João Seixas and Dr Gonçalo Bernardes.

I would like to thank PBS Biotech for the support part of this PhD work, especially to Dr Brian Lee, Daniel Giroux, Dr Yas Hashimura, Dr Robin Wesselschmidt for the guidance, enlightening discussions, and constructive criticism. To Daniel Giroux a very special thanks to you for the constant enthusiasm and challenging discussions which were crucial for the development of this work. I have learned a lot about bioreactor design and all the issues, challenges, and future trends of new bioreactor concept. Was a pleasure to work with you.

To Sartorius Stedim Biotech for our close and first collaboration with iBET in upstream processing. Special thank you to Dr Christel Fenge, Dr Jens Rupprecht, Dr Alexander Tappe and Dr Gerhard Greller for the unique opportunity. The valuable suggestions and the created synergy were essential to success of the work. To Lídia and Javier for being always there when I need something.

To Dr Ana Coroadinha, Dr Catarina Brito, Dr Inês Isidro, Dr Patrícia Alves and Dr Pedro Cruz for your confidence, motivation, timely guidance, but most importantly, for your friendship.

Downstream processing team headed by Dr Cristina Peixoto, thank you

for the support. To Bárbara Cunha for the precious help in depth filtration.

I want to thank to the late stage and Bioproduction Unit team, especially to António Cunha, Filipe Pinto, Helena Gonçalves, João Clemente, Rute Castro, Rute Eleutério, Sónia Mendes and Tiago Nunes.

I am deeply grateful to Alexandre (Fofo) Murad, Ana Raposo, Bárbara Fernandes, Daniel Simão, Marta Paiva, Maria João Sebastião and Ricardo Correia for support, loyalty, encouragement, laugh and friendship.

To former colleagues from iBET to who I must thank for the learning since ever: Carina Silva, Manuel Garrido and Sara Rosa.

To all my remaining colleagues of the Animal Cell Technology unit, present and former members, for the collective commitment creating a competitive but healthy working environment.

To all the professors (in particular, those from Molecular Biosciences PhD program), researchers, students, and friends I met in conferences and courses around the world, who inspired me and gave me that extra-motivation about my work. And to all the great people I met at this great institute ITQB who are also part of my PhD experience.

To Ana Barbas and Gonçalo Costa for pushing to a goal, to this thesis.

Aos meus amigos de sempre, Gaspar, Paulo, Pedro e Rui.

A Ari pel seu gran suport. Graciès bonica!

Não poderia terminar sem agradecer às pessoas a quem devo o que sou: aos meus pais e ao meu irmão, a quem dedico esta tese. Que me ensinaram a lidar com os Velhos do Restelo, a sorrir e a ser humilde, a defender e lutar por aquilo a que chamamos sonhos (como esta tese). Obrigado pelo apoio, carinho, amizade, paciência infindável, estímulo e por sempre acreditarem em mim. Aos meus avós, tios e primos o meu obrigado.

SUPERVISORS

Dr António Manuel Missionário Roldão
Investigator FCT, Head of Vaccine Development Laboratory at Animal Cell Technology Unit, iBET and ITQB António Xavier – UNL (Oeiras, Portugal).

Professor Manuel José Teixeira Carrondo
Vice-President of iBET, Head of Engineering Cellular Applications & Systems Biology Lab at Animal Cell Technology Unit, iBET (Oeiras, Portugal).

Jury

Dr Hela Kallel
Vaccines Process Development at UNIVERCELLS (Gosselies, Belgium).

Professor Francesc Godia Casablanc
Full Professor in Chemical Engineering at Universitat Autònoma de Barcelona (Barcelona, Spain).

Dr Margarida Diogo
Assistant Professor at the Department of Bioengineering and Institute for Bioengineering and Biosciences at Instituto Superior Técnico, Universidade de Lisboa (Lisboa, Portugal).

Dr Margarida Duarte
Researcher and Auxilliary Investigator in Virology Laboratory at Instituto Nacional de Investigação Agrária e Veterinária (Lisboa, Portugal).

PUBLICATIONS

Thesis publications:

Marcos F. Q. de Sousa, Marta M. Silva, Daniel Giroux, Yas Hashimura, Robin Wesselschmidt, Brian Lee, António Roldão, Manuel J. T. Carrondo, Paula M. Alves and Margarida Serra, 2015. Production of oncolytic adenovirus and human mesenchymal stem cells in a single-use, Vertical-Wheel bioreactor system: Impact of bioreactor design on performance of microcarrier-based cell culture processes. Biotechnology Progress, 31 (6) :1600-12. https://doi.org/10.1002/btpr.2158

Marcos F. Q. de Sousa, Christel Fenge, Jens Rupprecht, Alexander Tappe, Gerhard Greller, Paula M. Alves, Manuel J. T. Carrondo and António Roldão, 2019. Process intensification for Peste des Petites ruminants virus vaccine production. Vaccine, 37(47):7041-7051. https://doi.org/10.1016/j.vaccine.2019.07.009

Bárbara B. Sousa, **Marcos F. Q. de Sousa**, Marta C. Marques, João D. Seixas, José A. Brito, Pedro M. Matias, Gonçalo J. L. Bernardes and António Roldão, 2020. A scalable insect cell-based production process of the human recombinant BMX for in-vitro covalent ligand high-throughput screening. Bioprocess and Biosystems Engineering, In press. (https://doi.org/10.1007/s00449-020-02421-6

Other publications:

Ana C. Silva, Daniel Simão, Claudia Küppers, Tanja Lucas, **Marcos F. Q. de Sousa**, Pedro Cruz, Manuel J.T. Carrondo, Stefan Kochanek and Paula M. Alves, 2015. Human amniocyte-derived cells are a promising cell host for adenoviral vector production under serum-free conditions. Biotechnology Journal, 10:760–71. https://doi.org/10.1002/biot.201400765

Daniel Simão, Marta M. Silva, Ana P. Terrasso, Francisca Arez, **Marcos F.Q. de Sousa**, Narges Z. Mehrjardi, Tomo Šarić, Patrícia Gomes-Alves, Nuno Raimundo, Paula M. Alves and Catarina Brito, 2018. Recapitulation of Human Neural Microenvironment Signatures in iPSC-Derived NPC 3D Differentiation. Stem Cell Reports, 11(2):552-564. https://doi.org/10.1016/j.stemcr.2018.06.020

Ana S. Moreira, Ana C. Silva, **Marcos F. Q. de Sousa**, Åsa Hagner-McWhirterc, Gustaf Ahlénc, Mats Lundgren, Ana S. Coroadinha, Paula M. Alves, Cristina Peixoto and Manuel J. T. Carrondo, 2020. Establishing Suspension Cell Cultures for Improved Manufacturing of Oncolytic Adenovirus. Biotechnology Journal, 15(4): e1900411. https://doi.org/10.1002/biot.201900411

NOMENCLATURE

ATMPs	Advanced therapy medicinal products
BMX	Bone marrow tyrosine kinase on the chromosome X
BtB_{eff}	Bead-to-bead transfer efficiency of Vero cells (%)
CCI	Cell concentration at infection (x10^6 cell/mL)
CFU	Colony forming unit
cGMP	Current good manufacturing practices
D_{eff}	Detachment efficiency of Vero cells from microcarriers (%)
D	Perfusion rate (1/day)
D_i	Impeller diameter (m)
D_{VW}	Impeller diameter in PBS-VW (m)
DSP	Downstream processing
EDR	Energy dissipation rate, $\boldsymbol{\varepsilon}$
$\bar{\varepsilon}_{PBS}$	Mean specific energy dissipation rate in PBS-VW (W/m^3 or W/kg)
$(\varepsilon_{PBS})_{Max}$	Maximum local energy dissipation rate PBS-VW (W/m^3 or W/kg)
$\bar{\varepsilon}_{STB}$	Mean specific energy dissipation rate in STB (W/m^3 or W/kg)
$(\varepsilon_{STB})_{Max}$	Maximum local energy dissipation rate in STB (W/m^3 or W/kg)
FAO	Food and Agriculture of the United Nations
FDA	Fluorescein diacetate
hMSC	Human Mesenchymal Stem Cells
hpi	Hours post-infection
hrBMX	Human recombinant BMX
HCD	High cell density
Hi5	High Five
IC-BEVS	Insect cell – baculovirus expression vector system
ip	Infectious particles
KES	Kolmogorov eddy size, λ (μm)
KLS	Kolmogorov length scale, λ (μm)
M	Fluid mass (kg)
μ	Liquid viscosity (N.s/m^2)
MCB	Master cell bank
MOI	Multiplicity of infection (virus/cell)
N	Agitation rate (1/s or 1/rpm)

$N_{c,Max,}$	Maximum agitation rate for cell culture (1/s or 1/rpm)
$N_{c,Min}$	Minimum agitation rate for cell culture (1/s or 1/rpm)
N_{FS}	Agitation to resuspend microcarriers (1/s or 1/rpm)
NIH	National Institute of Health
OIE	World Organization for Animal Health
OV	Oncolytic virus
OV-Ad5	Oncolytic adenovirus type 5
P	Power input for STB (W)
P_{VW}	Power input for PBS-VW (W)
P_0	Impeller power number (-)
P/M	Mean specific energy dissipation rate (W/kg)
PBB	Packed-bed bioreactor
PBS-3	PBS Vertical-Wheel™ bioreactor 3L volume
PBS-VW	PBS Vertical-Wheel™ bioreactor
pfu/mL	Plate forming unit per milliliter
pi	Post-infection
PI	Propidium iodide
PPR	Peste des Petites ruminants
PPRV	Peste des Petites ruminants virus
Q	Volumetric flow rate in PBS-VW (m^3/min)
qPCR	Real-time quantitative PCR analysis
RB	Roller bottle
rBac	Recombinant baculovirus
RMB	Rocking-motion bioreactor
rpm	Rotation per minute
ρ_L	Liquid density (kg/m^3)
RT	Room temperature (ºC)
RUB	Re-usable bioreactor
SARS	Severe Acute Respiratory Syndrome
Sf-9	Spodoptera frugiperda clone 9
SFM	Serum-free medium
SSR	Shear stress rate, τ (N/m^2)
ST	Stirred-tank
STB	Stirred-tank bioreactor

SUB	Single-use bioreactor
T	Stirred-tank bioreactor diameter
$TCID_{50}$	Tissue culture infection dose 50
t_m	Mixing time (sec)
TOH	Time of harvesting (hour or day)
TS	Tip speed (m/s)
USP	Upstream processing
V	Volume
vvm	Volume of gas per volume of culture per minute
WCB	Working cell bank
wv	Working volume
W_{VW}	Impeller width for PBS-VW (cm)
VBA	Visual Basic Applications
VLP	Virus-like particle
υ	Kinematic viscosity (m^2/sec)

LIST OF FIGURES

LIST OF TABLES

ABSTRACT

The market demand for new biopharmaceuticals is increasing with the aging of the global population and associated (chronic) diseases, rising interest for targeted (cell and gene) therapy, and the advent of new infectious diseases (e.g. Covid-19 pandemics). It becomes evident the need to accelerate the development of commercial processes for the manufacturing of such biopharmaceuticals to meet such demand. This thesis targets such needs creating solid knowledge on the upstream processing of animal cell cultures for the production of complex biopharmaceuticals using bioreactors and microcarriers technology, perfusion and integrated biomanufacturing as optimization tools. The work developed attempted to cover some latitude of challenges based on differences in product characteristics: (i) recombinant protein for drug discovery (human recombinant Bone Marrow Tyrosine kinase on the chromosome X – hrBMX, **Chapter 2**), (ii) virus as vaccine candidate (Peste des Petites ruminants virus – PPRV – vaccine, **Chapter 3**), (iii) virus for cancer therapy (oncolytic adenovirus type 5 – OV-Ad5, **Chapter 4**), and (iv) stem cells for cell therapy (human Mesenchymal Stem Cells – hMSC, **Chapter 4**). System's complexity was embraced using bioreactors scale-down models and bioengineering correlations defining optimal process operation and scale-up.

The market demand for biopharmaceuticals and the challenges for its biomanufacturing are reviewed in **Chapter 1**. A special focus is put on the main streamlining tools for bioprocess development and optimization, namely (i) expression platforms for rapid production of recombinant proteins, (ii) microcarriers-based cultures in bioreactors, (iii) bioengineering correlations for process operation and scale-up, (iv) bioprocess intensification using perfusion and integration of upstream processing (USP) and downstream processing (DSP), and (v) new bioreactor designs for Advanced Therapy Medicinal Products (ATMPs) production.

The supply of biopharmaceuticals in high quantities and, most importantly, quality is often the bottleneck in drug discovery studies. This is particularly relevant at early development stages for proof-of-concept. Implementing robust and scalable platforms for rapid manufacturing of such material is thus essential. An end-to-end rapid production platform of high-quality hrBMX was developed in **Chapter 2**. The insect Sf-9 cell line combined with the baculovirus expression vector system (IC-BEVS) was the selected biological system. Baculoviruses encoding hrBMX were generated and used for screening the best infection conditions in small-scale shake flasks (15 mL): multiplicity of infection of 0.01 virus/cell, cell concentration at infection of $1x10^6$ cell/mL and time of harvest of 72 hours. Process scalability was demonstrated at 5 L scale using stirred-tank bioreactor (STB), with protein expression levels comparable to shake flasks cultures. Regarding purification, by remodeling the purification scheme traditionally used for this type of proteins (i.e. tyrosine kinases) into a 2-step chromatographic train, process time could be reduced by 75 % and, most importantly, protein quantity and stability could be substantially improved. In the end, 24 mg of highly pure hrBMX (> 99 %) could be obtained per L of bioreactor culture. Eventually, the quality of the protein produced enabled subsequent studies related to anti-cancer pharmacological applications.

Chapter 3 describes the development of a new and intensified seed-train strategy to produce PPRV vaccine candidate using microcarrier-based technology. Implementing such a strategy results from the need to reduce the mid-scale(s) of the traditional cell seed-train scheme and, with it, process time and cost. First, Vero cells were stepwise adapted to serum-free medium (SFM), with final specific growth rates similar to those achieved in serum-containing medium. Then, adapted Vero cells were grown in STB using perfusion operation mode, resulting in an increase of 2.5-fold in maximum cell concentration when compared to batch culture. At such high cell concentrations (and SFM), the efficiency of classical cells detachment protocols from microcarriers were as low as 29 %. Therefore, a new in-situ

enzymatic and mechanical cell detachment procedure was developed, reaching efficiencies above 85 %. Noteworthy, by combining this new method with perfusion, process scale-up to 20 L STB could be done directly from a 2 L STB, surpassing the need for a mid-scale platform (i.e. 5 L STB) and thus reducing seed train duration.

In recent decades, a myriad of bioreactor designs has been proposed to lessen the impact of shear stress on cell performance for product generation (quantity and quality) while considering other key factors such as operation mode, ease of handling, regulatory considerations and easiness of scale-up. In **Chapter 4**, the potential of a new single-use and low shear-stress bioreactor design, the Vertical-Wheel™ bioreactor (PBS-VW) for microcarriers-based cultures was explored head-to-head with the 2 L STB. Two cell models were used for that purpose: A549 cell line for OV-Ad5 production (for gene therapy) and hMSC (for cell therapy). The PBS-VW bioreactor induced higher A549 cell growth and the number of infectious OV-Ad5 per cell than the STB. Importantly, a lower total per infectious particles ratio was obtained in PBS-VW, thus indicating a higher OV-Ad5 quality. For the hMSC cell model, slightly higher volumetric cell concentrations were achieved in the PBS-VW bioreactor when compared to STB. Noteworthy, hMSC population generated in PBS-VW showed a significantly lower percentage of apoptotic cells and reduced levels of HLA-DR positive cells. Overall, the data herein generated demonstrated the potential of the new bioreactor design to support the production of microcarrier-based gene and cell therapy products.

Chapter 5 discusses the implications of the findings and main achievements of this thesis. The challenges and hurdles associated with biopharmaceutical upstream processing using animal cell cultures and their effects during the production process optimization and scale-up were discussed. The main pitfalls and ensuing outline strategies for future work are described.

Summarizing, this PhD thesis contributes to advance the state of the art on upstream processing of complex biopharmaceuticals providing a set of novel and improved optimization schemes for their production.

RESUMO

O crescimento de mercado dos biofármacos tem sido notório nos últimos anos devido ao surgimento de doenças crónicas associadas ao envelhecimento, novas doenças infeciosas (por exemplo, pandemia Covid-19) e crescente interesse em terapias direcionadas (como a celular e genética). Para acompanhar este crescimento e suprimir a necessidade de mercado, a indústria biofarmacêutica tem concentrado boa parte dos seus esforços na melhoria dos bioprocessos de produção de biofármacos.

O objetivo desta tese consiste em desenvolver estratégias inovadoras para a melhoria de bioprocessos de produção de biofármacos através do uso de ferramentas de otimização como tecnologias de bioreatores e microsuportes, e a intensificação e integração de bioprocessos. O bioreator é utilizado como modelo de pequena escala para estudos de desenvolvimento e o seu uso é suportado por corelações de bioengenharia essências na definição das condições de operação e correto dimensionamento de cada bioprocesso de produção. Na base dos desafios associados ao desenvolvido no presente trabalho encontram-se as características dos biofármacos produzidos: proteína recombinante para suporte ao desenvolvimento de drogas covalentes (tirosina quinase de medula óssea humana na forma recombinante – hrBMX, **capítulo 1**), vírus como candidato a vacina veterinária (vírus da peste dos pequenos ruminantes – PPRV, **capítulo 2**), produção de vírus oncolítico (adenovírus oncolítico do tipo 5 – OV/Ad5, **capítulo 4**) e expansão de células estaminais mesenquimais de origem humana (hMSC, **capítulo 4**).

As necessidades atuais de mercado para biofármacos e os desafios associados à sua produção são revistos no **capítulo 1**. Destacam-se as ferramentas de melhoramento para desenvolvimento e otimização de bioprocessos, nomeadamente: (i) plataformas de expressão para produção rápida de proteínas recombinantes, (ii) microsuportes para cultura de células

em bioreatores, (iii) correlações de bioengenharia para operação e aumento de escala de bioprocessos, (iv) intensificação de bioprocessos através de perfusão e integração das fases de produção e purificação; e (v) novo bioreator para produção de produtos medicinais para terapia avançada (ATMPs).

O fornecimento de biofármacos em quantidades e qualidade elevadas pode ser um fator limitante para estudos de desenvolvimento de novas terapias, particularmente importante nas fases iniciais de cada projeto ou em programas de desenvolvimento acelerado. Assim, torna-se fundamental desenvolver plataformas robustas e escaláveis para a rápida produção e fornecimento de biofármacos. No **capítulo 2** apresenta-se a metodologia para plataforma de produção rápida "end-to-end" aplicada à expressão da proteína hrBMX utilizando células Sf-9 e o sistema de expressão através de baculovirus recombinante (BEVS). Neste estudo foi construído um baculovírus que codifica a expressão da hrBMX e este foi posteriormente usado para determinar as condições ótimas para produção em frascos agitados de pequena escala (15 mL): multiplicidade de infeção de 0.01 vírus/célula e tempo de recolha de 72 horas após-infeção para uma concentração celular no momento da infeção de $1x10^6$ célula/mL. O aumento de escala das condições ótimas foi realizado com sucesso no bioreator de tanque agitado (STB) de 5 L, com níveis de expressão de hrBMX comparáveis entre as culturas de bioreator e frasco agitado. Relativamente ao processo de purificação, o esquema tradicionalmente utilizado para este tipo de proteínas (isto é, tirosina quinases) foi simplificado para 2 passos cromatográficos essenciais, reduzindo o tempo de processo em 75 % sem interferir na estabilidade final da hrBMX. No final do processo foi possível recuperar 24 mg de hrBMX pura (> 99 %) por L de cultura de bioreator. A qualidade da proteína foi avaliada na última fase da plataforma de produção rápida através dum conjunto de testes bioquímicos e biofísicos criteriosamente selecionado e com capacidade para validar o potencial da hrBMX produzida para estudos farmacológicos de inibidores covalentes

contra cancro.

O **capítulo 3** descreve a implementação de uma nova estratégia de intensificação do crescimento de células em microsuportes para produzir uma vacina contra PPRV. Isto resulta não só da necessidade de reduzir a(s) escala(s) intermediária(s) tradicionalmente utilizadas para obter células em número suficiente para alimentar a escala de produção, mas também a duração e o custo do bioprocesso. Primeiro, células Vero foram adaptadas de forma gradual ao meio de cultura sem soro (SFM) com taxas específicas de crescimento semelhantes às obtidas em meio com soro. De seguida, as células adaptadas foram cultivadas em STB em perfusão, resultando num aumento de 2.5 vezes na concentração máxima de células, quando comparado à cultura em “batch”. O protocolo tradicionalmente utilizado para a separação de células de microsuportes aplicado às novas condições de cultura (elevada concentração celular e meio sem soro) resultou num rendimento de separação de 29 %. Para colmatar este rendimento baixo foi desenvolvido um novo procedimento in-situ de separação enzimático e mecânico de células, resultando numa eficiência de separação células-microsuporte superior a 85 %. A combinação deste novo método com a perfusão permitiu gerar número de células suficientes para alimentar a escala de 20 L de STB (produção) diretamente a partir do STB de 2 L, eliminando a necessidade de uma escala intermédia (por exemplo de 5 L), reduzindo assim o tempo e custo de bioprocesso.

Nas últimas décadas, foram vários os projetos associados ao desenvolvimento de novos bioreatores com objetivo de diminuir o impacto da tensão de corte no desempenho da célula durante a expressão de produto em quantidade e, mais importante, qualidade. Outros fatores associados ao desenvolvimento do bioreator são o modo de operação, facilidade de manuseio, considerações regulatórias e facilidade para o aumento de escala. **No Capítulo 4**, explora-se o potencial de utilização de um novo bioreator descartável de baixa tensão de corte, Vertical-Wheel™

(PBS-VW), para culturas baseadas em microsuportes, em comparação com o STB de 2 L. Dois modelos de células foram utilizados para este fim: a linha celular A549 para produção de OV-Ad5 e hMSC com aplicação em terapia celular. O PBS-VW garantiu um maior crescimento das células A549 e mais elevada concentração especifica de OV-Ad5 infecioso por célula em comparação com o STB. Foi também obtida uma razão de partículas virais totais por infeciosas mais baixa no PBS, indicando uma maior qualidade do vírus produzido no novo bioreator. Para o modelo de células hMSC, foram alcançadas concentrações volumétricas de células ligeiramente superiores no bioreator PBS-VW quando comparado ao STB. De notar que a população de hMSC gerada no PBS-VW mostrou uma percentagem significativamente menor de células apoptóticas e níveis reduzidos de células positivas para HLA-DR. No geral, os dados obtidos demonstraram o potencial do novo bioreator para uma nova plataforma de produção escalável para produtos de terapia genética e celular (ATPMs) baseada no uso de microsuportes.

No **capítulo 5** são discutidas as implicações dos resultados apresentados nos capítulos anteriores. Especificamente são discutidos os obstáculos associados ao melhoramento de bioprocessos de produção de biofármacos utilizando culturas de células animais e seus efeitos durante a otimização e aumento de escala do bioprocesso de produção. No final, são abordadas as principais dificuldades e a robustez das estratégias delineadas para trabalhos futuros.

Em suma, a presente tese de doutoramento contribui para progresso no desenvolvimento de bioprocessos de produção de biofármacos complexos, fornecendo um conjunto de novos e aprimorados esquemas de otimização de produção.

Chapter 1

General Introduction

Author's contribution to the chapter:

Marcos F. Q. de Sousa wrote the chapter based on the referred bibliography.

CONTENTS

1. INTRODUCTION

Currently, the biopharmaceutical industry faces an increasing pressure to accelerate the development of commercial processes in response to market requirements (Deloite, 2019). The roadmap for successful process development entails process understanding and process optimization. Process understanding establishes relationships between inputs and outputs, defining optimum conditions and acceptable operating ranges (Tescione et al., 2015). These are product-dependent and rely on product quantity and quality critical attributes (Sandner et al., 2019). The outcome of process understanding is the identification of critical process parameters affecting production and tools for process intensification and improvement. Regarding the latter, selecting a representative scale-down model for process optimization studies is of paramount importance given the unfeasibility of conducting them at manufacturing scale (Tescione et al., 2015). In upstream processing, these representative models exist and have been used extensively to revamp old systems into flexible (Roberts, 2019), robust (Agalloco and Akers, 2019), continuous (Patil and Walther, 2018) or even multi-product (Crowell et al., 2018) manufacturing platforms. The recent Covid-19 pandemic (Callaway and Cyranoski, 2020) just renews the importance of streamlining upstream processing of complex biopharmaceuticals.

2. COMPLEX BIOPHARMACEUTICALS

Complex biopharmaceuticals are products derived from biological organisms for treating or preventing diseases. They represent some of the best accomplishments of modern science (Kesik-Brodacka, 2018) capable of targeting specific molecules, rarely causing the side effects associated with conventional small-molecule drugs (Gurevich and Gurevich, 2014). Also,

biopharmaceuticals exhibit high specificity and activity when compared with other therapeutic drugs (Mitragotri et al., 2014) facilitating the treatment of patients who respond poorly to synthetic drugs (Kesik-Brodacka, 2018). Biopharmaceuticals including recombinant antibodies and nucleic acid-based products, vaccines and genetically engineered cell-based products (Walsh, 2018). Importantly, an innovative class of heterogeneous research driven biopharmaceuticals for human use in gene therapy, cell and tissues products is the Advanced Therapy Medicinal Product (ATMPs) (Hanna et al., 2016). Applications include oncology (leading the way of the therapeutic trends), diabetes, rheumatology, antivirals (Walsh, 2018), blood disorders, metabolic, infectious and cardiovascular diseases (Sohail and Jaiswal, 2018) (**Figure 1.1**).

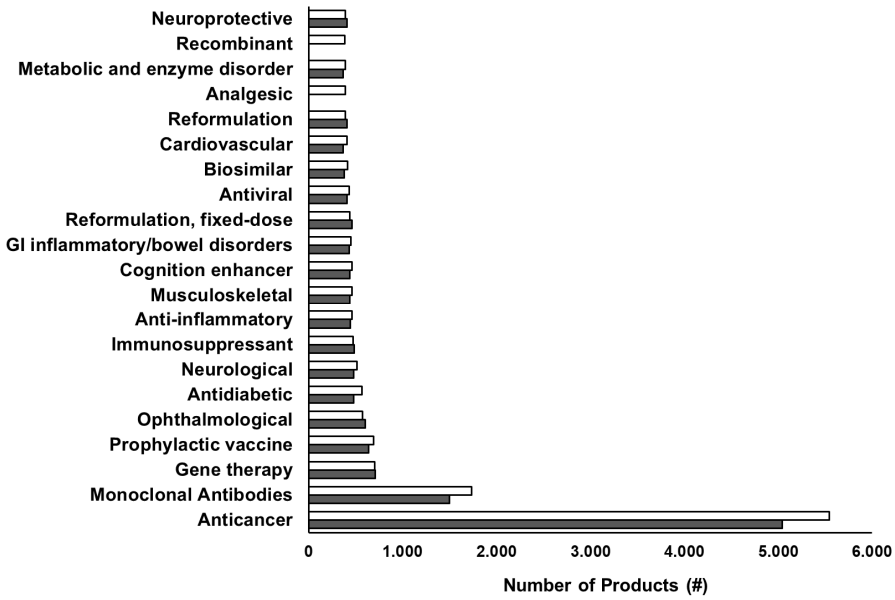

Figure 1.1. Top 25 therapeutic categories for 2018 (black bars) and 2019 (white bars). Data adapted from (PharmaProjects, Pharma intelligence, 2019).

The number of biopharmaceutical products has been significantly growing since the launch of recombinant insulin (Devlin, 1982). Presently, it

is the largest group in the pharma industry with outstanding contribution to public and animal health (Kesik-Brodacka, 2018) with hundreds of approved products (PharmaProjects, Pharma intelligence, 2019) and 40% of total drugs in the discovering pipelines (Long, 2017). Biopharmaceuticals growth is reflected in their market value, with an increase from $300 billion in 2014 to $450 billion in 2019, and an estimated value of $1.5 trillion by 2023 (Deloite, 2019). In addition, it is expected that biopharmaceuticals grow further as more diseases are understood at molecular and cellular levels (Hong et al., 2018).

2.1. Recombinant proteins

Recombinant proteins play a crucial role in the world of complex biopharmaceuticals acting as therapeutic drugs or as tools for developing new drugs. Recombinant proteins are expressed by in-vitro transfection of foreign genes into a host cell. Transfection process can be either mediated by a recombinant viral vector such as baculovirus (Kost and Kemp, 2016), adenovirus (Southgate et al., 2008) or retrovirus (Liao et al., 2017), or by chemical complexation (Pezzoli et al., 2017).

In clinic applications, recombinant proteins are known to be highly potent medicines, reasonably safe from off-target side effects (Bartfai and Lees, 2013). They can be used as pharmaceutical products including diagnostic, protein-based polymers for drug delivery, antibodies and enzymes for disease treatment, and as protein scaffolds for tissue engineering (PharmaProjects, Pharma intelligence, 2019). In drug discovery, recombinant proteins are used to understand disease-associated pathways towards the development of new therapeutic solutions (Puetz and Wurm, 2019). Various scientific methods are available to discover compounds of crucial importance for successful drug discovery (Sugiki et al., 2014). These involve the study of tertiary structure of disease-associated proteins and

respective protein-protein interactions at the atomic level. As therapeutics, large amounts of protein are required, needing high expression cell culture platforms.

2.2. Vaccines

Vaccination is the most effective medical intervention ever introduced, being responsible for reducing or eradicating some of the worst diseases in history (Bloom et al., 2017). Development of new vaccines has become critical with the growing concerns about potential public threats such as Ebola (O'Donnell and Marzi, 2020), H5N1 (avian flu) (Nogales and Dediego, 2020), pandemic strains of influenza (Shao et al., 2017), coronavirus (Chawla and Saxena, 2020) or the combined effects of multi-disease outbreaks (Verikios, 2020). Vaccine development pipelines are showing promising results against major infectious disease, including tuberculosis (30 vaccine candidates in 2016) (Cherry and Papoutsakis, 1988), malaria (RTS,S/AS01, first recombinant protein-based vaccine was approved in 2015; www.ema.europa.eu), Zika (Grubor-Bauk et al., 2019), Ebola (Feldmann et al., 2020), Flu (universal vaccine providing broad coverage against different strains within a subtype or even across subtypes) (Vogel and Manicassamy, 2020) and HIV (HVTN 702 and Ad26 in Clinical Trials Phase II/III; www.nih.gov). Equally important is the development of vaccines for non-infectious, neurodegenerative diseases. These are responsible for high morbidity associated with diabetes (Gao et al., 2016a) or Alzheimer's (Gao et al., 2016b), and the leading cause of death in cases of heart disease (Kadoglou et al., 2018), stroke (Fullerton et al., 2016) and cancer (Thomas and Prendergast, 2016). Regarding the latter, oncolytic viruses (OV) are a novel antitumor agent with the ability to selectively replicate and lyse tumor cells without affecting surrounding healthy cells (Davola and Mossman, 2019). Although being virus-specific, recent advances in molecular biology have allowed the genetic manipulation

of viruses to enhance tumor tropism (Russell et al., 2012). Several OV replicating preferentially in tumors have been examined for their cytotoxicity and efficacy in cancer therapy, namely adenovirus, measles, retroviruses, Newcastle disease virus, herpes simplex viruses, and vesicular stomatitis viruses (Raja et al., 2018). Notably, the therapeutic potential of OV is currently being studied for pancreatic (Sato-Dahlman and Yamamoto, 2017) and hepatocellular carcinomas (Abudoureyimu et al., 2019), malignant glioma (Foreman et al., 2017) and mesothelioma tumors (Scherpereel et al., 2018).

Veterinary vaccines play a major role in protecting animals and public health, reducing or even preventing transmission of zoonotic (e.g. brucellosis and leptospirosis) and foodborne infections to people (Roth, 2011). This field has seen many significant advances over the past twenty-five years with the introduction of vaccines based on novel recombinant genetic engineering (Rauch et al., 2018). These vaccines were able to successfully control diseases with prominent influence in human life such as Aujeszky's disease in pigs (Pejsak et al., 2000), West Nile (Hall and Khromykh, 2004), Rabies in wildlife (Rupprecht et al., 2005) and Rinderpest (Roeder et al., 2013). Remarkably, Rinderpest was the second disease after smallpox to be globally eradicated (Roth, 2011). Following the declaration of successful global eradication of Rinderpest, Peste des Petites ruminants disease (PPR) has been proposed as a candidate for global eradication (Cameron, 2019). The World Organization for Animal Health (OIE) and Food and Agriculture Organization of the United Nations (FAO) released a strategy in 2015 aiming for global eradication of PPR by 2030 (www.fao.org). Peste des Petites ruminants virus (PPRV) is a negative-strand RNA virus, acute and highly contagious (Baron, 2015), and economically important transboundary disease in Africa and Asia (Parida et al., 2015). PPRV infects a wide range of domestic and wild small ruminants, sheep and goats being the preferential

hosts (Abubakar et al., 2016); recently, the host spectrum has been updated to include camels (Rahman et al., 2020). Presently, licensed vaccines are based on attenuated viruses (PPRV/Nigeria/75, PPRV/Sungri/96, PPRV/Arasur/87 and PPRV/Coimbatore/97) prepared in monolayer cultures (Singh et al., 2015). To support the upcoming PPR global eradication program, novel vaccine production processes capable of surpassing the bottlenecks of these methodologies (i.e. high cost and limited scalability) are essential.

2.3. Stem cells

Four categories of stem cells have been isolated and cultured *in-vivo* to date: embryonic stem cells, fetal stem cells, adult stem cells and induced pluripotent stem cells. Within adult stem cells, human Mesenchymal Stem Cells (hMSC) have been showing promising results in a wide variety of applications, mostly due to their immunosuppressive, immunoregulating, migrating, and trophic properties. Furthermore, hMSC have proliferative capacity and potential to differentiate into osteocytes, chondrocytes, and adipocytes (Wei et al., 2007). Presently, more than 300 clinical trials (www.clinicaltrials.org) have been registered to evaluate the efficacy of hMSC in different types of cancer, diabetes, and treatment of graft vs host disease (Wei et al., 2007). From a manufacturing perspective, stem cells are the “product” and not the “substrate” as in recombinant proteins or vaccines production thus posing other, more challenging problems to process development. Processes and unit operations developed for biopharmaceuticals production have been successfully redesigned to cope with hMSC complexity (Serra et al., 2018). Other alternative, scalable platforms for production of hMSC are still needed to cope with the increasing demand for higher cell concentrations to feed the cell therapy market (Caplan, 2017).

3. BIOMANUFACTURING OF COMPLEX BIOPHARMACEUTICALS

3.1. Expression system

The most used platform today for the manufacturing of complex biopharmaceuticals is the mammalian cells expression system (**Figure 1.2**), mostly due to its capacity to (i) express large and complex molecules requiring specific post-translational modification (e.g. glycosylation) (Dumont et al., 2016), and (ii) secrete proteins, eliminating cell lysis and protein extraction steps as in another expression systems (e.g. bacteria) (McKenzie and Abbott, 2018).

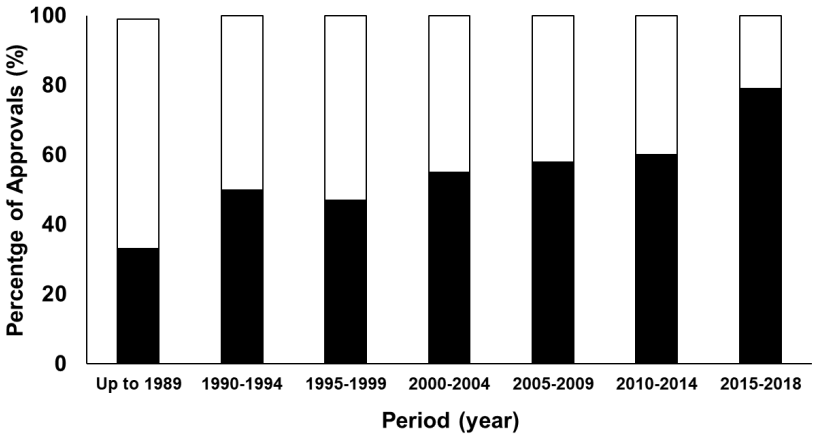

Figure. 1.2. Relative use of mammalian- (black) and non-mammalian (white) expression systems for complex biopharmaceuticals manufacturing. The data was adapted from (Walsh, 2018).

The downside in the use of mammalian cells relates to safety concerns regarding potential contamination with animal viruses (Owczarek et al., 2019), specific/complex nutritional requirements (Yao and Asayama, 2017), slow growth and sensitivity to shear conditions (Hu et al., 2011) (e.g. bioreactor), and high production time and cost (Sanchez-Garcia et al., 2016). Currently, CHO cells are the most used cell substrate in industry, typically to

produce recombinant proteins or monoclonal antibodies (Kunert and Reinhart, 2016). Other rodent (BHK, NS0, Sp2/0) (Butler and Spearman, 2014) (Butler and Spearman, 2014; Strohl and Strohl, 2012; Teixeira et al., 2009) and human cells (HEK293) (Estes and Melville, 2014) are also used to a lesser extent.

For viral-vectors and vaccine production, mammalian cell substrates such as A549 (Kovesdi and Hedley, 2010), Vero (Barrett et al., 2009), MRC-5 (Fletcher et al., 1998), MDCK (Fletcher et al., 1998), CEF and avian cell lines (Fletcher et al., 1998) have been successfully used for many years. The human lung carcinoma continuous cell culture A549 was first initiated by Giard et al. in 1973 (Giard et al., 1973) and further characterized by Lieber et al. in 1976 (Lieber et al., 1976) (**Table 1.1**). A549 cell line incorporated a reduced Adenovirus (Ad) type 5 sequence (nt505–4034) under the regulation of a non-Ad promoter, phosphoglycerate kinase (PGK) (Kovesdi and Hedley, 2010), to support replication of viral pathogens such as adenovirus (Landry et al., 1987). Unmodified A549 cells have been approved for cGMP production of replicating Ad vectors (e.g. OV, NIH) and, recently, Moreira and co-workers reported an adapted cell line to suspension culture in serum-free medium (SFM) for the production of oncolytic Ad5 (Moreira et al., 2020). Vero cells are permissible to infection by a wide variety of viruses, thus being an exceptional host to generate inactivated whole virus vaccines (e.g. influenza, West Nile, Chikungunya, Ross River and SARS) (Barrett et al., 2017). Indeed, Vero cells-based manufacturing platform currently accounts for 7 out of 20 mammalian cell-based vaccines, and many others are in the pipeline (CellCultureDish, 2020). Vero cells are anchorage-dependent, thus requiring a matrix to adhere to and grow in suspension (e.g. microcarriers in bioreactors) (Genzel, 2015). The lytic nature of most viruses poses an additional challenge to Vero cell cultures as one needs to preserve high cell viabilities (i.e. cell adherence to the matrix) during virus replication phase to

Table 1.1. Overview of the cell lines used within the scope of this PhD thesis.

Cell	Described	Origin	Culture	Application	References
A549	1972	Human/ Lung	Adherent*	Adenovirus Oncolytic adenovirus (replicative)	(Kovesdi and Hedley, 2010; Landry et al., 1987; Moreira et al., 2020) www.who.int
Vero	1962	Monkey/ Kidney	Adherent*	Polio Rabies Encephalites virus Human and animal Influenza SARS/MERS coronavirus Rotavirus Adenovirus Vaccinia Herpes Varicella	(Aaskov et al., 1997; Barrett et al., 2017; Fritz et al., 2012; Genzel, 2015; Tang et al., 2016) www.who.int
Sf9	1977	Clonal isolate from Sf21 derived from Armyworm/ Ovarian	Suspension	Virus-like particles of Influenza and rotavirus Virus protein from circovirus and papillomavirus Recombinant adenovirus-associated Recombinant glycoprotein	(Airenne et al., 2013; Jiang et al., 1998; Latham and Galarza, 2001; McPherson, 2008; Roldão et al., 2014; Urabe et al., 2002)
hMSC	1990	Human pericytes	Adherent	Arthritis Cardiovascular Autoimmune and gastrointestinal diseases Cancer Diabetes Graft versus host disease	(Bianco et al., 2008; Caplan, 2017; Serra et al., 2018) www.clinicaltrials.gov

* Reports in the literature described A549 and Vero cells adapted for cell growth in suspension but not licensed for biopharmaceuticals manufacturing (Moreira et al., 2020; Shen et al., 2019); Sf - *Spodoptera frugiperda*, hMSC - human Mesenchymal Stem Cell.

the downstream processing (DSP) (Silva et al., 2015). They preserve high cell viabilities (i.e. cell adherence to the matrix) during virus replication phase to ease the DSP (Silva et al., 2015). Their tumorigenic and/or oncogenic nature are also of concern (Levenbook et al., 1984). Recently, Chen and co-workers described the adaptation of Vero cells to suspension under commercial SFM (Shen et al., 2019). This cell line was reported as non-tumorigenic and shown to withstand high cell densities and improved production of vesicular stomatitis virus when compared to adherent Vero cells (Shen et al., 2019). Other cell lines have been used for viral vaccine production, e.g. PER.C6, CAP, AGE1.CR and EB66 cells (Léon et al., 2016; Lohr et al., 2014; Moreira et al., 2020; Pau et al., 2001; Wölfel et al., 2011). Nonetheless, some of these are under licensing, which turn expensive their use, in particular, for research and development proposes.

Insect cells, in combination with the Baculovirus Expression Vector System (BEVS), emerged as a powerful and versatile platform for vaccine production (Jordan and Sandig, 2014). The most common insect cell lines are Sf-9 and High Five (Hi5) (Roldão et al., 2011), which combined with the BEVS can efficiently express single recombinant proteins or complex protein structures (e.g. virus-like particle, VLP) as vaccine candidates. Recently, insect cells were described for stable expression of recombinant rotavirus (Fernandes et al., 2014), influenza and HIV-Gag VLP (Sequeira et al., 2018).

3.2. Cell culture system

Biopharmaceuticals manufacturing is highly influenced by the cell culture system: adherent or suspension. Except for cell lines derived from the blood system, tumors or some insects, most cell lines grow under adherent conditions (Merten et al., 2014). For specific products, adherent cell lines induce higher cell-specific productivity compared to suspension and adapted cell lines (Genzel, 2015). Anchorage-dependent cells have drawn great

attention due to their broad spectrum of applications, from biologics and vaccines to cell therapy and tissue engineering (Derakhti et al., 2019). Currently, most of these applications still rely on planar, two-dimension (2D) technologies. Roller bottles have been used for the cultivation of Vero cells and the production of important virus-based vaccines such as rabies virus (Jagannathan et al., 2015) and PPRV (Hegde et al., 2009). Multilayer cell culture devices such as cell stack have been successfully used for the expansion of hMSC (Panchalingam et al., 2015). However, surface limitations for cell growth make these traditional culture methods difficult to scale-up to an industrial setting. Comparing adherent to suspension cell culture methodologies, the difference relies on the way that sub-culturing is performed. While sub-culturing in suspension is performed by diluting cells in fresh medium, in adherent cells sub-culturing requires a complex process of cell detachment from the matrix and subsequent inoculation into a new, empty matrix. The impact of adherent and suspension culture becomes evident when scaling up the process. Suspension cultures can be scaled up easily from spinner vessels to lab-bench STB and from these to industrial scale (up to 30 000 L) STB (Warnock et al., 2006). In adherent cultures, scale-up is limited by the surface area available of the matrix used for cell growth. To overcome this limitation, cells have been adapted to suspension or, as largely adopted by the vaccine industry, to grow on microcarriers.

3.3. Bioprocess

Biopharmaceutical manufacturing consists of a sequence of unit operations divided in Upstream processing (USP) and DSP. Traditionally, USP starts with the preparation of the cell stocks (Cell bank) followed by a sequence of culture stages for expansion of cells (Cell seed-train) to feed the last stage of biopharmaceutical production in a bioreactor (Production) (**Figure. 1.3**). This manufacturing scheme is commonly implemented in industry and is

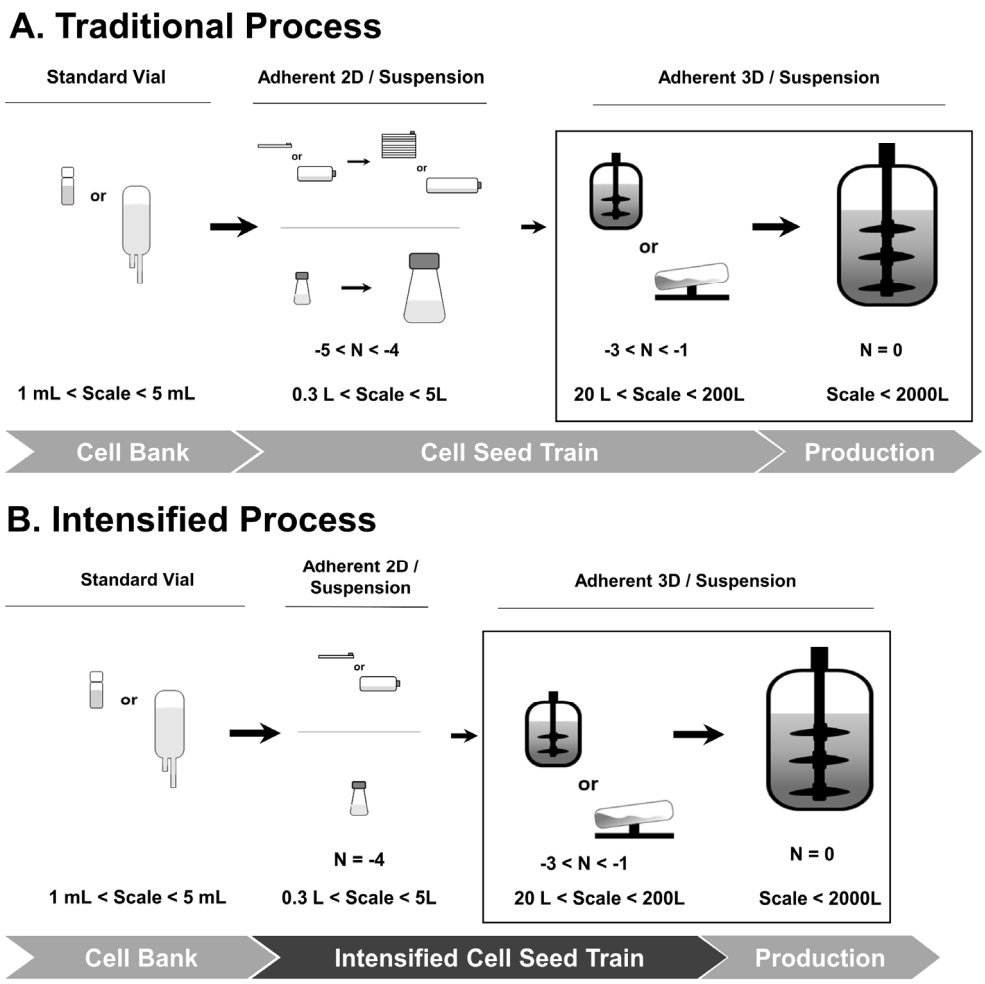

Figure 1.3. Workflows for **(A)** Traditional and **(B)** Intensified process using streamline tools for complex biopharmaceutical manufacturing.

based on principles focused on producing an exact set number of products each period and holding a reserve in case of unexpected demand/unavailability. Emerging technologies, process flexibility, cost-efficiency, speed-to-market, and market demands are driving biopharma companies to reconsider the traditional biomanufacturing workflow and, consequently, the production scales (Chen et al., 2018; Hong et al., 2018). The aim is to increase volumetric productivity (Kamen and Henry, 2004) while reducing timelines, contamination probability and facility footprint (e.g.

bioreactor scale) (DiCesare et al., 2016) (**Figure. 1.3**). A multitude of tools can be used to streamline the bioprocess, such as bioreactor technology (e.g. single vs reusable, stirred vs rocking motion), microcarriers technology, process intensification (e.g. batch vs perfusion or continuous, integrated USP and DSP), or scale-up (bioengineering tools). Combinations of these factors have been reported in the literature (van der Loo and Wright, 2016). These tools assist in process development, generating flexible, scalable, and multiproduct-driven production platforms. A bioreactor is key equipment for these processes, providing controlled environment to achieve optimal growth and/or product formation in the cell system employed. Process intensification has been described for viral vectors and vaccines (Alvim et al., 2019; Nikolay et al., 2018; Tapia et al., 2016; Venereo-Sanchez et al., 2017), recombinant proteins (Tripathi and Shrivastava, 2019), stem cells (Abecasis et al., 2017), and seed-train preparation (Kern et al., 2016; Wright et al., 2015). The latest innovations are using process intensification to reduce the seed train and ensure the highest possible process consistency under full process (Woodgate, 2018). Continuous processing has also the potential to positively impact on the bioprocess by integrating USP and DSP (Gupta et al., 2019). This strategy has been historically limited to labile products that are prone to degradation over time (Chen et al., 2018). Recent advances in both USP and DSP have accelerated their application to other products, allowing a significant reduction in production time and cost (Gronemeyer et al., 2014).

4. TOOLS FOR STREAMLINING UPSTREAM PROCESSING OF COMPLEX BIOPHARMACEUTICALS

To improve the upstream processing of complex biopharmaceuticals is a multidisciplinary task, requiring the use of bioengineering tools (e.g. bioreactor and microcarriers technology) and concepts (e.g. process intensification and scale-up) for its successful implementation. The ultimate

goal is to generate a manufacturing platform as flexible, scalable and multiproduct-driven as possible supporting population health primary needs and drug discovery studies.

4.1. Bioreactor technology

Progress has been made in recent decades towards the development of technologies to cope with cell characteristics (Heath and Kiss, 2007; Rodrigues et al., 2011). Today, cells are typically cultured in bioreactors as they provide the necessary levels of pH, oxygen concentration and temperature in a controlled way. Several engineering principles associated with gas and liquid management are essential for proper mechanical design of bioreactors (Catapano et al., 2009; Löffelholz et al., 2013). Mixing and fluid dynamics characterization ensure culture homogeneity, thus avoiding environmental variation that may impact negatively on cell viability and productivity (Clapp et al., 2018).

4.1.1. Bioreactors type

Two types of bioreactors are used for animal cell culture: reusable (RUB) and single-use (SUB). RUB are made of glass or stainless steel and are widely implemented in academic and industrial environments in a variety of scales (Pörtner et al., 2015). They require large capital investment for purchase and installation, cleaning and sterilization processes as well as skilled operators, thus increasing production cost and time. SUB technology is based on a disposable sterilized chamber/vessel in which cell culture is performed, minimizing the risk of cross-contamination and decreasing the amount of validation, cleaning, sterilization and maintenance needed (Sandle and Saghee, 2011). Besides, these market-ready bioreactors are of added-value for high-throughput applications, and exist in a multitude of scales and formats (e.g. PBS Vertical-Wheel™ bioreactor) (Obom et al., 2014). Although

concerns regarding their cost-effectiveness, sustainability and availability, and scalability still prevail (Clapp et al., 2018), SUB have been slowly earned their space in the bioreactor market (Löffelholz et al., 2013). Both types of bioreactors meet the basic needs for animal cell culture, i.e. good mixing to ensure that the culture environment is homogenous and low shear to avoid cell damage. Also, all RUB and SUB vessels include ports for inlet and outlet gas, ports for additions and harvesting, and probes for pH, DO, and temperature control and monitoring.

4.1.2. Bioreactor agitation systems

Three types of bioreactor agitation systems are used for animal cell culture: mechanically agitated, hydrodynamically driven and non-agitated.

Mechanically agitated stirred-tank bioreactor (STB) is the most well-known and used vessel design for animal cell culture. To cope with market demand, the capacity of STB has gradually increased over the past years, presently ranging from 2 L up to 20 000 L (Pörtner et al., 2015). STB can be made of glass (small scales and the workhorse in academic labs), stainless-steel (mid-to-large scales and widely implanted in the industry) or plastic (scales from 2 L to 2000 L and used mainly in the industry). All follow the same geometry basic principles (i.e. cylindrical or square-shaped), holding different impeller designs to sustain proper mixing and gas transfer for cell growth. Notably, the hydrodynamic stress in STB can be significantly higher than in other bioreactor systems (i.e. rocking-motion bioreactors). The use of stirrers (i.e. impellers) for mixing and spargers for gassing, and the combination of these factors induce high hydrodynamic and interfacial shear environments that can be harmful to cells (Woodgate, 2018). Since sparging cannot be avoided, particularly at large-scale (Woodgate, 2018), shear protective agents like serum or Pluronic® PF-68 have been developed (Clincke et al., 2011) and are today used in most (academic or industrial) cell

culture processes (Gigout et al., 2008).

Rocking-motion bioreactor (RMB) were the first SUB technology to reach the market (Singh, 1999) and the most used hydrodynamically driven bioreactor in the market. RMB are composed of pre-sterilized disposable plastic bags and typically small in scale (volumes ranging from 1 L to 100 L) (Eibl and Eibl, 2009). Mixing and gas transfer is created either by rocking back and forth or by bi-axial movement of the plastic bag, which can be adjusted according to rocking frequency and angle. RMB are normally used in seed-train preparation for vaccines manufacturing (Gallo-Ramírez et al., 2015) and stem cells expansion (Correia et al., 2014).

Packed-bed bioreactor (PBB) is one of the non-agitated bioreactors available in the market and consist of SU vessels filled with an immobilized-matrix providing a large cell growth area in a small volume (Warnock et al., 2005). However, sampling (e.g. for cell concentration and viability) and mixing (e.g. for oxygen supply) is normally cumbersome thus making it difficult to scale-up (Britton et al., 2018). PBB has been traditionally used for applications involving product-inhibited reactions (Britton et al., 2018) but, with recent advances in molecular and cell biology, their use has been expanding to other areas such as cell and gene therapy which depend highly on anchorage-dependent cells to thrive (Merten, 2015).

4.1.3. Bioreactor operation mode

Different bioreactor operation modes have been established over the years aiming at increasing production yields (**Figure 1.4**).

The most commonly used operation mode is batch. It is easy to operate and consists in the supply of all nutrients needed for cell growth at the start of the culture. No extra feeding is performed thus the risk of contamination is

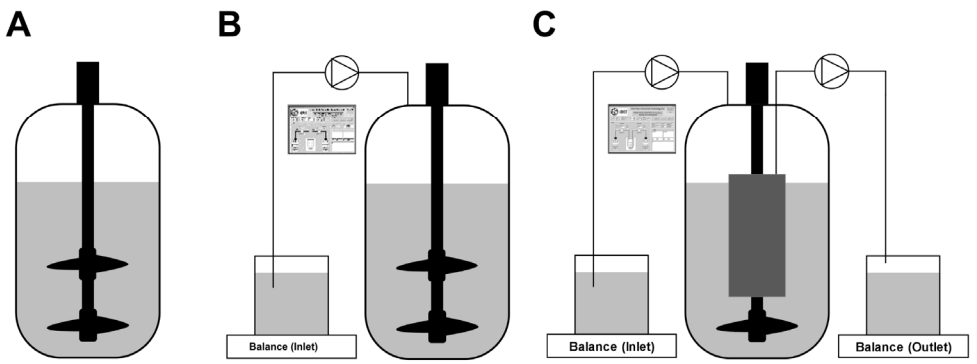

Figure. 1.4. Operation modes for animal cell culturing. **(A)** Batch, **(B)** Fed-batch and **(C)** Perfusion

minimized. There is no effective way to control the process state in batch, i.e. cells in culture are exposed to nutrient concentrations much higher than those required for biomass formation and biopharmaceuticals production. This commonly leads to high metabolic rates (glycolysis and glutaminolysis) and accumulation of inhibitory by-products, thus preventing the achievement of high cell densities and product titers (Cruz et al., 2000).

Fed-batch mode is complex to operate and aims at extending culture lifetime by supplementing limiting nutrients and/or reducing the accumulation of toxic by-products. Small volumes of highly concentrated key nutrients are fed to the bioreactor at specific times during the process, and the bioreactor is harvested at the end of the batch cycle. This has been one of the most effective operation modes for mammalian cell culture given its ability to concentrate the product within the bioreactor to levels higher than those of perfusion or continuous cultures (Gutiérrez-Granados et al., 2018). However, it requires the design of complex nutrient mixtures and feeding strategies to control the concentration of major carbon substrates, thus enabling a more efficient metabolism with lower production rates of inhibitory by-products (Pereira et al., 2018).

Perfusion mode consists in retaining cells within the bioreactor while continuously replacing used medium by fresh medium over an extended period. Besides providing a constant flow of nutrients and growth factors to cells, it allows the removal of inhibitory by-products from the bioreactor (Yang et al., 2014) thus ensuring optimal conditions for cell growth (Kropp et al., 2016). In addition, high cell density (HCD) perfusion processes offer the advantage of producing biopharmaceuticals in compact bioreactors; the bioreactor may be up to 10x smaller and still generate the same amount of product (Ozturk, 1996). Perfusion presents competitive advantages over fed-batch processes as residence times are normally lower favoring product consistency and quality. However, and similar to fed-batch, perfusion design and operation is complex, involving the manipulation of high volumes of medium (with its associated high cost and contamination risk) and requiring sophisticated process automation and feedback control tools (Fernandes-Platzgummer et al., 2014; Woodgate, 2018). Perfusion has been used since the 80s for the production of commercial molecules (e.g. recombinant follicle-stimulating hormone, interferon beta-1a, factor VIII, therapeutic antibodies) (Bielser et al., 2018). Recently, it appears to be gaining new interest from the biopharmaceutical industry within the context of process intensification (see below section 4.3 for details) (Jordan et al., 2018), with cell banking and cell culture seed train two of the many examples of successful use of perfusion (DiCesare et al., 2016; Seth et al., 2013). Nevertheless, scaling-up such processes is still a challenging task (Talò et al., 2018).

4.2. Microcarriers technology

A significant number of cell lines used in cell and gene therapy, vaccines production or bioassays are anchorage-dependent (Merten, 2015). The technologies available to culturing these cells are planar, two-dimensional (2D) (e.g. roller bottle, cell factory, cell stack) (Merten, 2015), or suspension

(three-dimensional) using either macroporous immobilized-matrixes (Pörtner and Barradas, 2007) or microcarriers technology (Cytiva Lifesciences, 2013). Since the development of microcarrier technology by van Wezel in 1967 (Van Wezel, 1967), microcarriers have become an attractive solution to address the limitations of 2D traditional culture methods. Microcarriers are microbeads with diameters of 90-350 μm (Alfred et al., 2011) with densities slightly higher than water and capable of supporting cell attachment and growth. Cells can grow either on the surface or within the pores of these structures in STB (Derakhti et al., 2019) or PBB (Pörtner and Barradas, 2007), making it possible to achieve high cell densities in relatively low volumes due to their high surface to volume ratio.

Traditionally, microcarrier-based cultures are performed in STB due to their controlled environment (pH, DO, temperature) and homogeneous mixing (nutrients, oxygen) for cell growth. However, the use of agitation for mixing proposes can lead to the generation of eddies (Kolmogorov length scale) negatively impacting cell growth (Cherry and Papoutsakis, 1988; Ibrahim and Nienow, 2004). Correct estimation of mixing values is thus critical to guarantee low shear environment for the cells while keeping microcarriers in suspension, and for that the bioengineering correlations developed in the last decades revealed valuable (further detail in section 4.4 below). Microcarrier-based cultures have been described for scales ranging from milliliters (e.g. spinner flasks stirred with magnetic bars or ball-shaped eccentrically rotating agitator) (Merten, 2015) to cubic meters (Montagnon et al., 1983). The largest microcarrier-based process reported is a 6 000 L STB for Influenza production using Vero cells (Barrett et al., 2009).

Microcarrier-based cultures have two critical stages: (i) cell adhesion and propagation to microcarriers, and (ii) cell detachment from microcarriers. Cell adhesion and propagation stage involve a series of seeding cultures with

increasing bioreactor volumes before reaching the production stage. In each seeding bioreactor, and after achieving confluence, cells must be subcultured. This requires cell detachment from microcarriers and re-attachment to new microcarriers in fresh medium (Merten, 2015). Cell detachment from microcarriers is usually performed via proteolytic enzyme treatment (e.g. trypsin) or mechanical scraping (Merten, 2015). Both methods can compromise cell membrane integrity and thus impact negatively on cell growth kinetics in the next seeding bioreactor and/or product quantity and quality at the production bioreactor. Recently, significant efforts have been made to develop procedures to facilitate cell harvesting and collection, with some relying on established bioengineering principles for its conceptual design (Rafiq et al., 2018) and others on cell-type-specific characteristics (Farid and Jenkins, 2018). Regarding the latter, bead-to-bead cell transfer has been gaining momentum due to its ease implementation and cost-effectiveness, when the cells so permit. It consists of the addition of empty microcarriers to the culture followed by intermittent or continuous agitation to allow cells to colonize the empty microcarriers that were added, not requiring enzymatic or mechanical treatment (Wang and Ouyang, 1999). However, this protocol has not been described in the open literature as a routine utilization at scales larger than 30 L (Shevitz et al., 1990).

Microcarrier technology has been extensively used to produce virus-based vaccines such as Herpes (Griffiths and Thornton, 1982), Rabies (Montagnon, 1989), Measles and Mumps (Sidorenko et al., 1989), Hepatitis A (Junker et al., 1994), Polio (Duchêne, 2006) and Influenza (George et al., 2010). Recently, with the advent of stem cell technologies and their potential for cell-based therapies, the interest in anchorage-dependent cell cultures increased (Merten, 2015). Several studies have been reporting the use of microcarrier-based technology to study stem cells expansion, differentiation

and function (Nienow et al., 2016b) in different operation modes (e.g. batch, perfusion) (Abeille et al., 2014; Serra et al., 2018). Combining microcarriers with bioreactor technology, production yields can increase significantly making a process cost-effective (Simaria et al., 2014). Today, revisiting microcarrier technology is essential to generate new methodologies for cell growth, scale-up/scale-out, and cell culture devices.

4.3. Process intensification

Process intensification in USP is associated with an increase in productivities (cell or product) using bioreactors operated in fed-batch (Xu et al., 2020). Recently, perfusion appears to be gaining new interest from the biopharmaceutical industry within the context of process intensification (Jordan et al., 2018). Many industries are slowly transitioning from batch or fed-batch to perfusion or hybrid (i.e. combination of fed-batch and perfusion) processes with significant benefits (Gupta et al., 2019; Jordan et al., 2018). Selecting the appropriate bioreactor and cell retention device is key for a successful perfusion process. The bioreactor needs to support high cell concentration while guaranteeing appropriate mixing/homogeneity at relatively low shear (Zhao et al., 2010). STB and, to a lesser extent, RMB are commonly used for perfusion processes (Woodgate, 2018). Increased productivities enable the reduction of bioreactor scale, size and complexity, falling into regimes where SUB can be applied (below 2 000 L) (Chen et al., 2018). On the other hand, the retention device needs to prevent cells from flowing out of the bioreactor, provide sufficient aeration to the cells while preventing harmful shear, guarantee long-term operation without failure (e.g. filter fouling), and operate across multiple perfusion rates and production scales (Chen et al., 2018). These devices can be either internal or external to the bioreactor: settling cyclones (Pinto et al., 2008), centrifuges (Voisard et al., 2003), acoustic resonance (Dalm et al., 2004) and spin filters (Fenge

et al., 1993). More recently, alternating or tangential flow filtration (ATF or TFF, respectively) technologies have been successfully reported as cell retention devices (Clincke et al., 2013).

Cell culture medium is another key factor to consider for process intensification. Traditionally, cell culture is performed in serum-containing media. However, its use implies many disadvantages such as the presence of animal-derived proteins and contaminants (e.g., fungi, bacteria and viruses), its non-defined composition, variable quality and high cost, and, more importantly, its negative impact on DSP. Adaptation of cells to SFM or chemically defined (CDM) medium is desirable not only from a biosafety perspective but also from a process understanding and optimization point of view. From the several attempts carried out so far to replace serum (Petiot et al., 2012; Rourou et al., 2007; Silva et al., 2008), important, specific components (e.g. growth factors, proteins, hydrolysates, cytokines, hormones, attachment factors, trace elements) responsible for cell survival and proliferation in vitro have been difficult to identify. For that reason, the adaptation of some cell lines to SFM or CDM have been a success while for others it failed redundantly. Most production processes require culture media capable of supporting cell growth and virus production (Genzel, 2015). Moreover, some media may require additional optimization for large-scale production, as cell adaptation is typically performed in shakers with different shear, pH and oxygen concentration (Hunter et al., 2019). The operation mode also defines the development of specific media formulations since cell requirements in batch, fed-batch and perfusion are significantly different (Bausch et al., 2019). Medium development knowledge for perfusion application, is many times mentioned as a key gap for the wider adoption of perfusion processing in biopharmaceuticals manufacturing (Bausch et al., 2019). Several formulations of SFM and protein-free media are commercially available for culturing several cell lines.

The full potential of USP for process intensification can be realized in the context of a fully continuous end-to-end integrated manufacturing unit (Karst et al., 2017). This integration can be a very useful tool when applied to a unit operation such as clarification, a mid-stage operation between UPS and DSP (Rathore et al., 2015). Its successful implementation requires time for process development. Bringing in new methods such as modelling and/or high-throughput-screening approaches may help in improving the integration process. Standardizing this unit operation results in a reliable and robust operation which can be applied to multi-products manufacturing platforms. In turn, this platform should be able to reduce time (Vicente et al., 2009) and effort in DSP development (Gupta et al., 2019) as well as in plant fingerprint (Godawat et al., 2015).

4.4. Process engineering parameters

Understanding the main bioreactor engineering parameters facilitates process optimization, scale-up and scale-down, and importantly, comparison between different bioreactor designs. The methodologies applied to estimate the bioengineering characteristics of a bioreactor must be common to different designs and capable of balancing the interactions between fluid dynamics and biological performance. The bioengineering principles used for process scale-up are the same as for scale-down (Sandner et al., 2019) and can be divided into scale-dependent and scale-independent (Löffelholz et al., 2013). Scale-independent parameters are the pH, DO, temperature, cell inoculum concentration or process duration, for example, and are maintained constant during scale-down or scale-up. Scale-dependent parameters are energy dissipation rate (EDR, ε) and volumetric flow rate (Nienow, 2006), Kolmogorov eddy size (KES, λ) (Croughan et al., 1987), volumetric mass transfer coefficient (k_La) (Schaepe et al., 2013), mixing time (t_m) and shear stress (SSR, τ) (Bailey and Ollis, 1986), residence time (Rodrigues et al.,

2012), heat transfer (Nagata, 1975) and tip speed (TS) (Nienow, 2006), for example. They depend on bioreactor geometry, agitation or aeration, and thus require adjustment according to the production scale. Typically, these parameters are assessed at small-scale and then used for scaling-up (or down) the process using appropriate criteria (e.g. constant ε, λ, τ and TS). When this data is not available, empirical correlations proposed using similar bioreactor geometries and scales can be used (Tescione et al., 2015). Details on the most important bioengineering correlation are discussed below.

4.4.1. Bioengineering correlations

Two important bioengineering correlations for process scale-up are the Reynolds number (Re) and the mean specific energy dissipation rate (ε).

The flow regime in bioreactors is defined by the Reynolds number:

$$\mathrm{Re} = \frac{\mathrm{N.T.}\rho}{\mu} \qquad \text{Equation 1.1}$$

where N (1/s) is the agitation rate, T (m) is the diameter of the bioreactor, ρ (kg/m^3) and μ (N.s.m^2) are liquid density and viscosity, respectively. Fluid flow can be laminar, transitional, or turbulent, with turbulent being the flow regime most commonly used in stirred systems such as STB. For new bioreactor designs, a modified Reynolds number has been proposed (Büchs, 2001; Eibl et al., 2009; Löffelholz et al., 2013).

The specific power-input (P/M), or mean specific energy dissipation rate ($\bar{\varepsilon}$), estimates the average local energy input which is often related to mechanical stress:

$$\frac{\mathrm{P}}{\mathrm{M}} = \bar{\varepsilon} = \frac{\mathrm{P_o.N^3.D_i^5}}{\mathrm{V}} \qquad \text{Equation 1.2}$$

where M (kg) is the fluid mass, P_0 (-) and D_i (m) are the power number and diameter of the impeller, respectively, and V (m^3) is bioreactor working volume. $\bar{\varepsilon}$ has been reported for ungassed (Cruz et al., 1998; Placek and Tavlarides, 1985) and gassed (Calderbank, 1958; Greaves and Kobbacy, 1981; Nagata, 1975) bioreactor systems as well as for different bioreactor designs (Anderlei et al., 2007; Chisti and Jauregui-Haza, 2002; Löffelholz et al., 2013; Nienow, 2006). Fluid flow in bioreactors can be very heterogeneous and thus the value of $\bar{\varepsilon}$ may not reflect the real impact of mechanical stress caused by agitation on cells behavior (Kaiser et al., 2011). It is known that agitation power is dissipated into a small fraction of bioreactors volume and thus the maximum/local dissipation rate at the microscale of turbulence, $(\varepsilon)_{\mathrm{Max}}$, can be orders of magnitude higher than the average (Li et al., 2018). The energy dissipation rate (ε) allows to estimate important advanced parameters such as Kolmogorov eddy size (λ) and shear stress rate (τ) under turbulent flow:

$$\lambda = \left(\frac{\upsilon}{\varepsilon}\right)^{1/4} \qquad \text{Equation 1.3}$$

$$\tau = \left(\frac{\varepsilon}{\upsilon}\right)^{1/2} . \mu \qquad \text{Equation 1.4}$$

where υ (m^2/s) is the kinematic viscosity. Shear forces impact negatively animal cells by acting at both the biochemical and physiological level (Trujillo-Roldán and Valdez-Cruz, 2006). They can induce sub-lethal effect on the cells, without causing cell death, but can also induce apoptosis (Godoy-Silva et al., 2009). Shear stress is also critical for the quality of the biopharmaceutical product whether this is a virus (Grein et al., 2019), recombinant protein (Keane et al., 2003) or stem cells (Wang et al., 2018). Shear stress threshold values can be estimated using methodologies applied for shear estimation (Galie et al., 2014; Wang et al., 2018), and are cell line

dependent (Godoy-Silva et al., 2009; Tanzeglock et al., 2009). For anchorage-dependent cells growing on microcarriers under agitation conditions, the effect of turbulent eddy sizes on cells are examined using Kolmogorov eddy size as defined in **Equation 1.3**. Several authors have shown that Kolmogorov eddy length can be correlated with specific cell growth rate (Cherry and Papoutsakis, 1988; Croughan et al., 1987), with Croughan and co-workers in 1987 being the first ones to demonstrate that cell growth is not compromised for eddy lengths comparable or larger to 2/3 of microcarrier's diameter. Others have later confirmed this relationship for microcarriers as well as for suspension cells (Cruz et al., 1998). To ensure successful culture of anchorage-dependent cells in suspension, microcarriers must be kept in suspension with minimum or no-gradient/local solids concentration. The most accepted equation to assess solid suspension characteristics of an impeller is the one developed by Zwietering (1958) (Mak, 1992). It estimates the agitation needed to avoid sedimentation of solids, designated as "Just Suspended Agitation", and is widely used for microcarriers-based cultures (Delafosse et al., 2018). However, significant differences have been observed between Zwietering correlation value and experimental data (George et al., 2010). Some reports suggest to visually assess microcarriers flow in bioreactor and estimate "Just Suspended Agitation" experimentally (Nienow et al., 2016a).

5. THESIS SCOPE

The market demand for new biopharmaceuticals is increasing with the aging of the global population and associated (chronic) diseases, rising interest for targeted (cell and gene) therapy, and advent of new infectious diseases (e.g. Covid-19 pandemics). To meet such demand, it becomes evident the need to accelerate the development of commercial processes for the manufacturing of such biopharmaceuticals.

This PhD thesis aims at contributing to such effort by revisiting old biomanufacturing platforms and developing new ones. A schematic representation of the bioengineering tools used in this thesis and essential to achieve an intensified upstream process are summarized in **Figure. 1.5**. More specifically, the topics addressed in the thesis are the following:

- Application of bioengineering correlations for (i) process optimization and scale-up in stirred-tank bioreactor (STB), and (ii) process transfer from standard STB to new single-use bioreactor (SUB) designs (**Chapter 2-4**),
- Establishing a rapid production platform for recombinant protein production to assist drug discovery studies (**Chapter 2**),
- Revisiting microcarrier technology to design a flexible and scalable seed-train strategy for virus-based vaccine production in anchorage-dependent cells (**Chapter 3**),
- Evaluating the impact of serum-free medium on microcarriers-based cell cultures in STB (**Chapter 3**),
- Integrating of upstream processing and downstream processing to generate a continuous biomanufacturing scheme for production of virus-based vaccines (**Chapter 3**),
- Evaluating the impact of SUB technology on the yields and quality of products obtained using microcarriers-based cultures (**Chapter 4**).

Summarizing, this thesis demonstrates the relevance of coupling bioengineering principles with fundamental biological understanding for streamlining upstream processing of biopharmaceuticals. Importantly, the tools here-in described can be applied to de-bottleneck the manufacturing platforms of other difficult to express human and animal biopharmaceuticals.

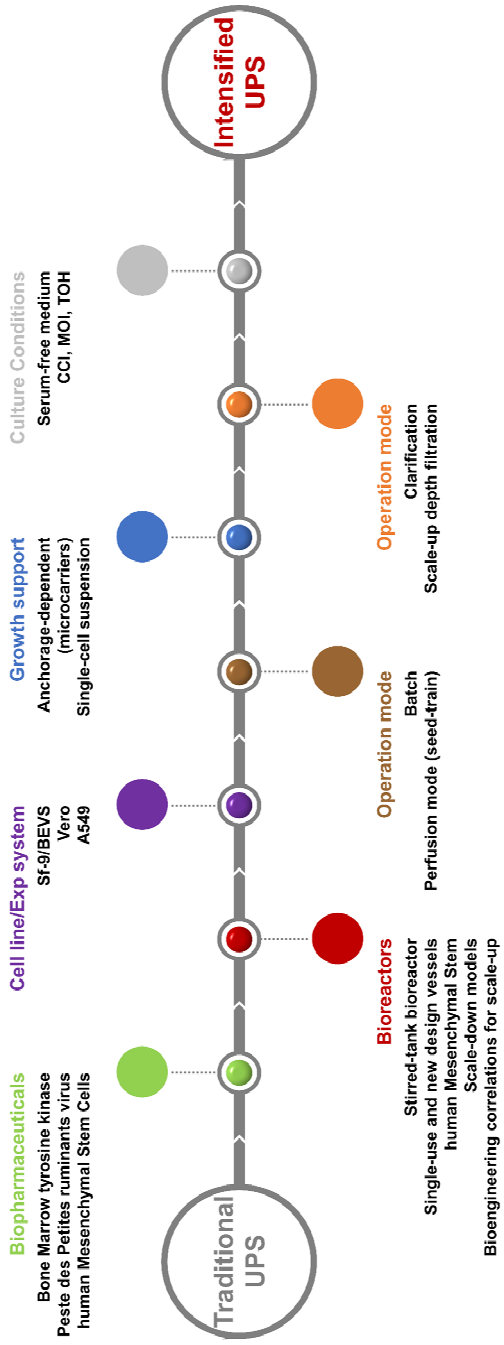

Figure. 1.5. A schematic representation of the bioengineering tools used in this thesis and essential to achieve an intensified upstream process. CCI: Cell concentration at infection. MOI: Multiplicity of infection. TOH: Time of harvesting.

6. REFERENCES

Aaskov J, Williams L, Yu S. 1997. A candidate Ross River virus vaccine: Preclinical evaluation. *Vaccine* **15**:1396–1404.

Abecasis B, Aguiar T, Arnault É, Costa R, Gomes-Alves P, Aspegren A, Serra M, Alves PM. 2017. Expansion of 3D human induced pluripotent stem cell aggregates in bioreactors: Bioprocess intensification and scaling-up approaches. *J. Biotechnol.* **246**:81–93. https://www.sciencedirect.com/science/article/pii/S0168165617300214?via%3Dihub.

Abeille F, Mittler F, Obeid P, Huet M, Kermarrec F, Dolega ME, Navarro F, Pouteau P, Icard B, Gidrol X, Agache V, Picollet-D'Hahan N. 2014. Continuous microcarrier-based cell culture in a benchtop microfluidic bioreactor. *Lab Chip* **14**:3510–8.

Abubakar M, Manzoor S, Wensman JJ, Torsson E, Ali Q, Munir M. 2016. Molecular and Epidemiological Features of Peste des Petits Ruminants Outbreak during Endemic Situation. *Br. J. Virol.* **3**:123–129.

Abudoureyimu M, Lai Y, Tian C, Wang T, Wang R, Chu X. 2019. Oncolytic Adenovirus - A Nova for Gene-Targeted Oncolytic Viral Therapy in HCC. *Front. Oncol.* **9**:1182.

Agalloco J, Akers J. 2019. Risk Assessment and Mitigation in Aseptic Processing. In: . *Parenter. Medicat.*, pp. 829–839.

Airenne KJ, Hu Y-C, Kost TA, Smith RH, Kotin RM, Ono C, Matsuura Y, Wang S, Ylä-Herttuala S. 2013. Baculovirus: an Insect-derived Vector for Diverse Gene Transfer Applications. *Mol. Ther.* **21**:739–749.

Alfred R, Radford J, Fan J, Boon K, Krawetz R, Rancourt D, Kallos M. 2011. Efficient Suspension Bioreactor Expansion of Murine Embryonic Stem Cells on Microcarriers in Serum-Free Medium. *Biotechnol. Prog.* **27**:811–823.

Alvim RGF, Itabaiana I, Castilho LR. 2019. Zika virus-like particles (VLPs): Stable cell lines and continuous perfusion processes as a new potential vaccine manufacturing platform. *Vaccine* **37**:6970–6977. http://www.sciencedirect.com/science/article/pii/S0264410X19307017.

Anderlei T, Mrotzek C, Bartsch S, Amoabediny G, Peter CP, Büchs J. 2007. New method to determine the mass transfer resistance of sterile closures for shaken bioreactors. *Biotechnol. Bioeng.* **9**:999–1007.

Bailey JE, Ollis DF. 1986. Biochemical engineering fundamentals. New York: McGraw-Hill. http://books.google.com/books?id=zdBTAAAAMAAJ.

Baron MD. 2015. The molecular biology of peste des petits ruminants virus. In: . *Peste Des Petits Ruminants Virus*, pp. 11–38.

Barrett PN, Mundt W, Kistner O, Howard MK. 2009. Vero cell platform in vaccine production: moving towards cell culture-based viral vaccines. *Expert Rev. Vaccines* **8**:607–18. http://informahealthcare.com/doi/abs/10.1586/erv.09.19.

Barrett PN, Terpening SJ, Snow D, Cobb RR, Kistner O. 2017. Vero cell technology for rapid development of inactivated whole virus vaccines for emerging viral diseases. *Expert Rev. Vaccines* **16**:883–894. https://doi.org/10.1080/14760584.2017.1357471.

Bartfai T, Lees G V. 2013. The need for medicines grows. In: . *Futur. Drug Discov.*, pp. 31–53.

Bausch M, Schultheiss C, Sieck JB. 2019. Recommendations for Comparison of Productivity Between Fed-Batch and Perfusion Processes. *Biotechnol. J.* **14**:1700721. https://doi.org/10.1002/biot.201700721.

Bianco P, Robey PG, Simmons PJ. 2008. Mesenchymal stem cells: revisiting history, concepts, and assays. *Cell Stem Cell* **2**:313–319. https://pubmed.ncbi.nlm.nih.gov/18397751.

Bielser J-MM, Wolf M, Souquet J, Broly H, Morbidelli M. 2018. Perfusion mammalian cell culture for recombinant protein manufacturing – A critical review. *Biotechnol. Adv.* **36**:1328–1340. https://www.sciencedirect.com/science/article/pii/S0734975018300831?via%3Dihub.

Bloom DE, Black S, Rappuoli R. 2017. Emerging infectious diseases: A proactive approach. *Proc. Natl. Acad. Sci. U. S. A.* **114**:4055–4059.

Britton J, Majumdar S, Weiss GA. 2018. Continuous flow biocatalysis. *Chem. Soc. Rev.* **47**:5891–5918. https://pubmed.ncbi.nlm.nih.gov/29922795.

Büchs J. 2001. Introduction to advantages and problems of shaken cultures. *Biochem. Eng. J.* **7**:91–98.

http://www.sciencedirect.com/science/article/pii/S1369703X00001066.

Butler M, Spearman M. 2014. The choice of mammalian cell host and possibilities for glycosylation engineering. *Curr. Opin. Biotechnol.* **30**:107–12.

Calderbank PH. 1958. Physical Rate Processes in Industrial Fermentation. Part I: The Interfacial Area in Gas- Liquid Contacting with Mechanical Agitation. *Trans. Inst. Chem. Eng.* **36**:443–463.

Callaway E, Cyranoski D. 2020. China coronavirus: Six questions scientists are asking. *Nature* **577**:605–607.

Cameron AR. 2019. Strategies for the global eradication of peste des petits ruminants: An argument for the use of guerrilla rather than trench warfare. *Front. Vet. Sci.* **6**:331.

Caplan AI. 2017. Mesenchymal stem cells: Time to change the name! *Stem Cells Transl. Med.* **6**:1445–1451.

Catapano G, Czermak P, Eibl R, Eibl D, Pörtner R. 2009. Bioreactor Design and Scale-Up. In: . *Cell Tissue React. Eng. Princ. Pract.*, pp. 173–259.

CellCultureDish. 2020. The Evolution of Vaccine Manufacturing – Past, Current, and Future Trends. *https://cellculturedish.com/the-evolution-of-vaccine-manufacturing-past-current-and-future-trends/*.

Chawla S, Saxena SK. 2020. Preparing for the Perpetual Challenges of Pandemics of Coronavirus Infections with Special Focus on SARS-CoV-2. *Coronavirus Dis. 2019*.

Chen C, Wong HE, Goudar CT. 2018. Upstream process intensification and continuous manufacturing. *Curr. Opin. Chem. Eng.* **22**:191–198.

Cherry RS, Papoutsakis ET. 1988. Physical mechanisms of cell damage in microcarrier cell culture bioreactors. *Biotechnol. Bioeng.* **32**:1001–14.

Chisti Y, Jauregui-Haza UJ. 2002. Oxygen transfer and mixing in mechanically agitated airlift bioreactors. *Biochem. Eng. J.* **10**:143–153.

Clapp K, Castan A, K. Lindskog E, Clapp K, Castan A, Lindskog E. 2018. Upstream Processing Equipment. In: . *Biopharm. Process. Dev. Des. Implement. Manuf. Process.*, pp. 457–476.

Clincke M-F, Guedon E, Yen F, Ogier V, Roitel O, Goergen J-L. 2011. Effect of surfactant pluronic F-68 on CHO cell growth, metabolism, production, and

glycosylation of human recombinant IFN-γ in mild operating conditions. *Biotechnol. Prog.* **27**:181–190.

Clincke M-F, Mölleryd C, Samani PK, Lindskog E, Fäldt E, Walsh K, Chotteau V. 2013. Very high density of CHO cells in perfusionby ATF or TFF in WAVE bioreactor™ – Part II: Applications for antibody production and cryopreservation. *Biotechnol. Prog.* **29**:754–67.

Correia C, Serra M, Espinha N, Sousa M, Brito C, Burkert K, Zheng Y, Hescheler J, Carrondo MJT, Šarić T, Alves PM. 2014. Combining Hypoxia and Bioreactor Hydrodynamics Boosts Induced Pluripotent Stem Cell Differentiation Towards Cardiomyocytes. *Stem Cell Rev. Reports* **10**:786–801.

Croughan MS, Hamel JF, Wang DI. 1987. Hydrodynamic effects on animal cells grown in microcarrier cultures. *Biotechnol. Bioeng.* **29**:130–41. http://www.ncbi.nlm.nih.gov/pubmed/18561137.

Crowell LE, Lu AE, Love KR, Stockdale A, Timmick SM, Wu D, Wang YA, Doherty W, Bonnyman A, Vecchiarello N, Goodwine C, Bradbury L, Brady JR, Clark JJ, Colant NA, Cvetkovic A, Dalvie NC, Liu D, Liu Y, Mascarenhas CA, Matthews CB, Mozdzierz NJ, Shah KA, Wu S-L, Hancock WS, Braatz RD, Cramer SM, Love JC. 2018. On-demand manufacturing of clinical-quality biopharmaceuticals. *Nat. Biotechnol.* **36**:988–995.

Cruz HJ, Moreira JL, Carrondo MJ. 2000. Metabolically optimised BHK cell fed-batch cultures. *J. Biotechnol.* **80**:109–118.

Cruz PE, Cunha A, Peixoto CC, Clemente J, Moreira JL, Carrondo MJT. 1998. Optimization of the production of virus-like particles in insect cells. *Biotechnol. Bioeng.* **60**:408–418.

Cytiva Lifesciences. 2013. Microcarrier cell culture: principles and methods. *https://www.cytivalifesciences.com/en/us/support/handbooks*.

Dalm MCF, Cuijten SMR, van Grunsven WMJ, Tramper J, Martens DE. 2004. Effect of feed and bleed rate on hybridoma cells in an acoustic perfusion bioreactor: part I. Cell density, viability, and cell-cycle distribution. *Biotechnol. Bioeng.* **88**:547–557.

Davola ME, Mossman KL. 2019. Oncolytic viruses: how “lytic” must they be for therapeutic efficacy? *Oncoimmunology* **8**:e1581528.

Delafosse A, Loubière C, Calvo S, Toye D, Olmos E. 2018. Solid-liquid suspension

of microcarriers in stirred tank bioreactor - Experimental and numerical analysis. *Chem. Eng. Sci.* **180**:52–63.

Deloite. 2019. 2019 Global life sciences outlook Focus and transform | Accelerating change in life sciences. *Glob. life Sci. outlook I Focus Transform | Accel. Chang. life Sci.*:1–54.

Derakhti S, Safiabadi-Tali SH, Amoabediny G, Sheikhpour M. 2019. Attachment and detachment strategies in microcarrier-based cell culture technology: A comprehensive review. *Mater. Sci. Eng. C. Mater. Biol. Appl.* **103**:109782.

Devlin J. 1982. New insulins and new ways with insulin. *Ir. Med. J.* **75**:344–346.

DiCesare C, Yu M, Yin J, Zhou W, Hwang C, Tengtrakool J, Konstantinov K. 2016. Development, qualification, and application of a bioreactor scale-down process: Modeling large-scale microcarrier perfusion cell culture. *Bioprocess Int.* **14**.

Duchêne M. 2006. Production, testing and perspectives of IPV and IPV combination vaccines: GSK biologicals' view. *Biologicals* **34**:163–166.

Dumont J, Euwart D, Mei B, Estes S, Kshirsagar R. 2016. Human cell lines for biopharmaceutical manufacturing: history, status, and future perspectives. *Crit. Rev. Biotechnol.* **36**:1110–1122.

Eibl R, Eibl D. 2009. Application of disposable bag bioreactors in tissue engineering and for the production of therapeutic agents. *Adv. Biochem. Eng. Biotechnol.*

Eibl R, Werner S, Eibl D. 2009. Bag Bioreactor Based on Wave-Induced Motion: Characteristics and Applications. *Adv. Biochem. Eng. Biotechnol.* **115**:55–87.

Estes S, Melville M. 2014. Mammalian Cell Line Developments in Speed and Efficiency. *Adv. Biochem. Eng. Biotechnol.* **139**:11–33.

Farid SS, Jenkins MJ. 2018. Chapter 44 - Bioprocesses for Cell Therapies. In: Jagschies, G, Lindskog, E, Łącki, K, Galliher, PBT-BP, editors. Elsevier, pp. 899–930. http://www.sciencedirect.com/science/article/pii/B978008100623800044X.

Feldmann H, Sprecher A, Geisbert TW. 2020. Ebola. *N. Engl. J. Med.* **382**:1832–1842. https://doi.org/10.1056/NEJMra1901594.

Fenge C, Klein C, Heuer C, Siegel U, Fraune E. 1993. Agitation, aeration and perfusion modules for cell culture bioreactors. *Cytotechnology* **11**:233–244. https://doi.org/10.1007/BF00749874.

Fernandes-Platzgummer A, Diogo MM, Lobato da Silva C, Cabral JMS. 2014.

Maximizing mouse embryonic stem cell production in a stirred tank reactor by controlling dissolved oxygen concentration and continuous perfusion operation. *Biochem. Eng. J.* **82**:81–90.

Fernandes F, Dias MM, Vidigal J, Sousa MFQ, Patrone M, Teixeira AP, Alves PM. 2014. Production of rotavirus core-like particles in Sf9 cells using recombinase-mediated cassette exchange. *J. Biotechnol.* **171**.

Fletcher MA, Hessel L, Plotkin SA. 1998. Human diploid cell strains (HDCS) viral vaccines. *Dev. Biol. Stand.* **93**:97–107.

Foreman PM, Friedman GK, Cassady KA, Markert JM. 2017. Oncolytic Virotherapy for the Treatment of Malignant Glioma. *Neurotherapeutics* **14**:333–344.

Fritz R, Sabarth N, Kiermayr S, Hohenadl C, Howard MK, Ilk R, Kistner O, Ehrlich HJ, Barrett PN, Kreil TR. 2012. A vero cell-derived whole-virus H5N1 vaccine effectively induces neuraminidase-inhibiting antibodies. *J. Infect. Dis.* **205**:28–34.

Fullerton HJ, Wintermark M, Hills NK, Dowling MM, Tan M, Rafay MF, Elkind MSV, Barkovich AJ, Deveber GA. 2016. Risk of recurrent arterial ischemic stroke in childhood: A prospective international study. *Stroke* **47**:53–59.

Galie PA, Nguyen D-HT, Choi CK, Cohen DM, Janmey PA, Chen CS. 2014. Fluid shear stress threshold regulates angiogenic sprouting. *Proc. Natl. Acad. Sci.* **111**:7968 LP – 7973. http://www.pnas.org/content/111/22/7968.abstract.

Gallo-Ramírez LE, Nikolay A, Genzel Y, Reichl U, Gallo–Ramírez LE, Nikolay A, Genzel Y, Reichl U, Gallo-Ramírez LE, Nikolay A, Genzel Y, Reichl U. 2015. Bioreactor concepts for cell culture-based viral vaccine production. *Expert Rev. Vaccines* **14**:1181–1195. https://doi.org/10.1586/14760584.2015.1067144.

Gao L, Tian M, Zhao HY, Xu QQ, Huang YM, Si QC, Tian Q, Wu QM, Hu XM, Sun LB, McClintock SM, Zeng Y. 2016a. TrkB activation by 7, 8-dihydroxyflavone increases synapse AMPA subunits and ameliorates spatial memory deficits in a mouse model of Alzheimer's disease. *J. Neurochem.* **136**:620–36.

Gao L Ben, Yu XF, Chen Q, Zhou D. 2016b. Alzheimer's disease therapeutics: Current and future therapies. *Minerva Med.* **107**:108–13.

Genzel Y. 2015. Designing cell lines for viral vaccine production: Where do we stand? *Biotechnol. J.*

George M, Farooq M, Dang T, Cortes B, Liu J, Maranga L. 2010. Production of cell culture (MDCK) derived Live Attenuated Influenza Vaccine (LAIV) in a fully

disposable platform process. *Biotechnol. Bioeng.* **106**:906–17.

Giard DJ, Aaronson SA, Todaro GJ, Arnstein P, Kersey JH, Dosik H, Parks WP. 1973. In Vitro Cultivation of Human Tumors: Establishment of Cell Lines Derived From a Series of Solid Tumors2. *JNCI J. Natl. Cancer Inst.* **51**:1417–1423. https://doi.org/10.1093/jnci/51.5.1417.

Gigout A, Buschmann M, Jolicoeur M. 2008. The fate of Pluronic F-68 in chondrocytes and CHO Cells. *Biotechnol. Bioeng.* **100**:975–987.

Godawat R, Konstantinov K, Rohani M, Warikoo V. 2015. End-to-end integrated fully continuous production of recombinant monoclonal antibodies. *J. Biotechnol.* **213**:13—19. https://doi.org/10.1016/j.jbiotec.2015.06.393.

Godoy-Silva R, Chalmers JJ, Casnocha SA, Ma N, Bass LA, Ma N. 2009. Quantitative Study of physiological responses of CHO cells to repetitive hydrodynamic stress. *Biotechnol. Bioeng.* **103**:1103–1117.

Greaves M, Kobbacy KAH. 1981. Power consumption and impeller dispersion effeciency in gas-liquid mixing. *FLUID Mix. SYMP. BRADFORD, U.K. MAR.24-26, 1981, RUGBY, U.K., INST. CHEM. ENGRS., 1981, Pap. L1, P.L1-L33. ICHEME*.

Grein T, Loewe D, Dieken H, Weidner T, Salzig D, Czermak P. 2019. Aeration and Shear Stress Are Critical Process Parameters for the Production of Oncolytic Measles. *Front. Bioeng. Biotechnol.* **7**:78.

Griffiths B, Thornton B. 1982. Use of microcarrier culture for the production of herpes simplex virus (type 2) in MRC-5 cells. *J. Chem. Technol. Biotechnol.* **32**:324–329. https://doi.org/10.1002/jctb.5030320137.

Gronemeyer P, Ditz R, Strube J. 2014. Trends in Upstream and Downstream Process Development for Antibody Manufacturing. *Bioeng. (Basel, Switzerland)* **1**:188–212.

Grubor-Bauk B, Wijesundara DK, Masavuli M, Abbink P, Peterson RL, Prow NA, Larocca RA, Mekonnen ZA, Shrestha A, Eyre NS, Beard MR, Gummow J, Carr J, Robertson SA, Hayball JD, Barouch DH, Gowans EJ. 2019. NS1 DNA vaccination protects against Zika infection through T cell–mediated immunity in immunocompetent mice. *Sci. Adv.* **5**:1–15.

Gupta SK, Dangi AK, Smita M, Dwivedi S, Shukla P. 2019. Chapter 11 - Effectual

Bioprocess Development for Protein Production. In: Shukla, PBT-AM and B, editor. *Appl. Microbiol. Bioeng.* Academic Press, pp. 203–227. http://www.sciencedirect.com/science/article/pii/B9780128154076000113.

Gurevich E V, Gurevich V V. 2014. Therapeutic potential of small molecules and engineered proteins. *Handb. Exp. Pharmacol.* **219**:1–12. https://pubmed.ncbi.nlm.nih.gov/24292822.

Gutiérrez-Granados S, Gòdia F, Cervera L. 2018. Continuous manufacturing of viral particles. *Curr. Opin. Chem. Eng.* **22**:107–114.

Hall RA, Khromykh AA. 2004. West Nile virus vaccines. *Expert Opin. Biol. Ther.* **4**:1295–305.

Hanna E, Rémuzat C, Auquier P, Toumi M. 2016. Advanced therapy medicinal products: current and future perspectives. *J. Mark. access Heal. policy* **4**:10.3402/jmahp.v4.31036. https://pubmed.ncbi.nlm.nih.gov/27123193.

Heath C, Kiss R. 2007. Cell Culture Process Development: Advances in Process Engineering. *Biotechnol. Prog.* **23**:46–51. https://doi.org/10.1021/bp060344e.

Hegde R, Gomes AR, Muniyellappa HK, Sonnahallipura B, Giridhar P, Renukaprasad C. 2009. A short note on peste des petits ruminants in Karnata, India. *Rev. Sci. Tech.* **28**:1031–1035.

Hong MS, Severson KA, Jiang M, Lu AE, Love JC, Braatz RD. 2018. Challenges and opportunities in biopharmaceutical manufacturing control. *Comput. Chem. Eng.* **110**:106–114.

Hu W, Berdugo C, Chalmers JJ. 2011. The potential of hydrodynamic damage to animal cells of industrial relevance: current understanding. *Cytotechnology* **63**:445–460. https://pubmed.ncbi.nlm.nih.gov/21785843.

Hunter M, Yuan P, Vavilala D, Fox M. 2019. Optimization of Protein Expression in Mammalian Cells. *Curr. Protoc. Protein Sci.* **95**:e77. https://doi.org/10.1002/cpps.77.

Ibrahim S, Nienow AW. 2004. Suspension of microcarriers for cell culture with axial flow impellers. *Chem. Eng. Res. Des.* **82**:1082–1088. https://www.sciencedirect.com/science/article/pii/S0263876204725940.

Jagannathan S, Rajendran V, Kuruba B, kukkaler channappa SK, Pachamuthu R, Mani K. 2015. Formulation, Efficacy and Immunogenicity Studies of a Liquid State Rabies Vaccine with Magnesium Chloride as Stabilizer. *J. Vaccines Vaccin.* **6**:1–

4.

Jiang B, Barniak V, Smith RP, Sharma R, Corsaro B, Hu B, Madore HP. 1998. Synthesis of rotavirus-like particles in insect cells: comparative and quantitative analysis. *Biotechnol. Bioeng.* **60**:369–374.

Jordan I, Sandig V. 2014. Matrix and backstage: cellular substrates for viral vaccines. *Viruses* **6**:1672–1700. https://pubmed.ncbi.nlm.nih.gov/24732259.

Jordan M, Mac Kinnon N, Monchois V, Stettler M, Broly H. 2018. Intensification of large-scale cell culture processes. *Curr. Opin. Chem. Eng.* **22**:253–257.

Junker BH, Seamans TC, Ramasubramanyan K, Aunins J, Paul E, Buckland BC. 1994. Cultivation of attenuated hepatitis A virus antigen in a titanium static mixer reactor. *Biotechnol. Bioeng.* **44**:1315–1324. https://doi.org/10.1002/bit.260441107.

Kadoglou NPE, Parissis J, Seferovic P, Filippatos G. 2018. Vaccination in Heart Failure: An Approach to Improve Outcomes. *Rev. Esp. Cardiol.* **71**:697–699.

Kaiser SC, Loffelholz C, Werner SS, Eibl D, Kaiser S, Löffelholz C, Werner SS, Eibl D, C. S, Loffelholz C, Werner SS, Eibl D. 2011. CFD for Characterizing Standard and Single-use Stirred Cell Culture Bioreactors. In: . *Comput. Fluid Dyn. Technol. Appl.*, pp. 97–122.

Kamen A, Henry O. 2004. Development and optimization of an adenovirus production process. *J. Gene Med.* **6**:S184-92.

Karst D, Steinebach F, Morbidelli M. 2017. Continuous integrated manufacturing of therapeutic proteins. *Curr. Opin. Biotechnol.* **53**:76–84.

Keane JT, Ryan D, Gray PP. 2003. Effect of shear stress on expression of a recombinant protein by Chinese hamster ovary cells. *Biotechnol. Bioeng.* **81**:211–220. https://doi.org/10.1002/bit.10472.

Kern S, Platas-Barradas O, Pörtner R, Frahm B. 2016. Model-based strategy for cell culture seed train layout verified at lab scale. *Cytotechnology* **68**:1019–1032. https://pubmed.ncbi.nlm.nih.gov/25795469.

Kesik-Brodacka M. 2018. Progress in biopharmaceutical development. *Biotechnol. Appl. Biochem.* **65**:306–322.

Kost TA, Kemp CW. 2016. Fundamentals of baculovirus expression and applications. *Adv. Exp. Med. Biol.* **896**:187–197.

Kovesdi I, Hedley SJ. 2010. Adenoviral producer cells. *Viruses* **2**:1681–703.

Kropp C, Kempf H, Halloin C, Robles-Diaz D, Franke A, Scheper T, Kinast K, Knorpp T, Joos TO, Haverich A, Martin U, Zweigerdt R, Olmer R. 2016. Impact of Feeding Strategies on the Scalable Expansion of Human Pluripotent Stem Cells in Single-Use Stirred Tank Bioreactors. *Stem Cells Transl. Med.* **5**:1289–1301.

Kunert R, Reinhart D. 2016. Advances in recombinant antibody manufacturing. *Appl. Microbiol. Biotechnol.* **100**:3451–3461. https://pubmed.ncbi.nlm.nih.gov/26936774.

Landry ML, Fong CKY, Neddermann K, Solomon L, Hsiung GD. 1987. Disseminated adenovirus infection in an immunocompromised host. Pitfalls in diagnosis. *Am. J. Med.* **83**:555–9.

Latham T, Galarza JM. 2001. Formation of wild-type and chimeric influenza virus-like particles following simultaneous expression of only four structural proteins. *J. Virol.* **75**:6154–6165.

Léon A, David AL, Madeline B, Guianvarc'h L, Dureau E, Champion-Arnaud P, Hebben M, Huss T, Chatrenet B, Schwamborn K. 2016. The EB66® cell line as a valuable cell substrate for MVA-based vaccines production. *Vaccine* **34**:5878–5885.

Levenbook IS, Petricciani JC, Elisberg BL. 1984. Tumorigenicity of Vero cells. *J. Biol. Stand.* **12**:391–398.

Li X, Scott K, Kelly WJ, Huang Z. 2018. Development of a Computational Fluid Dynamics Model for Scaling-up Ambr Bioreactors. *Biotechnol. Bioprocess Eng.* **23**:710–725.

Liao J, Wei Q, Fan J, Zou Y, Song D, Liu J, Liu F, Ma C, Hu X, Li L, Yu Y, Qu X, Chen L, Yu X, Zhang Z, Zhao C, Zeng Z, Zhang R, Yan S, Wu T, Wu X, Shu Y, Lei J, Li Y, Zhang W, Wang J, Reid RR, Lee MJ, Huang W, Wolf JM, He TC, Wang J. 2017. Characterization of retroviral infectivity and superinfection resistance during retrovirus-mediated transduction of mammalian cells. *Gene Ther.* **24**:333–341.

Lieber M, Todaro G, Smith B, Szakal A, Nelson-Rees W. 1976. A continuous tumor-cell line from a human lung carcinoma with properties of type II alveolar epithelial cells. *Int. J. Cancer* **17**:62–70.

Löffelholz C, Husemann U, Greller G, Meusel W, Kauling J, Ay P, Kraume M, Eibl R,

Eibl D. 2013. Bioengineering parameters for single-use bioreactors: Overview and evaluation of suitable methods. *Chemie-Ingenieur-Technik* **85**:40–56.

Lohr V, Hädicke O, Genzel Y, Jordan I, Büntemeyer H, Klamt S, Reichl U. 2014. The avian cell line AGE1.CR.pIX characterized by metabolic flux analysis. *BMC Biotechnol.* **14**:72. https://pubmed.ncbi.nlm.nih.gov/25077436.

Long G. 2017. The Biopharmaceutical Pipeline: Innovative Therapies in Clinical Development:1–36.

van der Loo JCM, Wright JF. 2016. Progress and challenges in viral vector manufacturing. *Hum. Mol. Genet.* **25**:R42-52.

Mak AT-C. 1992. Solid–liquid mixing In Mechanically Agitated Vessels. *Thesis Dr. Philos. Univ. London*.

McKenzie EA, Abbott WM. 2018. Expression of recombinant proteins in insect and mammalian cells. *Methods* **147**:40–49.

McPherson C. 2008. Development of a novel recombinant influenza vaccine in insect cells. *Biologicals* **36**:350–353.

Merten O-W. 2015. Advances in cell culture: anchorage dependence. *Philos. Trans. R. Soc. B Biol. Sci.* **370**:20140040. https://doi.org/10.1098/rstb.2014.0040.

Merten O-W, Schweizer M, Chahal P, Kamen AA. 2014. Manufacturing of viral vectors for gene therapy: part I. Upstream processing. *Pharm. Bioprocess.* **2**:183–203.

Mitragotri S, Burke PA, Langer R. 2014. Overcoming the challenges in administering biopharmaceuticals: Formulation and delivery strategies. *Nat. Rev. Drug Discov.* **13**:655–672.

Montagnon BJ. 1989. Polio and rabies vaccines produced in continuous cell lines: a reality for Vero cell line. *Dev. Biol. Stand.* **70**:27–47.

Montagnon B, Vincent-Falquet JC, Fanget B. 1983. Thousand litre scale microcarrier culture of vero cells for killed polio virus vaccine. *Dev Biol Stand* **55**:37–42.

Moreira AS, Silva AC, Sousa MFQ, Hagner-McWhirterc Å, Ahlénc G, Lundgren M, Coroadinha AS, Alves PM, Peixoto C, Carrondo MJT. 2020. Establishing Suspension Cell Cultures for Improved Manufacturing of Oncolytic Adenovirus. *Biotechnol. J.* **15**:1900411.

Nagata S. 1975. Mixing. Principles and applications.

Nienow AW, Coopman K, Heathman TRJ, Rafiq QA, Hewitt CJ. 2016a. Bioreactor Engineering Fundamentals for Stem Cell Manufacturing. In: . *Stem Cell Manuf.*

Nienow AW. 2006. Reactor engineering in large scale animal cell culture. *Cytotechnology* **50**:9–33. https://pubmed.ncbi.nlm.nih.gov/19003068.

Nienow AW, Hewitt CJ, Heathman TRJ, Glyn VAM, Fonte GNGN, Hanga MP, Coopman K, Rafiq QA. 2016b. Agitation conditions for the culture and detachment of hMSCs from microcarriers in multiple bioreactor platforms. *Biochem. Eng. J.* **108**:24–29. https://www.sciencedirect.com/science/article/pii/S1369703X15300309.

Nikolay A, Léon A, Schwamborn K, Genzel Y, Reichl U. 2018. Process intensification of EB66® cell cultivations leads to high-yield yellow fever and Zika virus production. *Appl. Microbiol. Biotechnol.* **102**:8725–8737.

Nogales A, Dediego ML. 2020. Influenza virus and vaccination. *Pathogens* **9**:220.

O'Donnell K, Marzi A. 2020. The Ebola virus glycoprotein and its immune responses across multiple vaccine platforms. *Expert Rev. Vaccines* **19**:267–277.

Obom KM, Cummings PJ, Ciafardoni JA, Hashimura Y, Giroux D. 2014. Cultivation of Mammalian Cells Using a Single-use Pneumatic Bioreactor System. *JoVE*:e52008. https://www.jove.com/t/52008.

Owczarek B, Gerszberg A, Hnatuszko-Konka K. 2019. A Brief Reminder of Systems of Production and Chromatography-Based Recovery of Recombinant Protein Biopharmaceuticals. Ed. Fabiano J Contesini. *Biomed Res. Int.* **8**:4216060. https://doi.org/10.1155/2019/4216060.

Ozturk SS. 1996. Engineering challenges in high density cell culture systems. *Cytotechnology* **22**:3–16. https://doi.org/10.1007/BF00353919.

Panchalingam KM, Jung S, Rosenberg L, Behie LA. 2015. Bioprocessing strategies for the large-scale production of human mesenchymal stem cells: A review Mesenchymal Stem/Stromal Cells - An update. *Stem Cell Res. Ther.* **23**:225.

Parida S, Muniraju M, Mahapatra M, Muthuchelvan D, Buczkowski H, Banyard AC. 2015. Peste des petits ruminants. *Vet. Microbiol.* **181**:90–106.

Patil R, Walther J. 2018. Continuous Manufacturing of Recombinant Therapeutic Proteins: Upstream and Downstream Technologies. *Adv. Biochem. Eng. Biotechnol.* **165**:277–322.

Pau MG, Ophorst C, Koldijk M, Schouten G, Mehtali M, Uytdehaag F. 2001. The

human cell line PER.C6 provides a new manufacturing system for the production of influenza vaccines. *Vaccine* **19**:2716–2721.

Pejsak Z, Mokrzycka A, Lipowski A. 2000. The results of serological monitoring for Aujeszky's disease in pigs performed during the period of 1991-1997. *Vet. Res.* **31**:156–157. https://doi.org/10.1051/vetres:2000040.

Pereira S, Kildegaard H, Andersen M. 2018. Impact of CHO Metabolism on Cell Growth and Protein Production: An Overview of Toxic and Inhibiting Metabolites and Nutrients. *Biotechnol. J.* **13**:1700499.

Petiot E, El-Wajgali A, Esteban G, Gény C, Pinton H, Marc A. 2012. Real-time monitoring of adherent Vero cell density and apoptosis in bioreactor processes. *Cytotechnology* **64**:429–441.

Pezzoli D, Giupponi E, Mantovani D, Candiani G. 2017. Size matters for in vitro gene delivery: Investigating the relationships among complexation protocol, transfection medium, size and sedimentation. *Sci. Rep.* **7**:1–11.

PharmaProjects, Pharma intelligence I. 2019. Pharma R&D Annual Review for 2019:1–32.

Pinto RC V, Medronho RA, Castilho LR. 2008. Separation of CHO cells using hydrocyclones. *Cytotechnology* **56**:57–67. https://pubmed.ncbi.nlm.nih.gov/19002842.

Placek J, Tavlarides LL. 1985. Turbulent flow in stirred tanks. Part I: Turbulent flow in the turbine impeller region. *AIChE J.* **31**:1113–1120.

Pörtner R, Barradas OBJ. 2007. Cultivation of Mammalian Cells in Fixed-Bed Reactors. In: . *Methods Biotechnol.*, pp. 353–369.

Pörtner R, Kern S, Eibl D. 2015. Decision tree for selection of suitable cultivation parameters for mammalian cell culture processes. *BMC Proc.* **9**:P45. https://doi.org/10.1186/1753-6561-9-S9-P45.

Puetz J, Wurm FM. 2019. Recombinant Proteins for Industrial versus Pharmaceutical Purposes: A Review of Process and Pricing. *Processes* **7**:476.

Rafiq QA, Ruck S, Hanga MP, Heathman TRJ, Coopman K, Nienow AW, Williams DJ, Hewitt CJ. 2018. Qualitative and quantitative demonstration of bead-to-bead transfer with bone marrow-derived human mesenchymal stem cells on microcarriers: Utilising the phenomenon to improve culture performance.

Biochem. Eng. J. **135**:11–21.

Rahman A-U-, Dhama K, Ali Q, Hussain I, Oneeb M, Chaudhary U, Wensman JJ, Shabbir MZ. 2020. Peste des petits ruminants in large ruminants, camels and unusual hosts. *Vet. Q.* **40**:35–42. https://pubmed.ncbi.nlm.nih.gov/31917649.

Raja J, Ludwig JM, Gettinger SN, Schalper KA, Kim HS. 2018. Oncolytic virus immunotherapy: future prospects for oncology. *J. Immunother. Cancer* **6**:140.

Rathore A, Agarwal H, Sharma AK, Pathak M, Kumar M. 2015. Continuous Processing for Production of Biopharmaceuticals. *Prep. Biochem. Biotechnol.* **45**:836–849.

Rauch S, Jasny E, Schmidt KE, Petsch B. 2018. New vaccine technologies to combat outbreak situations. *Front. Immunol.* **9**:1963.

Roberts JP. 2019. Single-Use Technology: Enjoy the Upsides, Handle the Downsides. *Genet. Eng. Biotechnol. News* **39**:S8, S10–S11. https://doi.org/10.1089/gen.39.S3.03.

Rodrigues C, Fernandes T, Diogo M, Silva C, Cabral J. 2011. Stem cell cultivation in bioreactors. *Biotechnol. Adv.* **29**:815–829.

Rodrigues ME, Costa AR, Henriques M, Azeredo J, Oliveira R. 2012. Wave characterization for mammalian cell culture: residence time distribution. *N. Biotechnol.* **29**:402–408.

Roeder P, Mariner J, Kock R. 2013. Rinderpest: The veterinary perspective on eradication. *Philos. Trans. R. Soc. B Biol. Sci.* **368**:20120139.

Roldão A, Silva AC, Mellado MCM, Alves PM, Carrondo MJT. 2011. Viruses and Virus-Like Particles in Biotechnology: Fundamentals and Applications. *Compr. Biotechnol. Second Ed.* **10**:625–649.

Roldão A, Cox M, Alves P, Carrondo M, Vicente T. 2014. Industrial Large Scale of Suspension Culture of Insect Cells. In: . *Ind. Scale Suspens. Cult. Living Cells*, pp. 348–389.

Roth JA. 2011. Veterinary Vaccines and Their Importance to Animal Health and Public Health. *Procedia Vaccinol.* **5**:127–136.

Rourou S, van der Ark A, van der Velden T, Kallel H. 2007. A microcarrier cell culture process for propagating rabies virus in Vero cells grown in a stirred bioreactor under fully animal component free conditions. *Vaccine* **25**:3879–3889.

Rupprecht CE, Hanlon CA, Slate D. 2005. Oral vaccination of wildlife against rabies:

Opportunities and challenges in prevention and control. In: . *Dev. Biol. (Basel).*, Vol. 119, pp. 173–184.

Russell SJ, Peng KW, Bell JC. 2012. Oncolytic virotherapy. *Nat. Biotechnol.* **30**:658–670.

Sanchez-Garcia L, Martín L, Mangues R, Ferrer-Miralles N, Vázquez E, Villaverde A. 2016. Recombinant pharmaceuticals from microbial cells: a 2015 update. *Microb. Cell Fact.* **15**:33. https://doi.org/10.1186/s12934-016-0437-3.

Sandle T, Saghee MR. 2011. Some considerations for the implementation of disposable technology and single-use systems in biopharmaceuticals. *J. Commer. Biotechnol.* **17**:319–329. https://doi.org/10.1057/jcb.2011.21.

Sandner V, Pybus LP, McCreath G, Glassey J. 2019. Scale-Down Model Development in ambr systems: An Industrial Perspective. *Biotechnol. J.* **14**:e1700766. https://doi.org/10.1002/biot.201700766.

Sato-Dahlman M, Yamamoto M. 2017. The Development of Oncoltyic Adenovirus Therapy in the Past and Future - For the Case of Pancreatic Cancer. *Curr. Cancer Drug Targets* **18**:153–161.

Schaepe S, Kuprijanov A, Sieblist C, Jenzsch M, Simutis R, Lübbert A. 2013. Biochemical Engineering/Bioprocess Engineering kLa of stirred tank bioreactors revisited. *J. Biotechnol.* **168**:576–583.

Scherpereel A, Wallyn F, Albelda SM, Munck C. 2018. Novel therapies for malignant pleural mesothelioma. *Lancet Oncol.* **19**:e161–e172.

Sequeira DP, Correia R, Carrondo MJT, Roldão A, Teixeira AP, Alves PM. 2018. Combining stable insect cell lines with baculovirus-mediated expression for multi-HA influenza VLP production. *Vaccine* **36**:3112–3123. https://linkinghub.elsevier.com/retrieve/pii/S0264410X17302463.

Serra M, Cunha B, Peixoto C, Gomes-Alves P, Alves P. 2018. Advancing manufacture of human mesenchymal stem cells therapies: technological challenges in cell bioprocessing and characterization. *Curr. Opin. Chem. Eng.* **22**:226–235.

Seth G, Hamilton RW, Stapp TR, Zheng L, Meier A, Petty K, Leung S, Chary S. 2013. Development of a new bioprocess scheme using frozen seed train intermediates to initiate CHO cell culture manufacturing campaigns. *Biotechnol.*

Bioeng. **110**:1376–1385.

Shao W, Li X, Goraya MU, Wang S, Chen JL. 2017. Evolution of influenza a virus by mutation and re-assortment. *Int. J. Mol. Sci.* **18**:4650.

Shen CF, Guilbault C, Li X, Elahi SM, Ansorge S, Kamen A, Gilbert R. 2019. Development of suspension adapted Vero cell culture process technology for production of viral vaccines. *Vaccine* **37**:6996–7002. http://www.sciencedirect.com/science/article/pii/S0264410X19308813.

Shevitz J, LaPorte TL, Stinnett TE. 1990. Production of viral vaccines in stirred bioreactors. *Adv. Biotechnol. Processes* **14**:1–35.

Sidorenko ES, Dorofeeva L V., Kaptsova TI, Steinberg LL, Zasorina IN, Sinitsyna OA, Boriskin YS. 1989. Experimental-scale measles and mumps vaccine production on microcarrier-grown cells. *Vaccine* **7**:554–556.

Silva AC, Delgado I, Sousa MFQQ, Carrondo MJTT, Alves PM. 2008. Scalable culture systems using different cell lines for the production of Peste des Petits ruminants vaccine. *Vaccine* **26**:3305–3311.

Silva AC, Roldão A, Teixeira A, Fernandes P, Sousa MFQ, Alves PM. 2015. Cell Immobilization for the Production of Viral Vaccines. In: . *Monit. Cell Cult.*, pp. 541–563.

Simaria AS, Hassan S, Varadaraju H, Rowley J, Warren K, Vanek P, Farid SS. 2014. Allogeneic cell therapy bioprocess economics and optimization: Single-use cell expansion technologies. *Biotechnol. Bioeng.* **111**:69–83.

Singh RK, K R, Dhanavelu M, Banyard A, Parida S. 2015. Vaccines Against Peste des Petits Ruminants Virus. *Peste Des Petits Ruminants Virus*:183–194.

Singh V. 1999. Disposable bioreactor for cell culture using wave-induced agitation. *Cytotechnology* **30**:149–158.

Sohail S, Jaiswal P. 2018. Biopharmaceuticals Market By Type (Monoclonal Antibody, Interferon, Insulin, Growth & Coagulation Factor, Erythropoietin, Vaccine, Hormone, and, Others) and Application (Oncology, Blood Disorder, Metabolic Disease, Infectious Disease, Cardiovascular Disea:1–255.

Southgate T, Kroeger KM, Liu C, Lowenstein PR, Castro MG. 2008. Gene transfer into neural cells In vitro using adenoviral vectors. *Curr. Protoc. Neurosci.* **4**.

Strohl WR, Strohl LMBT-TAE eds. 2012. 18 - Cell line development. In: . *Woodhead Publ. Ser. Biomed.* Woodhead Publishing, pp. 421–595.

http://www.sciencedirect.com/science/article/pii/B978190756837450018X.

Sugiki T, Fujiwara T, Kojima C. 2014. Latest approaches for efficient protein production in drug discovery. *Expert Opin. Drug Discov.* **9**:1189–204.

Talò G, Turrisi C, Arrigoni C, Recordati C, Gerges I, Tamplenizza M, Cappelluti A, Riboldi SA, Moretti M. 2018. Industrialization of a perfusion bioreactor: Prime example of a non-straightforward process. *J. Tissue Eng. Regen. Med.* **12**:405–415.

Tang H, Hammack C, Ogden SC, Wen Z, Qian X, Li Y, Yao B, Shin J, Zhang F, Lee EM, Christian KM, Didier RA, Jin P, Song H, Ming GL. 2016. Zika virus infects human cortical neural progenitors and attenuates their growth. *Cell Stem Cell* **18**:587–590.

Tanzeglock T, Soos M, Stephanopoulos G, Morbidelli M. 2009. Induction of Mammalian Cell Death by Simple Shear and Extensional Flows. *Biotechnol. Bioeng.* **104**:360–370.

Tapia F, Vázquez-Ramírez D, Genzel Y, Reichl U. 2016. Bioreactors for high cell density and continuous multi-stage cultivations: options for process intensification in cell culture-based viral vaccine production. *Appl. Microbiol. Biotechnol.* **100**:2121–2132.

Teixeira AP, Oliveira R, Alves PM, Carrondo MJT. 2009. Advances in on-line monitoring and control of mammalian cell cultures: Supporting the PAT initiative. *Biotechnol. Adv.* **27**:726–732.

Tescione L, Lambropoulos J, Paranandi MR, Makagiansar H, Ryll T. 2015. Application of bioreactor design principles and multivariate analysis for development of cell culture scale down models. *Biotechnol. Bioeng.* **112**:84–97.

Thomas S, Prendergast GC. 2016. Cancer vaccines: A brief overview. *Methods Mol. Biol.* **1403**:755–61.

Tripathi NK, Shrivastava A. 2019. Recent Developments in Bioprocessing of Recombinant Proteins: Expression Hosts and Process Development. *Front. Bioeng. Biotechnol.* **7**:420. https://pubmed.ncbi.nlm.nih.gov/31921823.

Trujillo-Roldán MA, Valdez-Cruz NA. 2006. Hydrodynamic stress: Death and cellular damage in agitated cultures. *Rev. Latinoam. Microbiol.* **48**:269–80.

Urabe M, Ding C, Kotin RM. 2002. Insect cells as a factory to produce adeno-

associated virus type 2 vectors. *Hum. Gene Ther.* **13**:1935–1943.

Venereo-Sanchez A, Simoneau M, Lanthier S, Chahal P, Bourget L, Ansorge S, Gilbert R, Henry O, Kamen A. 2017. Process intensification for high yield production of influenza H1N1 Gag virus-like particles using an inducible HEK-293 stable cell line. *Vaccine* **35**:4220–4228.

Verikios G. 2020. The dynamic effects of infectious disease outbreaks: The case of pandemic influenza and human coronavirus. *Socioecon. Plann. Sci.* **71**:100898.

Vicente T, Peixoto C, Carrondo MJT, Alves PM. 2009. Purification of recombinant baculoviruses for gene therapy using membrane processes. *Gene Ther.* **16**:766–775. https://doi.org/10.1038/gt.2009.33.

Vogel OA, Manicassamy B. 2020. Broadly Protective Strategies Against Influenza Viruses: Universal Vaccines and Therapeutics. *Front. Microbiol.* **11**:135.

Voisard D, Meuwly F, Ruffieux P-A, Baer G, Kadouri A. 2003. Potential of cell retention techniques for large-scale high-density perfusion culture of suspended mammalian cells. *Biotechnol. Bioeng.* **82**:751–765. https://doi.org/10.1002/bit.10629.

Walsh G. 2018. Biopharmaceutical benchmarks 2018. *Nat. Biotechnol.* **36**:1136–1145.

Wang P, Zhu S, Yuan C, Wang L, Xu J, Liu Z. 2018. Shear stress promotes differentiation of stem cells from human exfoliated deciduous teeth into endothelial cells via the downstream pathway of VEGF-Notch signaling. *Int. J. Mol. Med.* **42**:1827–1836.

Wang Y, Ouyang F. 1999. Bead-to-bead transfer of Vero cells in microcarrier culture. *Cytotechnology* **31**:221–4.

Warnock JN, Bratch K, Al-Rubeai M. 2005. Packed bed bioreactors. In: . *Bioreact. Tissue Eng. Princ. Des. Oper.*, pp. 87–113.

Warnock J, Merten O-W, Al-Rubeai M. 2006. Cell Culture Processes for the Production of Viral Vectors for Gene Therapy Purposes. *Cytotechnology* **50**:141–162.

Wei Y, Sun X, Wang W, Hu Y. 2007. Adipose-derived stem cells and chondrogenesis. *Cytotherapy* **9**:712–716.

Van Wezel AL. 1967. Growth of Cell-strains and Primary Cells on Micro-carriers in Homogeneous Culture. *Nature* **216**:64–65. https://doi.org/10.1038/216064a0.

Wölfel J, Essers R, Bialek C, Hertel S, Scholz-Neumann N, Schiedner G. 2011. CAP-T cell expression system: a novel rapid and versatile human cell expression system for fast and high yield transient protein expression. *BMC Proc.* **5**:133.

Woodgate JM. 2018. Perfusion N-1 Culture-Opportunities for Process Intensification. In: . *Biopharm. Process. Dev. Des. Implement. Manuf. Process.*, pp. 755–768.

Wright B, Bruninghaus M, Vrabel M, Walther J, Shah N, Bae S-A, Johnson T, Yin J, Zhou W, Konstantinov K. 2015. A novel seed-train process: Using high-density cell banking, a disposable bioreactor, and perfusion technologies. *Bioprocess Int.* **13**.

Xu J, Rehmann MS, Xu M, Zheng S, Hill C, He Q, Borys MC, Li ZJ. 2020. Development of an intensified fed-batch production platform with doubled titers using N-1 perfusion seed for cell culture manufacturing. *Bioresour. Bioprocess.* **7**:17. https://doi.org/10.1186/s40643-020-00304-y.

Yang WC, Lu J, Kwiatkowski C, Yuan H, Kshirsagar R, Ryll T, Huang YM. 2014. Perfusion seed cultures improve biopharmaceutical fed-batch production capacity and product quality. *Biotechnol. Prog.* **30**:616–25.

Yao T, Asayama Y. 2017. Animal-cell culture media: History, characteristics, and current issues. *Reprod. Med. Biol.* **16**:99–117.

Zhao H, Shao L, Chen JF. 2010. High-gravity process intensification technology and application. *Chem. Eng. J.* **156**:588–593.

Chapter 2

Rapid Manufacturing Platform for hrBMX Protein Production

This chapter is adapted from:

Bárbara B. Sousa, **Marcos F. Q. de Sousa**, Marta C. Marques, João D. Seixas, José A. Brito, Pedro M. Matias, Gonçalo J. L. Bernardes and António Roldão, 2020. A scalable insect cell-based production process of the human recombinant BMX for in-vitro covalent ligand high-throughput screening. Bioprocess and Biosystems Engineering: https://doi.org/10.1007/s0044 9-020-02421-6

Author's contribution to the chapter:

Marcos F. Q. de Sousa and Bárbara Sousa participated equally on the experimental setup, design and performed the experiments and analyzed the data. **Marcos F. Q. de Sousa** wrote the chapter.

CONTENTS

SUMMARY

Bone Marrow Tyrosine kinase on the chromosome X (BMX) is a tyrosine kinase expressed in hepatocellular carcinoma (TEC) family kinase associated with numerous pathological pathways in cancer cells. Covalent inhibition of BMX activity holds promise as a therapeutic approach against cancer. To screen for potent and selective covalent BMX inhibitors, large quantities of highly pure BMX are normally required which is challenging with the currently available production and purification processes. Here, we developed a scalable production process for human recombinant BMX (hrBMX) using the insect cells-baculovirus expression system (IC-BEVS). Comparable expression levels were obtained in small-scale shake flasks (15 mL) and stirred-tank bioreactor (STB) (5 L). A 2-step chromatographic-based process was implemented, reducing purification times by 75 % when compared to traditional processes, while maintaining hrBMX stability. The final production yield was 24 mg of purified hrBMX per liter of cell culture, with a purity of > 99 %. Product quality was assessed and confirmed through a series of biochemical and biophysical assays, including circular dichroism and dynamic light scattering. Overall, the platform herein developed was capable of generating more than 120 mg purified hrBMX from 5 L STB in just 34 days, thus having potential to assist in-vitro covalent ligand high-throughput screening for BMX activity inhibition.

Key Words: hrBMX production, IC-BEVS, bioprocess development, hrBMX crystallization, cancer therapy

1. INTRODUCTION

Bone Marrow Tyrosine kinase on the chromosome X (BMX) is member of tyrosine kinase expressed in hepatocellular carcinoma (TEC) family of non-receptor kinases (Tamagnone et al., 1994) and plays an important role in a variety of critical physiological and pathological processes, including tumorigenicity, cells motility, adhesion, angiogenesis, proliferation, and differentiation (Dai et al., 2010; Fox and Storey, 2015; Jiang et al., 2004; von Manstein et al., 2013; Zhang et al., 2003). Its involvement and integration in multiple and diverse cellular signaling pathways, has listed BMX as a potential therapeutic target for anti-cancer therapies, particularly for prostate cancer (Dai et al., 2010). Compounds with selectivity against BMX are desirable, since they offer pharmacological advantages including selectivity for cancer cells and thus fewer side effects (Jarboe et al., 2013; Rajantie et al., 2001).

The insect cells-baculovirus expression system (IC-BEVS) is a well-established platform for the production of human recombinant proteins, including the TEC family kinases (Miller, 1997). IC-BEVS has the advantage of being scalable, often resulting in short production times and high production yields (van Oers et al., 2015). Noteworthy, proteins expressed in insect cells can undergo post-translational modifications contrarily to other expression systems such as *E. coli* (Khow and Suntrarachun, 2012). Protein expression in IC-BEVS is commonly optimized by manipulating three key parameters, the multiplicity of infection (MOI), cell concentration at infection (CCI) and time of harvesting (TOH) (Maranga et al., 2003). Purification of insect cells-derived proteins is challenging and should be carried in the minimum possible number of steps, increasing product recovery yields. Besides, recombinant protein expression can be engineered to contain affinity tags for chromatographic purification (e.g. N- or C-terminal HIS-tag)

from their biological source; and for intracellularly expressed proteins, such as human recombinant BMX (hrBMX) (Muckelbauer et al., 2011), additional efficient cell-lysis and protein extraction methods should also be included (Wingfield, 2015). Assisting process development and optimization, in particular, when the produced proteins are to be used in biophysical and structural studies (e.g., thermal shift assay, surface plasmon resonance, and X-crystallography), it is essential to ensure protein sample quality and homogeneity. For this reason, it is crucial to perform a combination of complementary analytical methods, namely: SDS-PAGE, Western blot (WB), Dynamic light scattering (DLS), and Circular dichroism (CD) (Borgstahl, 2007; Kelly et al., 2005; Miles and Wallace, 2014).

In this study, we describe (i) the optimal bioprocess conditions to produce hrBMX using IC-BEVS and stirred-tank bioreactor, and (ii) the implementation of a 2-step chromatography-based strategy for the efficient purification of hrBMX. Homogeneity and chemical purity of purified hrBMX were confirmed by SDS-PAGE, WB, DLS and CD, meeting the standard for use in subsequent biophysical and structural studies.

2. MATERIALS AND METHODS

2.1. Cell culture conditions

Spodoptera frugiperda derived Sf-9 cells (89070101, ECCAC, UK) were routinely cultivated in shake flasks every 3-4 days in SF900II SFM (Gibco, USA) at 27 °C and 100 rpm. Cell concentration, viability and size were estimated using Cedex HiRes Analyser (Roche Diagnostic, Germany).

2.2. Generation of recombinant baculovirus

The human recombinant Bone Marrow Tyrosine kinase on the chromosome

X (hrBMX) gene was synthesized and assembled into pFastBac™ plasmid (Invitrogen, USA) as described elsewhere (Muckelbauer et al., 2011). The correct transposition of the target BMX gene sequence was analyzed by PCR, using primers specifically designed for the coding region of hrBMX catalytic domain 5′-GAGAACCTGTACTTCCAAGGC-3′ and 5′-TGTGGGCGGACAAAATAGTTG-3′. PCR product was evaluated by 1 % agarose gel. Sf-9 cells were transfected with the recombinant bacmid using Cellfectin™ II reagent and Bac-to-Bac® Expression System (according to manufacturer instructions, Invitrogen, USA) for the generation of P0 recombinant baculovirus (rBAC). The ensuing rBac were sequentially amplified twice for the generation of master virus stock P1 and P2 (Ciccarone et al., 1998). In both amplifications, rBac stocks were harvested when cell viability was approximately 80 % (corresponding to 96 h post-infection, hpi), and clarified by centrifugation (2 000 xg, 10 min). Stocks were titrated by cell growth cessation assay and MTT (3-(4,5-Dimethylthiazol-2-yl)-2,5-diphenyltetrazolium bromidefor) methods, as described in Roldão et al., 2009 (Roldão et al., 2009).

2.3. Production of hrBMX in small-scale shake flasks

To determine the best conditions for hrBMX production, Sf-9 cells were infected at $1x10^6$ cell/mL in shake flasks (15 mL working volume), using multiplicity of infection (MOI) of 0.001, 0.01, 0.1 and 1 plate forming unit (pfu)/cell. Cultures were maintained until cell viability dropped below 50 %. Samples were taken daily to assess cell growth and production kinetics.

2.4. Production of hrBMX in stirred-tank bioreactors

The production of hrBMX was performed in a 5 L working volume stirred/tank bioreactor (STB) (Sartorius Stedim Biotech, Germany). The dissolved oxygen parameter was controlled at 30 % automatically varying agitation rate

(60-210 rpm) corresponding to Kolmogorov eddy size and shear stress rate of 63-25 μm and 0.2-0.9 N/m^2, respectively. The temperature was set at 27 ºC. Cells were seeded at a concentration of $0.6x10^6$ cell/mL, allowed to grow up to $1.0x10^6$ cell/mL and infected with MOI of 0.01 pfu/cell. The culture was harvested at 72 hours post-infection (hpi), when cell viability reached 80 %. Harvested bulk was centrifuged at 500 xg, for 15 min at 4 ºC, and the cell pellet resuspended in five volumes of cold lysis buffer. Cells were disrupted by 3 consecutive cycles at 500 MPa using a high-pressure homogenizer (Avestin, Canada). The lysate was clarified by ultracentrifugation at 30 000 xg, for 30 min at 4 ºC. The purification of the 6His-BMX protein (32.5 kDa) was carried out by loading the clarified lysate onto HisTrap™ FF column (GE Healthcare Life Sciences, Sweden). Peak fractions were pooled and injected onto a HiLoad™ 10/300 Superdex™ 75 column (GE Healthcare Life Sciences, Sweden). Collected fractions were concentrated to 10 mg/mL and stored at -80 ºC. Buffer formulations were adapted from Muckelbauer et al., 2011 (Muckelbauer et al., 2011), with TRIS-base being used instead of HEPES. All purification steps were run at 4 ºC.

2.5. Analytical methods

2.5.1. Conventional SDS-PAGE gel and Mn^{2+}-Phos-tag™ SDS-PAGE

The electrophoresis was carried out according to Laemmli's method (Laemmli, 1970) and Kinoshita et al., 2006 (Kinoshita et al., 2006). Gels consisted of 4.5 % stacking and 12 % separating gel. Capturing of hrBMX phosphorylation was conducted in normal SDS-PAGE gel by adding 50 μM of the Phos-tag™ ligand (FUJIFILM, Japan) and 1 mM of $MnCl_2$. Protein bands were visualized by Coomassie blue staining. Protein band intensity was determined using ImageJ (National Institutes of Health, USA) and values were normalized with BSA band intensity (1 μg) to enable results analysis

between gels.

2.5.2. Western blot

Process and purified samples were subjected to SDS-PAGE (4.5-12 % gradient gels) and electroblotted to a PVDF membrane (Bio-Rad Laboratories, USA), according to standard procedures (Laemmli, 1970; Towbin et al., 1979). After transfer, membranes were incubated with 6x His-Tag mouse primary antibody at 1 µg/mL and with the goat anti-Mouse IgG (H+L) secondary antibody at 1:2000 (ThermoFisher Scientific, USA).

2.5.3. Circular dichroism

The Circular Dichroism (CD) spectra of the protein were acquired in a 195-300 nm wavelength range. Protein buffer exchange to PBS was carried out prior to CD. Samples were diluted to 0.25 mg/mL, experiments were made at 25 ºC and the final spectrum was an average of three consecutive scans. A known denaturing concentration of TCEP (5mM) was also added to the sample to obtain the curve of denatured protein. Collected data was normalized by adjusting the values of ellipticity (θ) to molar concentrations.

2.5.4. Dynamic light scattering

Particle size characterization in purified samples was performed using samples diluted to a final concentration of 0.25 mg/mL. Measurements were run at 4 ºC for 2 hours.

3. Results and Discussion

3.1. Optimization of infection conditions

A small-scale feasibility study was performed to determine the best multiplicity of infection (MOI) and time of harvesting (TOH) for human

recombinant Bone Marrow Tyrosine kinase on the chromosome X (hrBMX) expression (**Figure. 2.1**). Data shows that cell growth was inhibited after infection, more pronounced for the highest MOI (0.1 and 1 plate forming units (pfu)/cell) with a peak concentration of 0.8-1.0x10^6 cells/mL at 24 hours post-infection (hpi). Cells typically stop growing after infection (Roldão et al., 2009) and this growth inhibition is related to the amount of virus infecting cell population, thus more pronounced for the highest MOI (Maranga et al., 2003). A decrease in cell concentration and viability, together with an increase of 2-3 μm in cell size from 48 hpi on-wards, was observed for infected cultures when compared to non-infected control (**Figure 2.1.A-D**). Interestingly, a peak in cell size of 19 μm was observed at 72 hpi, which corresponds to the maximum productivity of hrBMX. The correlation between cell size and protein expression has been described as a method to predict maximum productivity (Sander and Harrysson, 2007). To quantify the amount of hrBMX produced, MOI of 0.01 and 0.001 pfu/cell were analyzed by Western blot (WB) (**Figure 2.1.E** and **Figure S2.1**). These conditions were selected based on (i) intracellular hrBMX expression and (ii) cell viability higher than 80 % at harvesting time (typical for intracellular recombinant protein expression). hrBMX expression was detected after 48 hpi, given that the expression of the foreign gene is driven by the polh promoter that is only transcribed during the late stages of infection (> 18 hpi) (Luckow et al., 1993). The highest protein expression was observed with MOI of 0.01 pfu/cell at 72 hpi, which correlates with the literature (Muckelbauer et al., 2011).

3.2. Production and purification of hrBMX

The production of hrBMX was successfully scaled-up to stirred-tank bioreactor (STB), i.e. similar production yields were obtained in shake-flask and STB (**Figure 2.1.F**), thus demonstrating the potential of Insect cell-baculovirus expression vector system (IC-BEVS) for large-scale production.

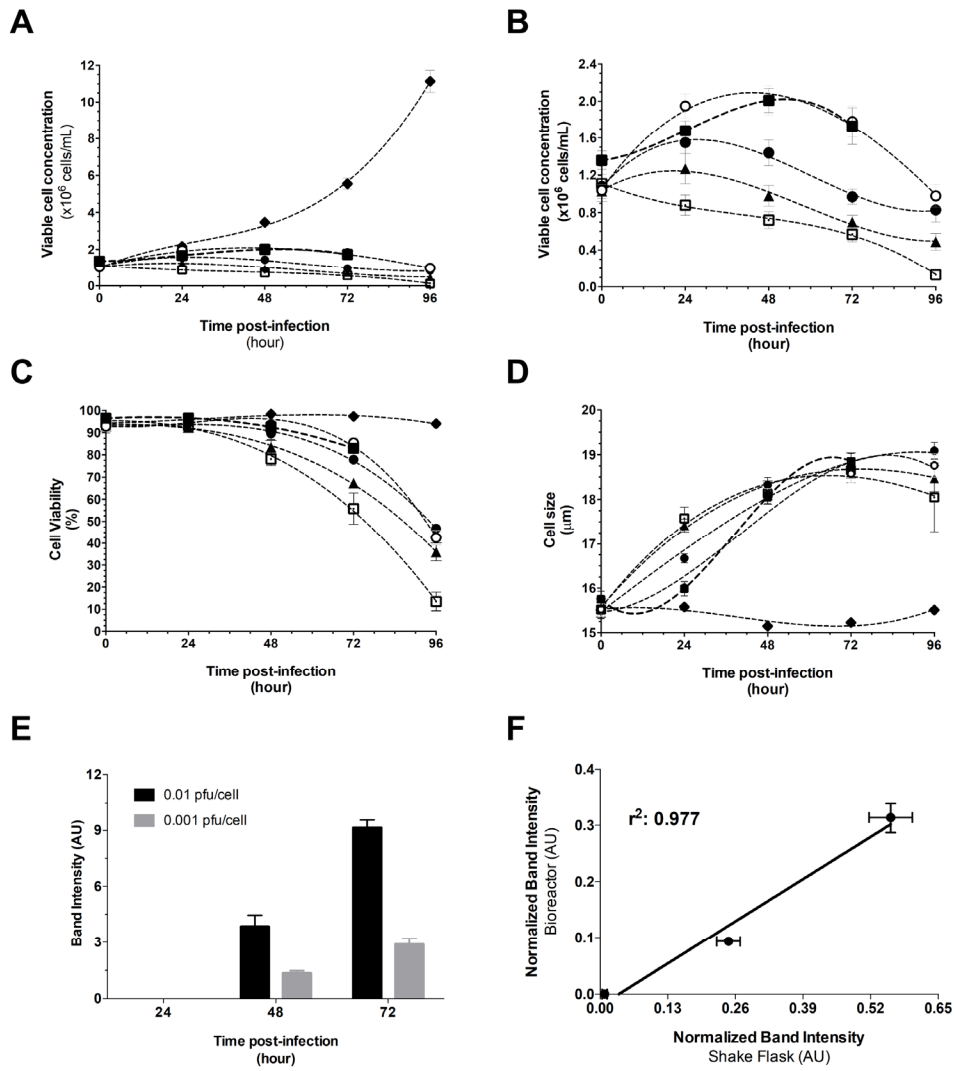

Figure 2.1. Production of human recombinant Bone Marrow Tyrosine kinase in the chromosome X (hrBMX). Cell growth kinetics after infection: **(A and B)** viable cell concentration, **(C)** cell viability and **(D)** cell size. CTL: control culture (i.e. without infection) (black diamond). MOI of 0.01 pfu/cell in the bioreactor (black square) and MOI of 0.001 pfu/cell (white circle), 0.01 pfu/cell (black circle), 0.1 pfu/cell (black triangle) and MOI of 1 pfu/cell (white square) in shake flask. hrBMX expression kinetics: **(E)** product quantification from WB band intensity and **(F)** product quantification from SDS-PAGE band intensity, normalized with BSA band intensity values (1µg). Data is the mean ± standard deviation obtained from at least three independent measurements (n=3). Lines represent the tendency of the experimental data. AU – Arbitrary Units. MOI - Multiplicity of infection.

Noteworthy, we describe for the first time a short purification process for hrBMX (**Figure 2.2.A-D**), reducing the overall number of purification steps and, consequently, total process time by 75 % when compared to other processes (Muckelbauer et al., 2011). Furthermore, based on buffer and additive screenings made before the starting of the experiments (data not shown), the buffering system was changed from HEPES to TRIS increasing hrBMX stability. Upon completion of the purification step, 24.3 mg of purified protein per liter of culture was obtained, a 4-fold increase when compared to the production yields of other phosphorylated proteins, already described (Díaz Galicia et al., 2019; Wang et al., 2008).

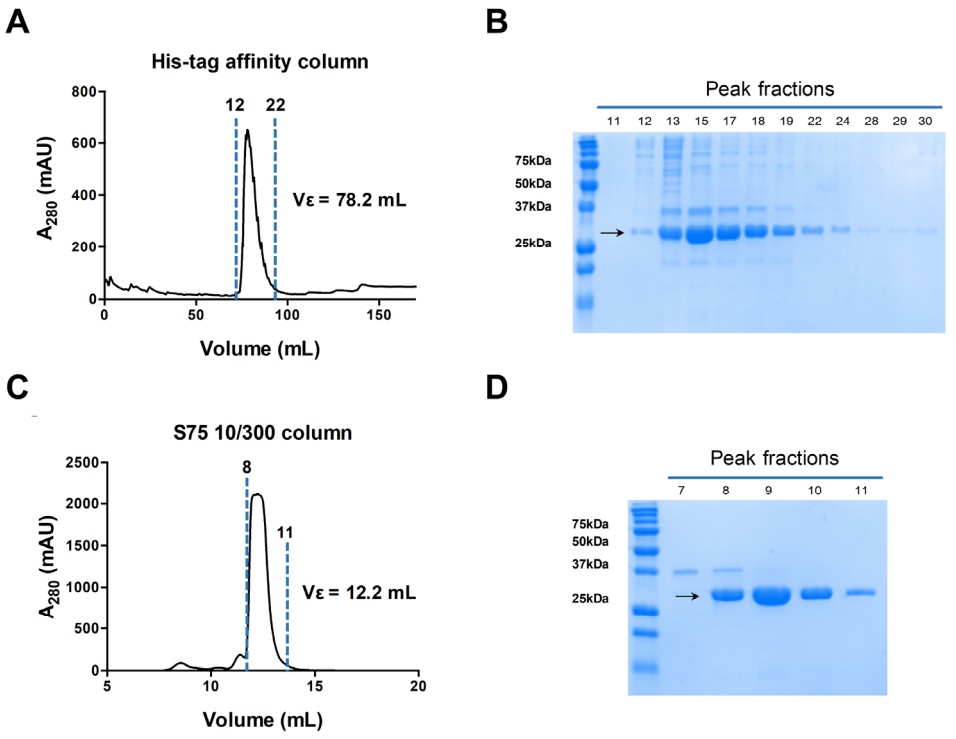

Figure 2.2. Purification of human recombinant Bone Marrow Tyrosine kinase in the chromosome X (hrBMX). Chromatogram of the **(A)** His-tagged hrBMX using a HisTrap™ FF column and **(B)** SDS-PAGE gel analysis of the collected fractions. Chromatogram of the His-tagged hrBMX using **(C)** Superdex^{TM} 75 column and **(D)** SDS-PAGE analysis of the collected fractions.AU - Arbitrary Units.

The IC-BEVS technology is widely used in industrial settings for the production of several recombinant proteins (Assenberg et al., 2013) given the easiness of use in small scale (for optimization or screening experiments) and scalability (for production runs) (Roldão et al., 2014). Proteins produced using the IC-BEVS guarantee more complete eukaryotic post-translational modifications than bacteria and yeast, and similar to human patterns (Davis and Wood, 1995). By combining benefits from other expression systems, this technology has been the most attractive platform used to produce a tyrosine kiı se expressed in hepatocellular carcinoma (TEC) (Bhoir et al., 2018; Muckelbauer et al., 2011). To our knowledge, no other expression system has been used for the expression of hrBMX and is the reason why was selected for our work. Under non-optimal conditions, IC-BEVS expression yields can be low. Evaluating key infection process parameters as described in Section 3.1, together with optimization of the purification steps, were of the most important towards maximizing protein expression in large-scale, thus contributing for a successful optimization of the method.

3.3. Biochemical and biophysical characterization of hrBMX

Biochemical and biophysical characterization of protein samples previous to crystallization assays is essential to increase the likelihood of protein crystal formation (Borgstahl, 2007). Analysis of the native and Mn^{2+}-Phos-tag gels showed that hrBMX product obtained from IC-BEVS is a mixture of non-phosphorylated and phosphorylated proteins (**Figure. 2.3.A**).

Interestingly, we have reported the crystal formation of hrBMX, preferentially of the non-phosphorylated structure, which enabled to characterize the irreversible inhibition of the protein at the atomic level (Seixas et al., 2020). Dynamic light scattering (DLS) measurement showed a correlation of function with a typical curve for monodisperse samples, although some degree of aggregation was detected over time (**Figure 2.3.B**).

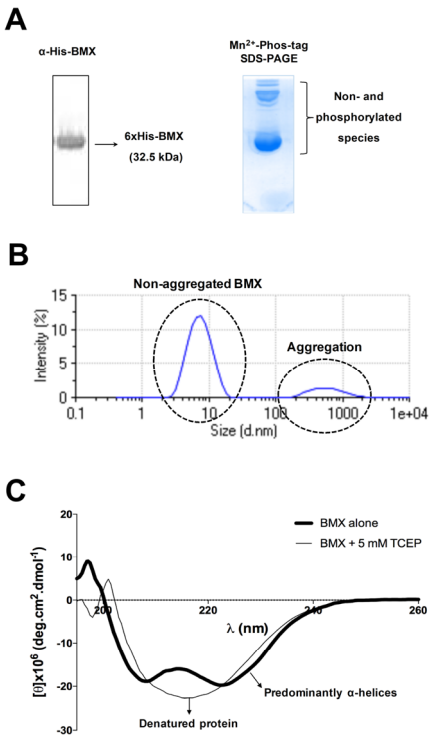

Figure 2.3. Biochemical and biophysical characterization of human recombinant Bone Marrow Tyrosine kinase in the chromosome X (hrBMX). **(A)** Western blot and Mn^{2+}-Phos-tag SDS gel of the final purified product. **(B)** Dynamic Light Scattering (DLS) spectrum of purified hrBMX, where the relative intensity (%) is displayed as a function of the diameter of the protein particle. **(C)** Circular Dichroism (CD) spectrum of purified hrBMX alone (native state) and with 5 mM TCEP (denatured protein). θ - values of ellipticity.

This may account for the mutagenesis strategy used, which consisted of the replacement of non-conserved residues by other residues that mimicked the crystal contacts of BTK, with to create packing opportunities for BMX crystal formation (Muckelbauer et al., 2011). Circular dichroism (CD) experiments **(Figure 2.3.C**) showed a pure protein in its native state, which was then ready for crystallization trials. The spectrum displays a curve typical of proteins that have a predominance of α-helices in their composition (Kelly et al., 2005), which is in good agreement with the published structural information (PDB: 3SXR and 3SXS).

In conclusion, this report describes optimal conditions to produce hrBMX in STB using the IC-BEVS and proposes a rapid and efficient purification protocol to assure high product quality (**Figure 2.4**). Optimization of the method was key for the large-scale production of hrBMX and the ensuing production platform has the potential to be used for other recombinant proteins with therapeutic interest. It also provides substantial information regarding the biochemical and biophysical characterization of hrBMX that could be used as future guidelines for follow-up studies. In particular, we expect this new protocol to efficiently produce high purity hrBMX to accelerate the study of hrBMX inhibition. In turn, the new knowledge generated will guide the design of ligands with improved potency and selectivity.

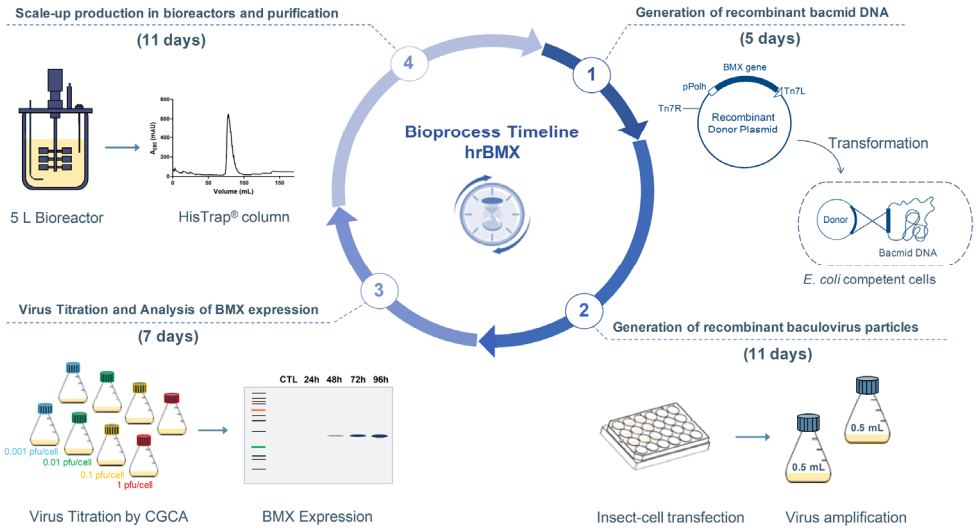

Figure 2.4. Bioprocess workflow for human recombinant Bone Marrow Tyrosine kinase in the chromosome X (hrBMX) production. The hrBMX gene was cloned into a baculovirus shuffle vector in competent E. coli cells and expression of the target protein was carried out by transfecting Sf-9 insect cells to produce stock recombinant baculovirus particles. Viral stock concentration was determined by the cell growth cessation assay and MTT titration methods, and viruses were used to infect insect cells in stirred-tank bioreactors for large-scale BMX production.

4. ACKNOWLEDGMENTS

This work has received funding from the European Union Horizon 2020 research and innovation program, under grant agreement No 702428. Royal Society to G.J.L.B. (URF\R\180019), FCT Portugal (iFCT to G.J.L.B., IF/00624/2015, Postdoctoral Fellowship SFRH/BPD/95253/2013 and PTDC/MED-QUI/28764/2017 to J.D.S., Marie Sklodowska-Curie IF (grant agreement No. 702428 to J.D.S. Investigador FCT programme 2014 (IF/01704/2014 and IF/01704/2014/CP1229/CT0001) to A.R. and from iNOVA4 Health Research Unit (LISBOA-01-0145-FEDER-007344) FCT/MCTES, FEDER, and Programa Operacional Competitividade e Internacionalização (POCI) are also acknowledged. FCT SFRH/BPD/118731/2016 to M.C.M. FCT SFRH/BD/143583/2019 to B.B.S. FCT LISBOA-01-0145-FEDER-007660 to J.A. B.

5. SUPPORTING INFORMATION

5.1. Supplementary material

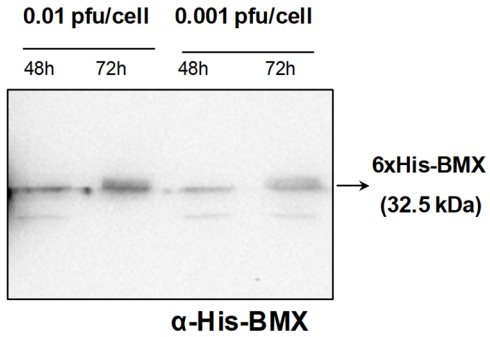

Figure S2.1 - Western Blot for the detection of human recombinant Bone Marrow Tyrosine kinase in the chromosome X (hrBMX) in the cell lysate. The presence of BMX was confirmed at 48 hpi and at 72 hpi. The blotting was carried out on the baculovirus-infected Sf-9 cells with 6x HisTag mouse primary antibody and goat anti-Mouse IgG (H+L) secondary antibody. hpi - hours post-infection. pfu - plate forming unit.

6. REFERENCES

Assenberg R, Wan PT, Geisse S, Mayr LM. 2013. Advances in recombinant protein expression for use in pharmaceutical research. *Curr. Opin. Struct. Biol.* **23**:393–402.

Bhoir S, Shaik A, Thiruvenkatam V, Kirubakaran S. 2018. High yield bacterial expression, purification and characterisation of bioactive Human Tousled-like Kinase 1B involved in cancer. *Sci. Rep.* **8**:4796. https://doi.org/10.1038/s41598-018-22744-5.

Borgstahl GEO. 2007. How to use dynamic light scattering to improve the likelihood of growing macromolecular crystals. *Methods Mol. Biol.* **363**:109–29.

Ciccarone VC, Polayes D a, Luckow V a. 1998. Generation of Recombinant Baculovirus DNA in E.coli Using a Baculovirus Shuttle Vector. *Methods Mol. Med.* **13**:213–235.

Dai B, Chen H, Guo S, Yang X, Linn DE, Sun F, Li W, Guo Z, Xu K, Kim O, Kong X, Melamed J, Qiu S, Chen H, Qiu Y. 2010. Compensatory upregulation of tyrosine kinase Etk/BMX in response to androgen deprivation promotes castration-resistant growth of prostate cancer cells. *Cancer Res.* **70**:5587–5596.

Davis TR, Wood HA. 1995. Intrinsic glycosylation potentials of insect cell cultures and insect larvae. *Vitr. Cell. Dev. Biol. - Anim. J. Soc. Vitr. Biol.* **31**:659–663.

Díaz Galicia ME, Aldehaiman A, Hong SB, Arold ST, Grünberg R. 2019. Methods for the recombinant expression of active tyrosine kinase domains: Guidelines and pitfalls. In: Shukla, AKBT-M in E, editor. *Methods Enzymol.* Academic Press, Vol. 621, pp. 131–152. http://www.sciencedirect.com/science/article/pii/S0076687919300461.

Fox JL, Storey A. 2015. BMX negatively regulates BAK function, thereby increasing apoptotic resistance to chemotherapeutic drugs. *Cancer Res.* **75**:1345–55.

Jarboe JS, Dutta S, Velu SE, Willey CD. 2013. Mini-Review: Bmx Kinase Inhibitors

for Cancer Therapy. *Recent Pat. Anticancer. Drug Discov.* **8**:228–238.

Jiang T, Guo Z, Dai B, Kang M, Ann DK, Kung H-J, Qiu Y. 2004. Bi-directional regulation between tyrosine kinase Etk/BMX and tumor suppressor p53 in response to DNA damage. *J. Biol. Chem.* **279**:50181–9.

Kelly SM, Jess TJ, Price NC. 2005. How to study proteins by circular dichroism. *Biochim. Biophys. Acta - Proteins Proteomics* **1751**:119–139. http://www.sciencedirect.com/science/article/pii/S1570963905001792.

Khow O, Suntrarachun S. 2012. Strategies for production of active eukaryotic proteins in bacterial expression system. *Asian Pac. J. Trop. Biomed.* **2**:159–162. https://pubmed.ncbi.nlm.nih.gov/23569889.

Kinoshita E, Kinoshita-Kikuta E, Takiyama K, Koike T. 2006. Phosphate-binding Tag, a New Tool to Visualize Phosphorylated Proteins. *Mol. Cell. Proteomics* **5**:749–57.

Laemmli UK. 1970. Cleavage of structural proteins during the assembly of the head of bacteriophage T4. *Nature* **227**:680–685.

Luckow V a, Lee SC, Barry GF, Olins PO. 1993. Efficient generation of infectious recombinant baculoviruses by site-specific transposon-mediated insertion of foreign genes into a baculovirus genome propagated in Escherichia coli. *J. Virol.* **67**:4566–4579.

von Manstein V, Yang CM, Richter D, Delis N, Vafaizadeh V, Groner B. 2013. Resistance of Cancer Cells to Targeted Therapies Through the Activation of Compensating Signaling Loops. *Curr. Signal Transduct. Ther.* **8**:193–202. https://pubmed.ncbi.nlm.nih.gov/25045345.

Maranga L, Brazao TF, Carrondo MJTT. 2003. Virus-like particle production at low multiplicities of infection with the baculovirus insect cell system. *Biotechnol. Bioeng.* **84**:245–53.

Miles AJ, Wallace BA. 2014. Circular Dichroism Spectroscopy for Protein

Characterization: Biopharmaceutical Applications. In: . *Biophys. Charact. Proteins Dev. Biopharm.*, pp. 109–137.

Miller LK. 1997. Introduction to the Baculoviruses. In: . *The Baculoviruses*.

Muckelbauer J, Sack JS, Ahmed N, Burke J, Chang CY, Gao M, Tino J, Xie D, Tebben AJ. 2011. X-ray crystal structure of bone marrow kinase in the X chromosome: A Tec family kinase. *Chem. Biol. Drug Des.* **78**:739–748.

van Oers MM, Pijlman GP, Vlak JM. 2015. Thirty years of baculovirus-insect cell protein expression: From dark horse to mainstream technology. *J. Gen. Virol.* Vol. 96.

Rajantie I, Ekman N, Iljin K, Arighi E, Gunji Y, Kaukonen J, Palotie A, Dewerchin M, Carmeliet P, Alitalo K. 2001. Bmx tyrosine kinase has a redundant function downstream of angiopoietin and vascular endothelial growth factor receptors in arterial endothelium. *Mol. Cell. Biol.* **21**:4647–4655. https://pubmed.ncbi.nlm.nih.gov/11416142.

Roldão A, Cox M, Alves P, Carrondo M, Vicente T. 2014. Industrial Large Scale of Suspension Culture of Insect Cells. In: . *Ind. Scale Suspens. Cult. Living Cells*, pp. 348–389.

Roldão A, Oliveira R, Carrondo MJT, Alves PM. 2009. Error assessment in recombinant baculovirus titration: Evaluation of different methods. *J. Virol. Methods* **159**:69–80.

Sander L, Harrysson A. 2007. Using cell size kinetics to determine optimal harvest time for Spodoptera frugiperda and Trichoplusia ni BTI-TN-5B1-4 cells infected with a baculovirus expression vector system expressing enhanced green fluorescent protein. *Cytotechnology* **54**:35–48. https://pubmed.ncbi.nlm.nih.gov/19003016.

Seixas JD, Sousa BB, Marques MC, Guerreiro A, Traquete R, Rodrigues T, Albuquerque IS, Sousa M, Lemos AR, Sousa PMF, Bandeiras TM, Wu D, Doyle SK, Robinson C V, Koehler A, Corzana F, Matias P, Bernardes G. 2020.

Rationally Designed Potent BMX Inhibitors Reveals Mode of Covalent Binding at the Atomic Level. https://chemrxiv.org/articles/preprint/Rationally_Designed_Potent_BMX_Inhibitors_Reveals_Mode_of_Covalent_Binding_at_the_Atomic_Level/11558310.

Tamagnone L, Lahtinen I, Mustonen T, Virtaneva K, Francis F, Muscatelli F, Alitalo R, Smith CI, Larsson C, Alitalo K. 1994. BMX, a novel nonreceptor tyrosine kinase gene of the BTK/ITK/TEC/TXK family located in chromosome Xp22.2. *Oncogene* **9**:3683–8.

Towbin H, Staehelin T, Gordon J. 1979. Electrophoretic transfer of proteins from polyacrylamide gels to nitrocellulose sheets: procedure and some applications. *Proc. Natl. Acad. Sci. U. S. A.* **76**:4350–4354.

Wang L, Foster M, Zhang Y, Tschantz WR, Yang L, Worrall J, Loh C, Xu X. 2008. High yield expression of non-phosphorylated protein tyrosine kinases in insect cells. *Protein Expr. Purif.* **61**:204–211.

Wingfield PT. 2015. Overview of the purification of recombinant proteins. *Curr. Protoc. protein Sci.* **80**:6.1.1-6.1.35.

Zhang R, Xu Y, Ekman N, Wu Z, Wu J, Alitalo K, Min W. 2003. Etk/Bmx Transactivates Vascular Endothelial Growth Factor 2 and Recruits Phosphatidylinositol 3-Kinase to Mediate the Tumor Necrosis Factor-induced Angiogenic Pathway. *J. Biol. Chem.* **278**:51267–76.

Chapter 3

Process Intensification for a PPRV Vaccine Production

This chapter is adapted from:

Marcos F. Q. de Sousa, Christel Fenge, Jens Rupprecht, Alexander Tappe, Gerhard Greller, Paula M. Alves, Manuel J. T. Carrondo and António Roldão, 2019. Process intensification for Peste des Petites Ruminants Virus vaccine production. Vaccine, 37(47):7041-7051. https://doi.org/10.1016/j.vaccine.2019.07.009

Author's contribution to the chapter:

Marcos F. Q de Sousa participated in the conceptualization, experimental setup and design, performed most of the experimental work, analyzed the data, and wrote the chapter.

CONTENTS

SUMMARY

Peste des Petites ruminants Virus (PPRV) vaccine production in anchorage-dependent Vero cells is challenging, involving a substantial amount of bioprocess development.

In this study, we describe the implementation of a new, scalable bioprocess for PPRV vaccine production in Vero cells using serum-free medium (SFM), microcarrier technology in stirred-tank bioreactor (STB), in-situ cell detachment from microcarriers and perfusion. Vero cells were successfully adapted to ProVero^{TM}-1 SFM, reaching growth rates similar to serum-containing cultures (0.030 1/h vs 0.026 1/h, respectively). An in-situ cell detachment method was successfully implemented, with efficiencies above 85 %. Up to 2.5-fold increase in maximum cell concentration was obtained using perfusion when compared to batch culture. Combining perfusion with the in-situ cell detachment method enabled the scale-up to 20 L STB directly from a 2 L STB, surpassing the need for a mid-scale platform (i.e. 5 L STB) and thus reducing seed train duration. Head-to-head comparison of cell growth and PPRV production in the 2 L and 20 L STB was performed, and no significant differences could be observed. Estimated infectious PPRV titers in Tissue Culture Infectious Dose 50 ($TCID_{50}$) ($TCID_{50}$/mL = $5x10^6$ and $TCID_{50}$/cell = 5) are within the log-range reported in the literature for PPRV production in STB and SFM by Silva et al. 2008 (Silva et al., 2008), thus confirming the feasibility and scalability of the seed train designed.

The novel and scalable vaccine production process herein proposed has the potential to assist the upcoming Peste des Petites ruminants (PPR) Global Eradication Program, targeted by Food and Agriculture of the United Nations (FAO) for 2030, by providing African local and/or regional

manufacturers with a platform capable of generating over 25 000 doses of Nigeria 75/1 strain in just 19 days using a 20 L STB.

Key Words: Vero cells, microcarrier technology, in-situ cell detachment, perfusion, scale-up.

1. INTRODUCTION

Peste des Petites ruminants (PPR) is a highly contagious disease affecting small ruminants in Africa, the Middle East and India (Parida et al., 2015). The disease is caused by a Morbillivirus virus from the Paramyxoviridae family, antigenically related to the Rinderpest virus (Gibbs et al., 1979; Parida et al., 2015). With a relevant negative economic impact of 1.45-2.1 billion USD per year (de Haan et al., 2015), it is estimated that more than 60 % of the global domestic small ruminant population (> 1.2 billion) is at risk of getting infected with Peste des Petites ruminants virus (PPRV) (FAO, 2009); PPR has become the next veterinary disease for eradication, targeted by Food and Agriculture of the United Nations (FAO) for 2030, after the successful eradication of Rinderpest in 2011 (Dhinakar Raj et al., 2015; Mariner et al., 2016).

Presently, the most effective manner to control PPR in endemic regions is vaccination (Bora et al., 2018). PPR vaccine Nigeria strain 75/1 is the only vaccine authorized for sheep and goats immunization conferring solid protection for periods of 3 years using low viral concentration vaccine doses of 10^3 Tissue Culture Infectious Dose 50 ($TCID_{50}$)/dose (Diallo et al., 1989; Diallo, 2004; Diallo et al., 2007; Singh et al., 2009; Taylor, 1979). PPRV Nigeria strain 75/1 was attenuated in Vero (African green monkey kidney) cell cultures (Diallo et al., 1989) and is currently produced using the same cell line in planar, two-dimension (2D) culture systems (e.g. roller-bottle and cell factory) (Silva et al., 2008). To support the upcoming PPR global eradication program, a novel vaccine production process capable of surpassing the bottlenecks of these methodologies (i.e. high cost and limited scalability) is essential. The platform implemented by Silva et al. (2008) provides already a step forward in that direction, with microcarrier-based agitation cultures (spinner flasks) and serum-free medium (SFM) being used

for PPR vaccine production (Silva et al., 2008). However, further developments are still needed such as the implementation of scalable production systems (e.g. stirred-tank bioreactor – STB) and reduction of production time using process intensification (e.g. in-situ cell detachment and perfusion).

Vero cells are traditionally cultured in serum-containing medium (Barrett et al., 2009; Gallo-Ramírez et al., 2015; Montagnon et al., 1984). Nevertheless, the un-defined composition, batch-to-batch variability and contamination source of serum make it a highly undesirable supplement in vaccine production processes (Falkner et al., 2006). Adapting a cell to SFM might be challenging, as the beneficial effect of serum on protecting cells from shear stress is lost, commonly interfering with its growth and virus production ability (Merten, 2015). This becomes more evident in large-scale, with the added (negative) impact of O_2 and CO_2 gradients on the cell's physiological state (Clapp et al., 2018). Despite the difficulties, Vero cells growth in SFM has been successfully demonstrated (Butler et al., 2000; Petiot et al., 2012; Rourou et al., 2007; Silva et al., 2008).

Anchorage dependent cell culture at an industrial scale requires the use of microcarrier's technology. Determining the agitation requirements for microcarrier-based bioreactor cultures is key for a successful scale-up strategy. It must guarantee a homogenous environment while avoiding exposing cells to shear stress levels that induce cell growth cessation, detachment or death (Merten, 2015). An engineering evaluation of culture systems and operating conditions is critical for a successful implementation of this technology during the scale-up of a vaccine production process (Sousa et al., 2015). In stirred-tank bioreactor (STB), scale-up is generally performed keeping constant bioengineering parameters such as energy dissipation rate (EDR, ε), Kolmogorov eddy size (KES,λ) and shear stress

rate (SSR, τ) (Cruz et al., 1998; Maranga et al., 2004). Several authors have established threshold for those parameters (Cherry and Papoutsakis, 1988; Cherry and Papoutsakis, 1989; Croughan et al., 1987; Croughan et al., 1988). Nonetheless, scale-up is not linear (Varley and Birch, 1999) and must be dealt on the case-by-case basis; keeping low shear levels while maintaining STB homogenous state, avoiding microcarriers sedimentation (Merten, 2015) and maintaining cell growth (Cruz et al., 1998; Maranga et al., 2004).

The culture of anchorage-dependent cells for seed-train preparation requires cell detachment from microcarriers. This is mostly performed by enzymatic digestion using recombinant and non-animal derived proteases or trypsin-like enzymes and requires complex steps such as PBS washing (removal of proteases inhibition proteins) and addition of proteases inhibitors (Merten, 2003). Non-enzymatic procedures are less reported, but theoretically reduce cell damaged or limit changes cell's phenotype (Li et al., 2015; Rappaport, 2003). Cell migration by bead-to-bead cell transfer is one example (Wang and Ouyang, 1999), a technique highly dependent on cell line and nature of the microcarrier (Merten, 2003; Rafiq et al., 2018). Recently, Nienow and co-workers (2014) described a new protocol for Mesenchymal Stem Cells harvesting combining enzymatic and mechanical detachment (Nienow et al., 2014). The method is based on the theory that short periods of intense agitation in the presence of a suitable enzyme should enhance cell detachment from relatively large microcarriers. The results shown by the authors are promising; however, this routine has not been described for larger-scale settings than 5 L STB.

Perfusion is a commonly used operation mode to control the macro-environment of a given culture, maximizing cell growth and product formation (Bielser et al., 2018). It can be also used to achieve high-cell density cultures

during seed-train preparation (Castilho and Medronho, 2002; Clincke et al., 2013), surpassing mid-scale platform and thus reducing seed-train preparation time.

In this study, we developed a new, scalable bioprocess for PPRV vaccine production in Vero cells using SFM, microcarrier technology in STB, in-situ cell detachment from microcarriers and perfusion. This platform can generate over 25 000 doses of Nigeria 75/1 strain in just 19 days using a 20 L STB.

2. MATERIALS AND METHODS

2.1. Cell line and culture conditions

Vero African Green monkey kidney cells (84113001, ECACC) routinely culture in DMEM supplemented with 10 % (v/v) of FBS (both from Gibco, USA) were adapted to grow in ProVero™-1 SFM (Lonza, USA) supplemented with 5 μg/L of Epithelial Growth Factor and 0.1 % (v/v) Pluronic® F-68 (Sigma, USA). At the end of the adaptation process, a master cell bank was generated by freezing cells in CryoStor® CS-10 cryopreservation medium (Sigma, USA) and stored in N_2 liquid (vapor phase).

2.1.1. Growth in static culture

Cells were routinely sub-cultured to 1-2x10^4 cell/cm^2 every 3-4 days when confluency is reached in t-flask (225 cm^2) or roller-bottle (1 700 cm^2) using TrypLE™ Select Enzyme (1x) (TrypLE Select) (Gibco, USA) for cell detachment and trypsin inhibitor (1 mg/mL, dissolved in cell culture medium) (Sigma, USA) for protease inactivation when using serum-free medium (SFM). Cultures were kept at 37 ºC in a humidified atmosphere of 5 % CO_2.

2.1.2. Growth in stirred tank

Spinner cultures were performed in Wheaton® vessels (125 mL working volume – wv) at 37 ºC and 50 rpm. Cells were seeded at a concentration of $0.1x10^6$ cell/mL and cultured on 3 g/L of Cytodex™-1 microcarrier (prepared according to manufacturing instructions, GE Healthcare Life Sciences, Sweden). Microcarrier colonization was promoted using continuous agitation.

Bioreactor cultures were performed in the stirred-tank bioreactors (STB) Biostat DCU-3 (2 L wv) and Biostat Cplus (20 L wv) (Sartorius Stedim Biotech, Germany). All bioreactors were equipped with two 3-blade segment impellers, 30° angled, appropriate for homogeneous mixing at low shear rates. An internal stainless-steel spin-filter (cell-microcarrier retention device) of pore size 75 μm (Sartorius Stedim Biotech, Germany) was mounted on the 2 L STB only for perfusion cultures. STB process control and monitoring were carried out using Multi Fermenter Control Software (Sartorius Stedim Biotech, Germany). Dissolved oxygen was controlled at 40 % (in air) by sequentially varying the percentage of N_2 and O_2 in gas inlet using a dual aeration strategy: (i) 0-2 days post-inoculation, aeration was performed via headspace at 0.1 volume of gases per volume of culture per min (vvm); (ii) > 2 days post-inoculation, aeration was performed via submerged ring-sparger with pore diameter of 0.8 mm (0.005 vvm). Anti-foam C (Sigma, USA) at a concentration of 0.01% (v/v) was added before starting sparging aeration. pH was controlled at 7.2 using the addition of CO_2 or $NaHCO_3$. The temperature was set to 37 ºC. Agitation conditions were defined based on bioengineering correlations (see Section 2.5 and **Table 3.1**). Cells were seeded at a concentration of $0.1x10^6$ cell/mL and cultured on 3 g/L of Cytodex™-1 microcarrier. Microcarrier colonization was promoted using intermittent agitation for 5 h: ON for 2 min at corresponding N_{FS} (**Table 3.1**)

and OFF for 18 min. For perfusion cultures, cells were grown to $0.4x10^6$ cell/mL (day 2), after which a dilution rate of 0.5-1 (1/d) was applied to maintain glutamine and glucose above limiting concentrations of 1.5 mM and 5 mM, respectively.

2.2. Vero cells detachment from microcarriers

2.2.1. Enzymatic method

The enzymatic method consisted in (i) turn off agitation and allow microcarriers to settle-down for 15 min; (ii) remove spent medium and wash microcarriers twice with PBS at 50 rpm (Spinner) or 60 rpm (2 L STB) for 10 min; (iii) remove PBS and add TrypLE Select (ratio of 1.5 volumes of TrypLE Select to 1 volume of settled microcarriers); (iv) agitate continuously the cell-microcarriers suspension for 20-25 min at 50 rpm (Spinner) or 60 rpm (2 L STB); (v) add trypsin inhibitor (1 mg/mL, dissolved in SFM) (ratio of 1 volume of trypsin inhibitor to 1 volume of TrypLE Select) once maximum cell detachment is reached; (vi) turn off agitation and allow microcarriers to settle-down for 20 min; (vii) harvest supernatant-containing cells and centrifuge at 200 xg for 10 min; and (viii) re-suspend cell pellet in SFM. All steps were performed at 37º C.

2.2.2. Enzymatic-mechanical method

The enzymatic and mechanical method consisted in (i) turn off agitation and allow microcarriers to settled-down; (ii) remove spent medium and add TrypLE Select at a ratio of 1.5 volumes of TrypLE Select to 1 volume of settled microcarriers; (iii) agitate continuously the cell-microcarriers suspension for 4 cycles of 7 min at 155 rpm, with a 5 seconds pulse at 250 rpm in between cycles; (iv) add trypsin inhibitor (1 mg/mL, dissolved in SFM) once maximum cell detachment is reached, at a ratio of 1 volume of trypsin

inhibitor to 1 volume of TrypLE Select. All steps were performed at 37 ºC.

2.2.3. Enzymatic and Enzymatic-mechanical methods efficiency

The detachment efficiency of Vero cells from microcarriers, D_{eff} (%), was defined as:

$$D_{eff}(\%) = \frac{N_{VC,AD}}{N_{VC,BD}}.100\% \qquad \text{Equation 3.1}$$

where $N_{vc,AD}$ is the number of viable cells in suspension obtained after the detachment protocol and $N_{vc,BD}$ is the number of viable cells expected in the culture prior to detachment from microcarriers as estimated by crystal violet staining and trypan blue dye exclusion methods (details in Section 2.6.1).

2.3. Bead-to-bead transfer of Vero cells

Vero cells were cultured on 3 g/L of Cytodex®-1 microcarrier in a 2 L STB until confluence is reached. Confluent microcarriers were then seeded to a new 2 L STB containing bare microcarriers at a ratio of 4:1 (bare:confluent) and bead-to-bead cell transfer promoted by intermittent mode of agitation, i.e. 2 min ON at 80-100 rpm and 28 min OFF, for 48 h. All steps were performed at 37º C.

2.3.1. Bead-to-bead transfer efficiency

The bead-to-bead transfer efficiency of Vero cells, BtB_{eff} (%), was defined as:

$$BtB_{eff}(\%) = \frac{N_{cMC}}{N_{bMC}}.100\% \qquad \text{Equation 3.2}$$

where N_{cMC} is the number of colonized microcarriers and N_{bMC} is the total number of microcarriers in the culture after the bead-to-bead cell transfer.

2.4. Production of PPRV

Vero cells at 0.2x10^6 cell/mL were infected with Peste des Petites ruminants virus (PPRV) Nigeria 75/1 virus strain, kindly provided by Dr Geneviève Libeau (CIRAD-EMVT, France), at multiplicity of infection (MOI) of 0.01 Tissue Culture Infectious Dose 50 ($TCID_{50}$)/cell. Before infection, one complete medium exchange was performed. Cultures were harvested at day 5-6 post-infection (pi). For bioreactor cultures, microcarriers were allowed to settle-down and PPRV bulk clarified using depth filters with 75 μm pore size and 0.018 m^2 (Sartopure PP3, 2 L STB) or 0.12 m^2 (Sartopure PP3, 20 L STB) area (both from Sartorius Stedim Biotech, Germany).

2.5. Bioengineering correlations

Operational conditions including agitation rate and scale-up criteria were estimated using the bioengineering correlations Kolmogorov eddy size, shear stress rate and tip speed, as described elsewhere (Cherry and Papoutsakis, 1988; Croughan et al., 1987; Nienow et al., 2014) and are summarized in **table 3.1**.

The power input, P (W or $kg.m^2/s^3$), throughout the STB can be determined by:

$$P = P_o . \rho_L . N^3 . D_i^5 \qquad \text{Equation 3.3}$$

where P_o (-) is the power number for the impeller (1.2 for both 2 L and 20 L STB, (Kaiser et al., 2011)), ρ (kg/m^3) is medium density, N (1/s) is the agitation rate, and D_i (m) the impeller diameter.

The specific power input, P/M, or mean specific energy dissipation rate, $\bar{\varepsilon}_{STB}$ (W/kg or m^2/s^3), can be estimated by:

$$\frac{P}{M} = \bar{\varepsilon}_{STB} = \frac{P_o.N^3.D_i^5}{V} \quad \text{Equation 3.4}$$

where M (kg) is the fluid mass and V (m^3) is the STB working volume. Despite the substantial data already known on the flow and turbulence levels in STB, the estimation of remains challenging with multiple approximate relations that can be used for such. In this study, two different assumptions (Asm) were considered for estimating $(\varepsilon_{STB})_{Max}$: assumption 1 (Asm#1) from Placek and Tavlarides, 1985 (Placek and Tavlarides, 1985) and assumption 2 (Asm#2) from McManamey, 1979 and Pacek et al., 1999 (McManamey, 1979; Pacek et al., 1999:

$$(\varepsilon_{STB})_{Max,Asm\#1} = \bar{\varepsilon}_{STB}.\frac{T^2H}{D_i^3} \quad \text{Equation 3.5}$$

$$(\varepsilon_{STB})_{Max,Asm\#2} = (\varepsilon_{STB})_{Imp} = \frac{P}{\rho.V_{Imp}} \quad \text{Equation 3.6}$$

where T (m) is the STB diameter, H (m) the STB height, and V_{Imp} (m^3) is the volume swept out by the impeller as it rotates. V_{Imp} is defined by $(\pi/4).D_i^2W_i$ (Nienow, 1998), in which W_i (m) is the impeller blade width. Based on these, $(\varepsilon_{STB})_{Max}$ was estimated by:

$$(\varepsilon_{STB})_{Max,Asm\#1} = P_o.N^3.D_i^2.\frac{T^2H}{V} \quad \text{Equation 3.7}$$

$$(\varepsilon_{STB})_{Max,Asm\#2} = \frac{P_o.N^3.D_i^3}{(\pi/4).W_i} \quad \text{Equation 3.8}$$

The Kolmogorov eddy size (KES), λ (μm), and the shear stress rate (SSR), τ (N/m^2), can be estimated by:

$$\lambda = \left(\frac{\upsilon}{\varepsilon}\right)^{1/4} \quad \text{Equation 3.9}$$

$$\tau = \left(\frac{\varepsilon}{\upsilon}\right)^{1/2} . \mu \qquad \text{Equation 3.10}$$

where υ (m^2/s) is the kinematic viscosity, and μ ($N.s/m^2$) is the viscosity of the fluid. The kinematic viscosity ($7.0x10^{-7}$ m^2/s) and viscosity of the fluid (0.00071 $N.s/m^2$) used for calculations were taken from literature for a microcarrier-based cell culture performed at 37 ºC (Croughan et al., 1987). The tip speed, TS (m/s) can be estimated by:

$$TS = \pi . N . D_i \qquad \text{Equation 3.11}$$

The agitation rate needed for off-bottom suspension of microcarriers, i.e. fully re-suspend settled-down microcarriers, N_{FS} (1/s), can be calculated using the Zwietering equation as proposed by Ibrahim and Nienow (2004) (Ibrahim and Nienow, 2004):

$$N_{FS} = S.\ \nu^{0.1} . d_p^{0.2} . \left(g . \frac{\Delta\rho}{\rho}\right)^{0.45} . \frac{X^{0.13}}{D_i^{0.85}} \qquad \text{Equation 3.12}$$

where S (6.4 from Atiemo-Obeng et al., 2004 (Atiemo-Obeng et al., 2004)) is a dimensionless parameter, d_p is the diameter of microcarriers (147-248 μm for Cytodex™-1, with an average diameter of approximately 190 μm according to manufacturer), g is the gravity acceleration (9.8 m/s^2), $\Delta\rho$ (kg/m^3) is the density difference between submerged microcarriers and fluid, and X (%, w/w) is the weight ratio between microcarriers and fluid.

2.6. Analytics

2.6.1. Cell counting and viability

Total cell concentration was estimated using crystal violet staining. Briefly, after cells disruption with a solution of 0.1 M citric acid with 1 % (v/v) Triton

Table 3.1. Operational conditions for microcarrier-based bioreactor cultures.

Bioreactor scale (L)			**2**	**20**
Agitation rate for off-bottom suspension of microcarriers, N_{FS} (rpm)			120	65
Agitation rate for cell culture, N ($N_{c,Min}$-$N_{c,Max}$, rpm)			70-99	33-47
Mean specific energy dissipation rate, $\bar{\varepsilon}_{STB}$ (x10³ W/kg or m²/s³)				
$\bar{\varepsilon}_{STB} = \frac{P_0 . N^3 . D_i^5}{V}$	Average		0.5-1.4	0.5-1.4
Maximum local energy dissipation rate, $(\varepsilon_{STB})_{Max}$ (x10³ W/kg or m2/s³)				
$(\varepsilon_{STB})_{Max} = P_0 . N^3 . D_i^2 . \frac{T^2 H}{V}$	At impeller	Asm #1	8-22	5-14
$(\varepsilon_{STB})_{Max} = \frac{P_0 . N^3 . D_i^3}{(\pi/4) . W_i}$	At impeller	Asm #2	20-57	11-31
Kolmogorov eddy size, λ (μm)				
$\lambda = \left(\frac{\upsilon}{\varepsilon}\right)^{1/4}$	Average		164-126	164-126
	At impeller	Asm #1	82-63	91-70
	At impeller	Asm #2	64-50	75-58
Shear stress rate, τ (N/m²)				
$\tau = \left(\frac{\varepsilon}{\nu}\right)^{\frac{1}{2}} . \mu$	Average		0.02-0.03	0.02-0.03
	At impeller	Asm #1	0.07-0.12	0.06-0.10
	At impeller	Asm #2	0.12-0.20	0.09-0.15
Tip speed, TS (m/s)				
$TS = \pi . N . D_i$	At Impeller		0.20-0.29	0.24-0.34
Bioreactor and impeller specifications				
Bioreactor	Type		B DCU-3	B Cplus
	Working volume (L)		2	20
	Diameter (m)		0.122	0.26
	Height (m)		0.18	0.38
Impeller	Type		3-blade segment, 30° angled	
	Diameter (m)		0.055	0.136
	Width (m)		0.02	0.06

D_i (m) - impeller diameter; H (m) - STB height; Nc (1/s) - agitation rate; $N_{c,Min}$ and $N_{C,Max}$ – Minimum and Maximum Nc, respectively; NFS - agitation rate to re-suspend settled-down microcarriers;. P_0 (dimensionless) - power number for the impeller; T (m) - STB diameter; V (m^3) - STB working volume; V_{imp} (m^3) - volume swept out by the impeller as it rotates; W_i (m) - impeller blade width; ν (m^2/s) - kinematic viscosity; μ (N.s/m^2) - viscosity of the fluid.

X-100 incubated for at least 1 h at 37 ºC with agitation, nuclei were stained with 0.1 % (w/v) crystal violet and counted in a hemocytometer chamber.

Viable cell concentration was estimated using Fuchs–Rosenthal hemocytometer chamber and trypan blue dye exclusion method. Microcarrier colonization was assessed by staining cells with fluorescein diacetate (FDA, green, viable cells) and propidium iodide (PI, red, dead cells) followed by visual inspection under a fluorescence microscope as described in Serra et al. (2010) (Serra et al., 2010).

2.6.2. Metabolite analysis

Glutamine, glucose and lactate concentrations were determined using YSI 7100MBS (YSI Life Sciences, USA). Ammonia concentration was quantified enzymatically using a commercially available UV test (Nzytech, Portugal). All samples were analyzed in triplicate. The specific consumption or production rates, q_{Met} (μmol/10^6 cell.h) were estimated applying a general mass balance equation for a batch or perfusion system as described elsewhere (Abecasis et al., 2017).

2.6.3. PPRV titration

Virus titer was determined using the $TCID_{50}$ protocol as described by Silva et al. (2008) (Silva et al., 2008). Briefly, 100 μL of viral samples 10-fold serial diluted in MEM supplemented with 10 % (v/v) of FBS and 100 μL of Vero cells suspension (2×10^4 cell/well) were prepared and transfer to the 96-well microtiter plate. Plates were kept at 37 ºC in a humidified atmosphere of 5 % CO_2 and cytopathic effect checked microscopically at day 10. Data collected was analyzed using GraphPad Prism software (4-parameters variable slope) estimating virus titers in $TCID_{50}$.

3. RESULTS

3.1. Vero cells adaptation to Provero™-1 serum-free medium

Vero cells adaptation to ProVero™-1 SFM was performed using a step-wise strategy. It consisted of sub-culturing cells in tissue culture flasks using serum-free medium (SFM) supplemented with progressively reduced percentages of FBS, namely 5 %, 2.5 %, 1.25 % and 0 %. Before each FBS reduction stage, at least 3 cell passages were needed to achieve a constant specific growth rate (μ). Results are shown in **Figure 3.1**.

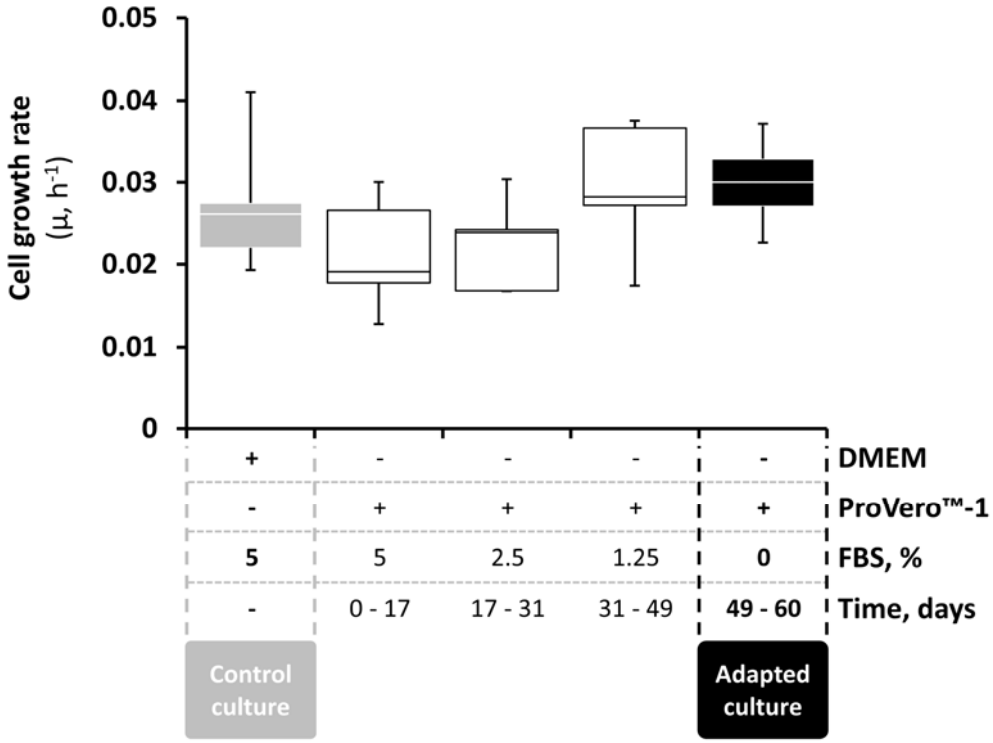

Figure 3.1. Whiskers chart of Vero cells growth rate (μ) during the adaptation process to serum-free medium conditions. Control culture: cells growing in DMEM supplemented with 5% (v/v) of FBS. Adapted culture: cells growing in ProVero™-1 SFM. Horizontal lines are medians, boxes represent the interquartile range and error bars show the full range of estimated rates. μ - specific growth rate.

Control culture (DMEM supplemented with 5 % FBS) and adapted culture (ProVero™-1 SFM) have similar growth rates, μ = 0.026 $\pm$ 0.006 h^{-1} vs μ = 0.030 $\pm$ 0.006 h^{-1}, respectively. Likewise, maximum cell concentrations achieved in control (1.9 $\pm$ 0.5 x10^5 cell/cm^2) and adapted (1.8 $\pm$ 1.0 x10^5 cell/cm^2) cultures were remarkably similar. These results confirm that Vero cells adaptation to SFM was successfully achieved.

3.2. Determining agitation requirements for microcarrier-based bioreactor cultures

The minimum agitation rate for cell culture, $N_{c,min}$, was defined as the agitation needed to ensure that microcarriers are uniformly suspended and oxygen mass transfer is sufficient to support cell growth and product formation. The $N_{c,min}$ used for the 2 L stirred-tank bioreactor (STB) has been selected based on work previously done at iBET (Fernandes et al., 2012; Marcelino et al., 2006). To define the $N_{c,min}$ of the 20 L STB, hydrodynamic parameters were computed, including the energy dissipation rate (EDR, ε), Kolmogorov eddy size (KES, λ), shear stress (SSR, τ) and tip speed (TS) (**Equation 3.3 to 3.11**). By retaining constant the mean specific energy dissipation rate, $\bar{\varepsilon}_{STB}$, as the scale-up criteria from 2 L to 20 L, it was possible to estimate the $N_{c,min}$ of the 20 L STB (33 rpm) (**Table 3.1**).

The maximum agitation rate for cell culture, $N_{c,max}$, was defined as the agitation needed to start inducing cell growth inhibition and/or cell death. The study of Croughan and co-workers on the correlation between Kolmogorov length scale (KLS) and cell growth was herein used to assist the definition of $N_{c,max}$ for the 2 L and 20 L STB (Croughan et al., 1987). The theory is that KLS lower than 2/3 of microcarrier's diameter have significant, immediate impact on cell growth (Croughan et al., 1987). Assuming that average diameter of Cytodex™-1 microcarrier is approximately 190 μm, the agitation

rate inducing a KES of 126 μm in the 2 L STB is 99 rpm, and thus this was the rate considered as $N_{c,max}$ (**Table 3.1**). By retaining constant the mean specific energy dissipation rate, $\bar{\varepsilon}_T$, as the scale-up criteria 2 L to 20 L, it was possible to estimate the $N_{c,max}$ of the 20 L STB (47 rpm) (Table 1).

Overall, the operational conditions ($N_{c,min}$ and $N_{c,max}$) defined for the 2 L and 20 L STB were within non-detrimental SSR (< 0.2 N/m^2, (Cherry and Papoutsakis, 1988; Cherry and Papoutsakis, 1989)) and tip speed (< 0.4 m/s, (Cherry and Papoutsakis, 1988; Cherry and Papoutsakis, 1989)) values (**Table 3.1**).

The agitation rate needed for off-bottom suspension of microcarriers, i.e. fully re-suspend settled-down microcarriers, N_{FS}, was calculated using Equation 3.12 (Ibrahim and Nienow, 2004). The values obtained for the 2 L and 20 L STB were 155 rpm and 73 rpm, respectively. In-situ testing revealed that these agitation rates were 12-29 % higher than those experimentally assessed by visual inspection and monitoring. Therefore, to minimize the impact of agitation on cell growth, the N_{FS} observed experimentally for the 2 L (120 rpm) and 20 L (65 rpm) STB were the ones used throughout the experiments (**Table 3.1**).

3.3. Improved seed-train process for inoculation of 20 L bioreactors

Conventional seed-train process for inoculation of a 20 L STB begins with the thawing of a cryopreserved working cell bank vial, followed by successive expansions into larger culture vessels: i) 225 cm^2 t-flask, ii) 1 700 cm^2 roller bottle, iii) 2 L STB, and iv) 5 L STB. This approach presents two mains challenges: i) the strategy for scale-up of Vero cells in microcarrier-based bioreactor cultures, and ii) the number of N-1 seed train bioreactors needed.

3.3.1. Detachment-reattachment as strategy for scale-up of Vero cells in microcarrier-based bioreactor cultures

Two strategies for scale-up of Vero cells in microcarrier cultures were evaluated: **I.** bead-to-bead transfer, and **II.** detachment-reattachment (**Figure 3.2**).

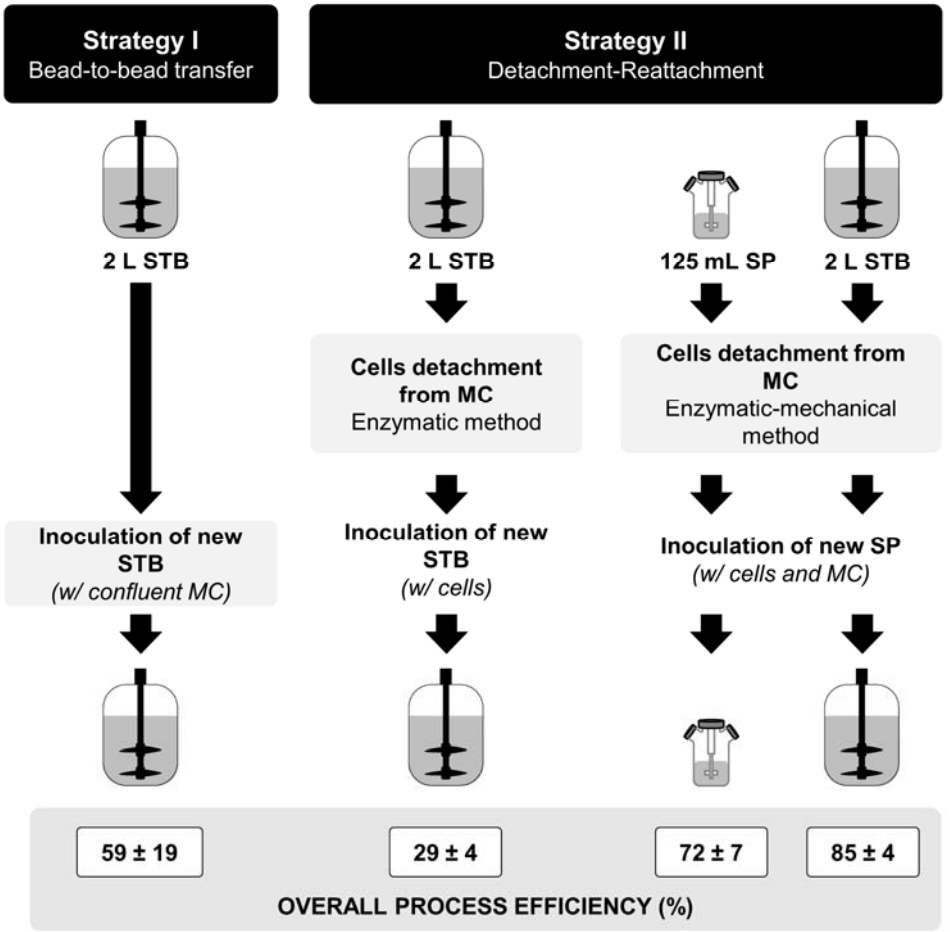

Figure 3.2. Strategies for scale-up of Vero cells in microcarrier-based bioreactor cultures. Overall process efficiency (%) using bead-to-bead transfer (**Strategy I**) and detachment-reattachment (**Strategy II**). Data are mean ± standard deviation obtained from at least three independent biological replicates (n=3). MC - Microcarrier. SP - spinner. STB - Stirred-tank bioreactor.

Experiments were performed in 2 L STB. In **Strategy I**, bead- to-bead cell transfer was promoted as described in Material and Methods (see Section 2.3), with overall process efficiency (BtB_{eff}, Equation 3.2) of 59 ± 18 %, meaning that over 41 % of microcarriers remained empty until the end of the production run. In **Strategy II**, cells were detached from microcarriers using the enzymatic method as described in Material and Methods (see Section 2.2.1), with detachment efficiency (D_{eff}, Equation 2.1) of 35 ± 7 %. Two reasons for this low value were: (i) inefficient detachment process as cells remained attached to microcarriers even after 20-25 min in TrypLE™ Select Enzyme (1x) (TrypLE Select), and (ii) cell loss during PBS washing and harvesting procedures. The reattachment process was more efficient (95 ± 4 %), giving an overall process efficiency of 29 ± 4 %. Cells obtained from both strategies were then used for Peste des Petites ruminants virus (PPRV) production (**Figure 3.3**).

3.3.2. Improving detachment efficiency using an enzymatic-mechanical method

To better understand the basics of Vero cells detachment from microcarriers, and therefore, optimize detachment efficiency (D_{eff}), a set of experiments were designed and run in 125 mL spinner flasks (**Figure 3.4**). The results obtained show that: (i) increasing the concentration of TrypLE Select does not improve D_{eff} and has a negative impact on cell viability; (ii) combining short period of intense agitation with the presence of TrypLE Select increases D_{eff} without impacting on cell viability; and (iii) removing the PBS washing step prior to cell detachment has no impact on D_{eff} (**Figure 3.4A**).

Based on this data, an enzymatic-mechanical method for Vero cells detachment from microcarriers was proposed (see Material and Methods, Section 2.2.2). Head-to-head comparison of cells obtained from the two

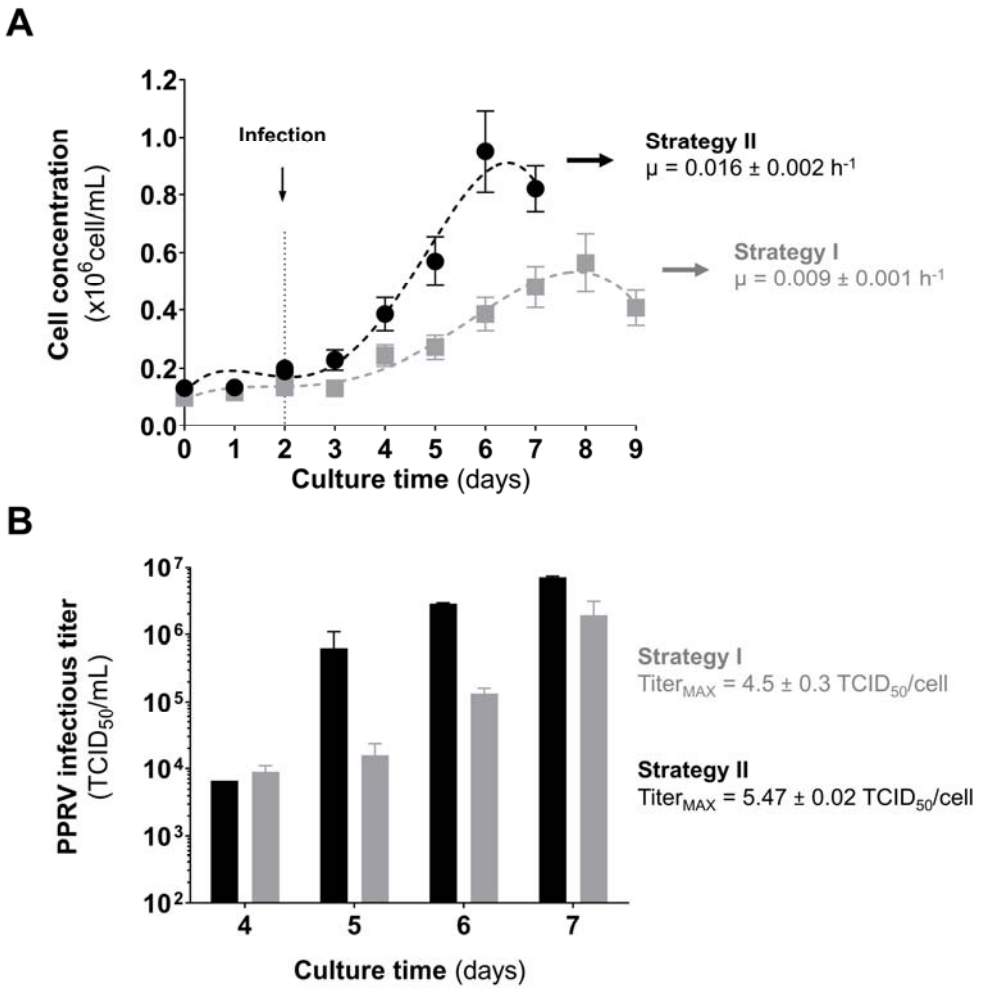

Figure 3.3. Impact of the strategy for scale-up of Vero cells in microcarrier-based bioreactor cultures on **(A)** growth kinetics and **(B)** PPRV production. Strategy I: bead-to-bead transfer; Strategy II: detachment-reattachment using the enzymatic method. Experiments were performed in 2 L STB. Data are mean ± standard deviation obtained from at least three independent measurements (n=3). PPRV - Peste des Petites ruminants virus. $TCID_{50}$ - Tissue Culture Infectious Dose 50.

methods (enzymatic vs enzymatic-mechanical) was performed in 125 mL spinner flasks, with no significant differences in the kinetics of cells reattachment to microcarriers, cell growth and PPRV production (**Figure**

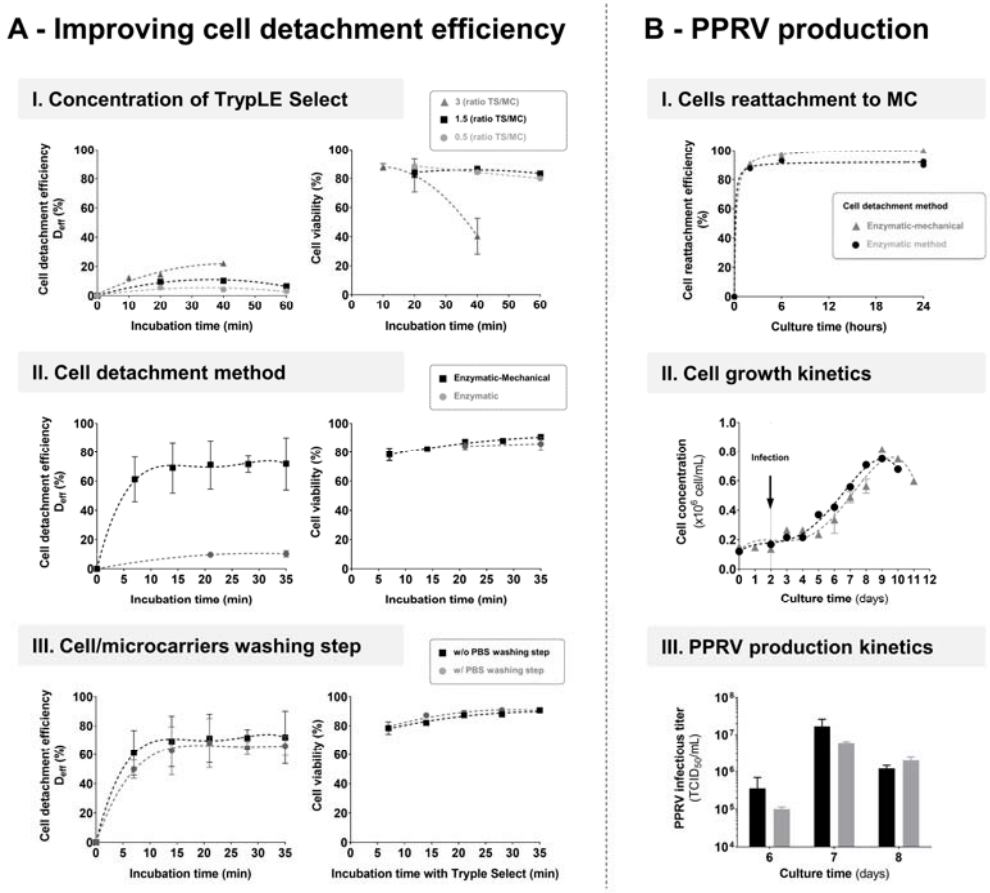

Figure 3.4. Implementation of an enzymatic-mechanical method for Vero cells detachment from microcarriers. **Panel A** - Improving cell detachment efficiency by evaluating the impact of **(I)** cell-dissociation enzyme, **(II)** cell detachment method, and **(III)** cell/microcarriers PBS washing step, on cell detachment efficiency (D_{eff}, %) and cell viability. **Panel B** - Head-to-head comparison of two cell detachment methods for **(I)** cell reattachment efficiency, **(II)** cell growth kinetics, and **(III)** PPRV production kinetics. Experiments were performed in Wheaton® spinner vessels (125 mL working volume). Data are mean ± standard deviation obtained from at least three independent measurements (n=3). MC - Microcarriers. PPRV - Peste des Petites ruminants virus. $TCID_{50}$ - Tissue Culture Infectious Dose 50. TS/MC - Ratio TrypLE Select per microcarrier.

3.4B). The in-situ cells detachment method was successfully scaled-up to 2 L STB, with D_{eff} of 85 ± 4 % (**Figure 3.2**).

3.3.3. Perfusion strategy to reduce the number of N-1 seed train bioreactors needed

To achieve higher cell densities in the N-1 seed train bioreactor, and thus reduce the time to production bioreactor, a perfusion strategy was explored. First, we evaluated the impact of perfusion on Vero cells growth in 2 L STB (**Figure 3.5A**).

Growth rate and cell confluence on microcarriers were higher in perfusion than in batch. Also, cell concentration of up to $2.4x10^6$ cell/mL could be achieved using perfusion, contrasting with the $1x10^6$ cell/mL obtained in batch. The metabolic profiles of cells were assessed, and specific rates estimated (**Table 3.2**). No significant differences in major nutrients (glucose and glutamine) consumption or by-product (lactate) formation were observed between both culture systems and within the normally obtained for animal cell cultures (Zeng et al., 1998). The exception is the specific ammonia (NH_3) production rate, which was 2-fold higher in perfusion than in batch. The follow-up study consisted of assessing the effect of cell concentration on detachment efficiency (D_{eff}) (**Figure 3.5B**). Experiments were performed in 2 L STB operated in perfusion and using the enzymatic-mechanical method as cell detachment strategy. Results show that D_{eff} is dependent on the cell concentration at time of harvest, with the highest D_{eff} ($\approx$ 88 %) being achieved at cell concentration of $1.7x10^6$ cell/mL. Lastly, the impact of perfusion on PPRV production was assessed by comparing the performance of two 2 L STB, one seeded with cells originated from batch mode and another seeded with cells originated from perfusion mode. Results are shown in **Figure 3.5C** and demonstrate that perfusion had no impact on cell growth and PPRV production as similar kinetics (i.e. regression coefficient (b) and Pearson's correlation (r) close to 1) were obtained in both conditions tested.

Based on the aforementioned data, the perfusion strategy for the N-1 seed

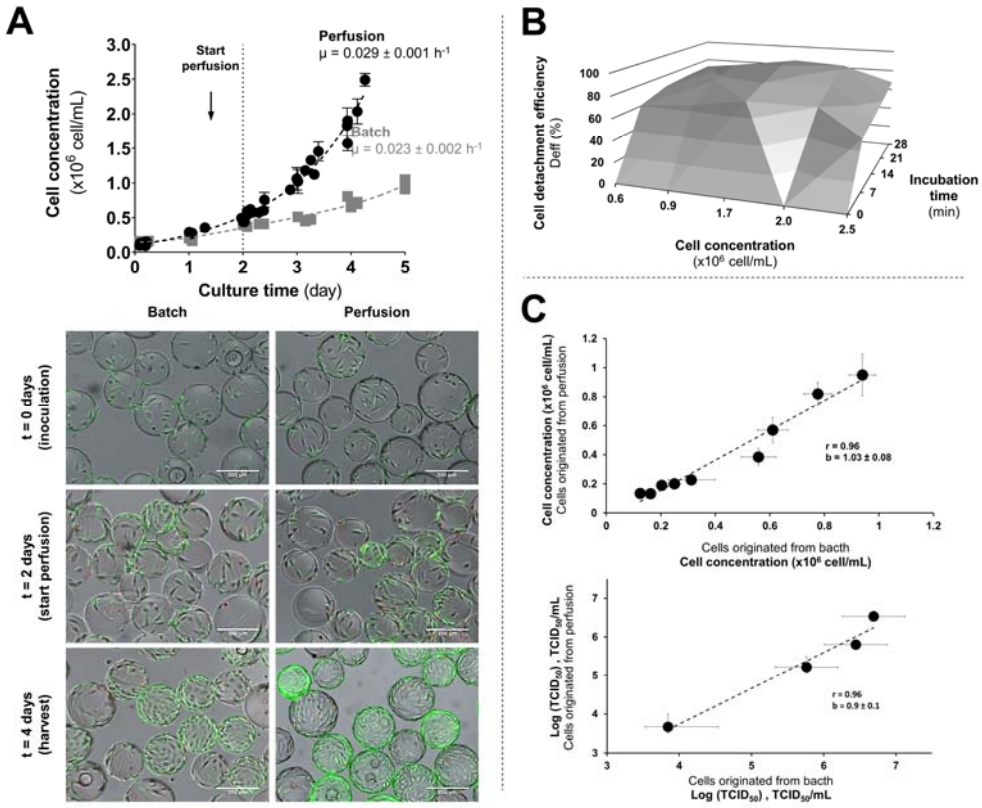

Figure 3.5. Impact of perfusion on Vero cells growth and PPRV production. **(A)** Cell growth kinetics in batch (grey symbols) and perfusion (black symbols); experiments were performed in 2 L STB. Immunofluorescence microscopy images of cells growing in batch and perfusion are shown (green: live cells stained with fluorescein diacetate; red: dead cells stained with propidium iodide; scale bars: 200 μm). **(B)** Correlation of cell detachment efficiency (D_{eff}, %) with cell concentration and incubation time with cell-dissociation enzyme; experiments were performed in 125 mL spinner flasks. **(C)** Linear regression of total cell concentration (upper panel) and PPRV infectious titer ($TCID_{50}$/mL) (lower panel) from cells originated from batch and perfusion, with ensuing Pearson's correlation (r) and regression coefficient (b); experiments were performed in 2 L STB. Data are mean ± standard deviation obtained from at least three independent biological replicates (n=3). PPRV - Peste des Petites ruminants virus. STB - Stirred-tank bioreactor. $TCID_{50}$ - Tissue Culture Infectious Dose 50.

train bioreactor will be implemented when scaling-up PPRV vaccine production from 2 L to 20 L STB.

Table 3.2. Specific rates of nutrient consumption and by-product formation during (i) Vero cells growth in batch and perfusion, and (ii) PPRV production in 2 L and 20 L STB.

Process Phase	Operation mode/Scale	Specific metabolic consumption or production rates (q_{Met}, µmol/10^6 cell.h)			
		Glucose Rate ± SD	Glutamine Rate ± SD	Lactate Rate ± SD	Ammonia Rate ± SD
Vero cells growth	Batch	-0.30 ± 0.03	-0.042 ± 0.004	0.55 ± 0.06	0.025 ± 0.005
	Perfusion	-0.32 ± 0.02	-0.051 ± 0.003	0.48 ± 0.04	0.053 ± 0.003
PPRV production	2 L STB	-0.31 ± 0.07	-0.04 ± 0.01	0.5 ± 0.1	0.024 ± 0.006
	20 L STB	-0.22 ± 0.01	-0.058 ± 0.005	0.30 ± 0.03	0.05 ± 0.02

Cultures were performed as described in Materials and Methods. Three independent biological replicates (n=3) were considered for assessing specific rates during Vero cells growth; a single production run (n=1) was considered for assessing specific rates during PPRV production. Negative values indicate nutrient consumption. SD - standard deviation. q_{Met} - Specific consumption or production rates. PPRV - Peste des Petites ruminants virus.

3.4. Sale-up PPRV vaccine production from 2 L to 20 L STB

The feasibility and scalability of the seed-train strategy herein proposed (i.e. perfusion for the N-1 bioreactor followed by detachment-reattachment using the enzymatic-mechanical cell detachment method) was demonstrated by comparing performances of the 2 L and 20 L STB for cell growth and PPRV production (**Figure 3.6**).

The kinetics of microcarrier colonization for the two STB are presented in **Figure 3.6A**. More than 90 % of microcarriers were colonized within the first 24 h post-inoculation, with no significant differences being observed between both culture systems. Likewise, cell growth and PPRV production in the 2 L and 20 L STB followed similar kinetics (**Figure 3.6B**). Cells were able to grow until day 4 post-infection (pi), reaching maximum concentrations of 0.9-1x10^6 cell/mL, after which cell concentration and viability started decreasing. This growth kinetics is typical of cell cultures infected at low MOI(< 1 virus/cell) and/or with viruses having impaired replication capacity (e.g. attenuated PPRV Nigeria 75/1 virus strain herein used), and has been previously observed elsewhere (Diallo et al., 1989; Silva et al., 2008). The morphology of Vero cells during PPRV infection process is shown in **Figure**

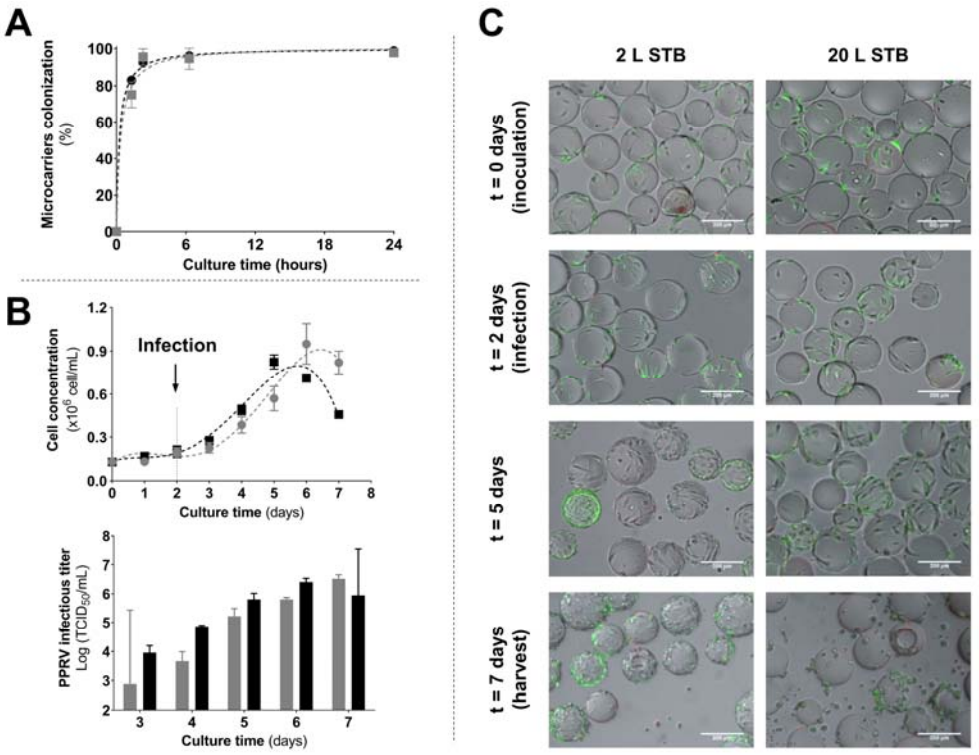

Figure 3.6. Scale-up PPRV vaccine production from 2 L to 20 L STB. Kinetics of **(A)** microcarriers colonization, **(B)** cell growth and PPRV production for the 2 L STB (grey symbols and bars) and 20 L STB (black symbols and bars) using MOI of 0.01 $TCID_{50}$/cell. **(C)** Immunofluorescence microscopy images of cells growing in the two culture systems (green: live cells stained with fluorescein diacetate; red: dead cells stained with propidium iodide; scale bars: 200 μm). Data expressed as mean ± standard deviation (relative to three measurements of microcarriers colonization, cell concentration and PPRV titer). PPRV - Peste des Petites ruminants virus. STB - Stirred tank bioreactor. $TCID_{50}$ - Tissue Culture Infectious Dose 50.

3.6C. In both STB, cells are attached and spread on microcarriers at the time of infection (day 0 pi), become swollen as the infection progresses (day 3 pi), and start lysing and/or detaching from microcarriers at day 5 pi. Metabolic profiles of cells before and after infection were assessed, and specific rates estimated (**Table 2.2**). No significant differences were observed between

both systems, and recorded values are within those normally obtained for batch cultures [50]. Infectious PPRV titers of approx. $5x10^6$ $TCID_{50}$/mL or 5 $TCID_{50}$/cell were achieved at day 4-5 pi irrespective of the culture system. These titers are within those reported in literature for PPRV production in STB and SFM (Silva et al., 2008). Finally, PPRV recovery yields after clarification by depth filtration were comparable (85 ± 9 % in the 2L STB and 90 ± 17 % in the 20L STB).

4. DISCUSSION

Process intensification for PPRV vaccine production in anchorage-dependent Vero cells is challenging, involving a substantial amount of bioprocess development. In this study we developed a new, scalable bioprocess for Peste des Petites ruminants virus (PPRV) vaccine production based on Vero cells and microcarrier technology in bioreactors, using ProVero™-1 as serum-free medium (SFM), an enzymatic-mechanical method for in-situ cell detachment from microcarriers, and perfusion. This process will ultimately support the eradication program of Peste des Petites ruminants (PPR) targeted by the Food and Agriculture Organization (FAO) for 2030 (Bora et al., 2018; Dhinakar Raj et al., 2015; Mariner et al., 2016).

One of the aims of this work was to adapt Vero cells to SFM. SFM is preferable not only from an economic perspective (process costs are potentially reduced) but also from a safety standpoint (eliminates the risk of unwanted contamination originated from the use of bovine serum) (Giangaspero, 2013). Using a stepwise adaptation strategy, we were able to minimize the impact of switching from serum-containing medium to SFM on cell's physiological state, with growth rates varying from 0.022 1/h to 0.029 1/h throughout the adaptation process (**Figure 3.1**). Cell's ability to attach and detach from microcarriers was not compromised, and aggregation was

not observed. Importantly, cell growth rate in SFM is similar to control culture and literature data (Petiot et al., 2012; Quesney et al., 2003; Rourou et al., 2007; Silva et al., 2008).

Determining the agitation requirements for microcarrier-based bioreactor cultures is key for a successful scale-up strategy. Cells growing on microcarriers are sensible to increases on energy dissipation and shear forces, associated to the agitation and aeration rates applied for homogenous mixing (microcarriers are uniformly suspended) and efficient oxygen transfer (Sousa et al., 2015). Aiming at providing bioengineering correlations to guide bioprocess engineers during process development, Croughan et al. (1987) have established a relationship between Kolmogorov length scale (KLS) and cell growth identifying a critical Kolmogorov eddy size (KES) threshold above which no harm to cells occurs (Croughan et al., 1987). In microcarrier-based cultures this corresponds to 2/3 of microcarrier's diameter, which for our culture system using Cytodex™-1 would be 126 μm. Recently, Nienow et al. (2016) reported that KLS as small as 30 % of microcarrier diameter can be used for human mesenchymal stem cell cultures without negatively impacting on cell proliferation and quality attributes (Nienow et al., 2016). Based on these results, one could speculate that Vero cells may withstand higher shear levels than those reported in earlier studies. However, since this has not been experimentally validated, the KES threshold of 2/3 of microcarrier's diameter as described by Croughan et al. (1987) was kept as our main criteria for setting the agitation requirements (Croughan et al., 1987). In two other studies, Nienow (1998) and Cherry and Papoutsakis (1989) proposed that cell damage is proportional to the increase in average energy dissipation rate and microcarriers size (Cherry and Papoutsakis, 1988; Nienow, 1998). It is stated that shear stress rate (SSR) below 0.7 N/m^2 and tip speed (TS) below 0.4 m/s have reduced impact on cell growth. To comply with these limits, the

maximum agitation rates for the 2 L and 20 L stirred-tank bioreactor (STB) were set to 99 rpm and 47 rpm, respectively (**Table 3.1**). At such operational conditions, KES, SSR and TS are below their respective thresholds, thus ensuring optimal process conditions for cell growth.

Another parameter to account for in microcarrier-based cultures is the agitation rate needed for off-bottom suspension of microcarriers (N_{FS}). Settled-down microcarriers must be fully re-suspended at a minimized power input per unit of volume to limit the impact of agitation on cell growth. This is particularly important during the seed train process, as often multiple N-1 bioreactors are needed and microcarrier colonization is promoted via intermittent agitation. N_{FS} can be estimated using the Zwietering equation (Ibrahim and Nienow, 2004). However, in over 50% of carefully executed microcarrier studies (incl. our study), its value is overestimated (Ibrahim and Nienow, 2004). George et al. (2010) observed identical discrepancies but using a different bioreactor design (George et al., 2010). Nienow et al. (2016) strongly suggest to visual assess the N_{FS} value and, then, estimate S value for that impeller type (Nienow et al., 2016). These findings suggest that N_{FS} determination must be done experimentally, as done in our study (**Table 3.1**).

The ability of Vero cells in microcarrier-based cultures to detach and reattach or to migrate to new/bare microcarriers is limited, posing a major problem for process seed train and scale-up (Merten, 2003). Therefore, revising the basis of cell detachment and reattachment to microcarriers is important, in particular when cells are cultivated in SFM and non-animal origin reagents. Recently, a new protocol for mesenchymal stem cell harvesting from microcarriers has been proposed, which is based on the theory that short periods of intense agitation in the presence of a suitable enzyme should enhance cell detachment from relatively large microcarriers (Nienow et al., 2014). Once in suspension, cells should not be damaged

since their diameter is smaller than KES. Based on this theory, we developed an enzymatic-mechanical method for in-situ Vero cells detachment from Cytodex™-1 microcarriers. Upon fine-tuning (i.e. elimination of PBS washing before cell detachment and centrifugation for removal of protease-inhibitor mix), this method provided a significant improvement in overall process efficacy (≈ 85 %) when compared to detachment-reattachment strategy using the enzymatic method (≈ 29 %) or bead-to-bead transfer (≈ 59 %) (**Figure 3.2**). This value is in-line with what is reported in literature for Vero cells growing in SFM (Rourou et al., 2007).

The number of N-1 seed train bioreactors is critical for the economic viability of any vaccine production platform. Keeping this number to its minimum reduces process time and production cost. Therefore, strategies capable of maximizing cell concentration before detachment must be considered and evaluated accordingly. In this study, perfusion was explored as a strategy to achieve higher cell densities in the N-1 seed train bioreactor. Up to 2-fold increase in growth rate and cell concentration was obtained when compared to batch processes, with peak cell density being achieved one day earlier (**Figure 3.5**). The perfusion strategy combined with the in-situ cell detachment enabled scale-up to 20 L directly from 2 L, surpassing a mid-scale platform (i.e. 5 L STB) and thus reducing seed train duration.

Head-to-head comparison of cell growth and PPRV production in the 2 L and 20 L STB was performed (**Figure 3.6**). No significant differences were observed between both culture systems, with infectious PPRV titers of $5x10^6$ Tissue Culture Infectious Dose 50 ($TCID_{50}$)/mL being achieved 4-5 days post-infection (pi). Silva et al. (2008) reported similar values for PPRV production in STB and SFM, i.e. maximum infectious PPRV titers around 10^6 $TCID_{50}$/mL and 5-8 $TCID_{50}$/cell achieved between day 4 and 6 pi (Silva et al., 2008).

Together, the results confirm the feasibility and scalability of the new bioprocess for PPRV vaccine production in Vero cells herein proposed (**Figure 3.7**).

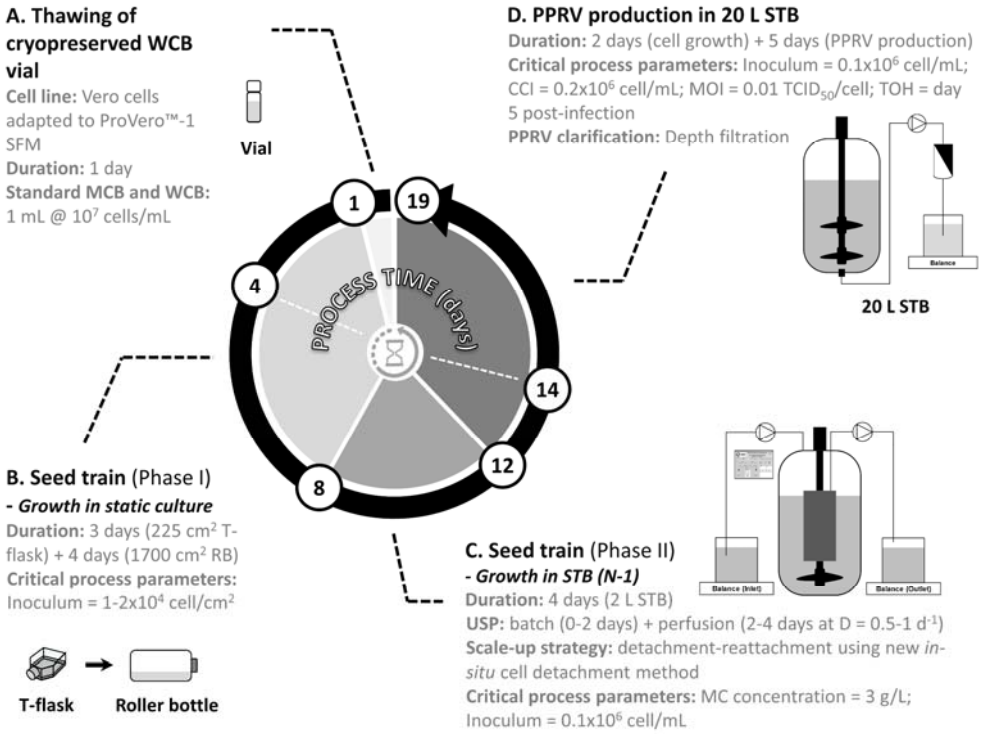

Figure 3.7. New, scalable bioprocess for PPRV vaccine production in Vero cells using SFM and microcarrier technology in STB. MCB - Master cell bank. PPRV - Peste des Petites ruminants virus. STB - Stirred-tank bioreactor. WCB - Working cell bank. $TCID_{50}$ - Tissue Culture Infectious Dose 50

5. CONCLUSION

This work demonstrates the suitability of a new, scalable bioprocess for Peste des Petites ruminants virus (PPRV) vaccine production in Vero cells using serum-free medium and microcarrier technology in bioreactors (**Figure 3.7**). Over 25 000 doses of Nigeria 75/1 strain can be potentially generated in just 19 days using a 20 L stirred-tank bioreactor. Due to its small footprint

and fast turn-around time, this process may allow African local and/or regional manufacturers to produce high quantities of PPRV vaccine in short time-frames, supporting the eradication program of Peste des Petites ruminants (PPR) targeted by Food and Agriculture of the United Nations (FAO) for 2030.

6. ACKNOWLEDGMENTS

This work was supported by Sartorius Stedim Biotech and by the Portuguese "Fundação para a Ciência e a Tecnologia" (EXPL/BBB-BIO/1541/2013 and IF/01704/2014/CP1229/CT0001). The authors wish to thank Carina Silva, Margarida Serra and João Clemente for technical and scientific support. The authors are also grateful to Dr Geneviève Libeau (CIRAD-EMVT, France) for providing the PPR vaccine strain. The authors express their gratitude to Dr Carlos Augusto for the fruitful discussions during the setup of this work. Conflict of interest: all authors declare no conflict of interest and agree with the submission of the manuscript, which was not submitted for publication elsewhere.

7. REFERENCES

Abecasis B, Aguiar T, Arnault É, Costa R, Gomes-Alves P, Aspegren A, Serra M, Alves PM. 2017. Expansion of 3D human induced pluripotent stem cell aggregates in bioreactors: Bioprocess intensification and scaling-up approaches. *J. Biotechnol.* **246**:81–93. https://www.sciencedirect.com/science/article/pii/S0168165617300214?via%3Dihub.

Atiemo-Obeng VA, Penney WR, Kresta SM. 2004. Solid–Liquid Mixing. In: Paul, E, Atiemo-Obeng, VA, Kresta, SM, editors. *John Wiley Sons*. Wiley-Interscience, John Wiley & Sons, Inc., pp. 543–584.

Barrett PN, Mundt W, Kistner O, Howard MK. 2009. Vero cell platform in vaccine production: moving towards cell culture-based viral vaccines. *Expert Rev. Vaccines* **8**:607–18. http://informahealthcare.com/doi/abs/10.1586/erv.09.19.

Bielser J-MM, Wolf M, Souquet J, Broly H, Morbidelli M. 2018. Perfusion mammalian

cell culture for recombinant protein manufacturing – A critical review. *Biotechnol. Adv.* **36**:1328–1340. https://www.sciencedirect.com/science/article/pii/S0734975018300831?via%3Dihub.

Bora M, Yousuf RW, Dhar P, Singh RP. 2018. An overview of process intensification and thermo stabilization for upscaling of Peste des petits ruminants vaccines in view of global control and eradication. *VirusDisease* **29**:285–296.

Butler M, Burgener A, Patrick M, Berry M, Moffatt D, Huzel N, Barnabé N, Coombs K. 2000. Application of a Serum-Free Medium for the Growth of Vero Cells and the Production of Reovirus. *Biotechnol. Prog.* **16**:854–858.

Castilho L, Medronho R. 2002. Cell Retention Devices for Suspended-Cell Perfusion Cultures. *Adv. Biochem. Eng. Biotechnol.*:129–169.

Cherry RS, Papoutsakis ET. 1989. Growth and death rates of bovine embryonic kidney cells in turbulent microcarrier bioreactors. *Bioprocess Eng.* **4**:81–89.

Cherry RS, Papoutsakis ET. 1988. Physical mechanisms of cell damage in microcarrier cell culture bioreactors. *Biotechnol. Bioeng.* **32**:1001–14.

Clapp K, Castan A, K. Lindskog E, Clapp K, Castan A, Lindskog E. 2018. Upstream Processing Equipment. In: . *Biopharm. Process. Dev. Des. Implement. Manuf. Process.*, pp. 457–476.

Clincke MF, Mölleryd C, Zhang Y, Lindskog E, Walsh K, Chotteau V. 2013. Very high density of CHO cells in perfusion by ATF or TFF in WAVE bioreactor™: Part I: Effect of the cell density on the process. *Biotechnol. Prog.* **29**:754–67.

Croughan MS, Hamel JF, Wang DI. 1987. Hydrodynamic effects on animal cells grown in microcarrier cultures. *Biotechnol. Bioeng.* **29**:130–41. http://www.ncbi.nlm.nih.gov/pubmed/18561137.

Croughan MS, Hamel JPJP, Wang DIC. 1988. Effects of microcarrier concentration in animal cell culture. *Biotechnol. Bioeng.* **32**:975–982.

Cruz PE, Cunha A, Peixoto CC, Clemente J, Moreira JL, Carrondo MJT. 1998. Optimization of the production of virus-like particles in insect cells. *Biotechnol. Bioeng.* **60**:408–418.

Dhinakar Raj G, Thangavelu A, Munir M. 2015. Strategies and Future of Global Eradication of Peste des Petits Ruminants Virus. In: Munir, M, editor. *Peste des Petits Ruminants Virus*. Berlin, Heidelberg, Heidelberg: Springer Berlin Heidelberg, pp. 227–254. https://doi.org/10.1007/978-3-662-45165-6_13.

Diallo A, Minet C, Le Goff C, Berhe G, Albina E, Libeau G, Barrett T. 2007. The threat of peste des petits ruminants: progress in vaccine development for disease control. *Vaccine* **25**:5591–7.

Diallo A. 2004. Peste des Petits ruminants. Manual of Diagnostic Tests and Vaccines for Terrestrial Animals, vols. I and II. *OIE* **I and II**.

Diallo A, Taylor WP, Lefèvre PC, Provost A, Lefevre PC, Provost A. 1989. Attenuation of a strain of rinderpest virus: potential homologous live vaccine. *Rev. Elev. Med. Vet. Pays Trop.* **42**:311–9. http://www.ncbi.nlm.nih.gov/pubmed/2485537.

Falkner E, Appl H, Eder C, Losert UM, Schöffl H, Pfaller W. 2006. Serum free cell culture: The free access online database. *Toxicol. Vitr.* **20**:395–400.

FAO. 2009. Peste Des Petitis Ruminants (PPR): A Challenge for Small Ruminants' Production. Animal Production and Health Division.

Fernandes P, Peixoto C, Santiago VM, Kremer EJ, Coroadinha AS, Alves PM. 2012. Bioprocess development for canine adenovirus type 2 vectors. *Gene Ther.* **20**:353–360. https://doi.org/10.1038/gt.2012.52.

Gallo-Ramírez LE, Nikolay A, Genzel Y, Reichl U, Gallo–Ramírez LE, Nikolay A, Genzel Y, Reichl U, Gallo-Ramírez LE, Nikolay A, Genzel Y, Reichl U. 2015. Bioreactor concepts for cell culture-based viral vaccine production. *Expert Rev. Vaccines* **14**:1181–1195. https://doi.org/10.1586/14760584.2015.1067144.

George M, Farooq M, Dang T, Cortes B, Liu J, Maranga L. 2010. Production of cell culture (MDCK) derived Live Attenuated Influenza Vaccine (LAIV) in a fully disposable platform process. *Biotechnol. Bioeng.* **106**:906–17.

Giangaspero M. 2013. Pestivirus Species Potential Adventitious Contaminants of Biological Products. *Trop. Med. Surg.* **1**:1–6.

Gibbs DPJ, Taylormichael WP, Lawman JP, Bryant J. 1979. Classification of peste des petits ruminants virus as the fourth member of the genus morbillivirus. *Intervirology* **11**:268–274.

de Haan NC, Kimani T, Rushton J, Lubroth J. 2015. Why Is Small Ruminant Health Important—Peste des Petits Ruminants and Its Impact on Poverty and Economics? In: Munir, M, editor. *Peste Des Petits Ruminants Virus*. Berlin, Heidelberg: Springer Berlin Heidelberg, pp. 195–226. https://doi.org/10.1007/978-3-662-45165-6_12.

Ibrahim S, Nienow AW. 2004. Suspension of microcarriers for cell culture with axial flow impellers. *Chem. Eng. Res. Des.* **82**:1082–1088. https://www.sciencedirect.com/science/article/pii/S0263876204725940.

Kaiser SC, Loffelholz C, Werner SS, Eibl D, Kaiser S, Löffelholz C, Werner SS, Eibl D, C. S, Loffelholz C, Werner SS, Eibl D. 2011. CFD for Characterizing Standard and Single-use Stirred Cell Culture Bioreactors. In: . *Comput. Fluid Dyn. Technol. Appl.*, pp. 97–122.

Li B, Wang X, Wang Y, Gou W, Yuan X, Peng J, Guo Q, Lu S. 2015. Past, present,

and future of microcarrier-based tissue engineering. *J. Orthop. Transl.* **3**:51–57.

Maranga L, Cunha A, Clemente J, Cruz P, Carrondo MJT. 2004. Scale-up of virus-like particles production: Effects of sparging, agitation and bioreactor scale on cell growth, infection kinetics and productivity. *J. Biotechnol.* **107**:55–64.

Marcelino I, Sousa MFQ, Veríssimo C, Cunha AE, Carrondo MJT, Alves PM. 2006. Process development for the mass production of Ehrlichia ruminantium. *Vaccine* **24**:1716–1725. https://www.sciencedirect.com/science/article/pii/S0264410X05010200?via%3Dihub.

Mariner JC, Jones BA, Rich KM, Thevasagayam S, Anderson J, Jeggo M, Cai Y, Peters AR, Roeder PL, J.C. M, B.A. J, K.M. R, S. T, J. A, M. J, Y. C, A.R. P, Roeder P.L. AO - Anderson Andrew R.; ORCID: http://orcid.org/0000-0001-6273-2862 AO - Roeder, Peter L.; ORCID: http://orcid.org/0000-0002-2981-6113 JO http://orcid. org/000.-0001-9592-6137 AO-P. 2016. The Opportunity to Eradicate Peste des Petits Ruminants. *J. Immunol.* **196**:3499–506. http://www.jimmunol.org/content/196/9/3499.full.pdf+html%5Cnhttp://ovidsp.ovid.com/ovidweb.cgi?T=JS&PAGE=reference&D=emed18&NEWS=N&AN=610862573.

Merten O-W. 2003. Cell Detachment. In: . *Encycl. Cell Technol.* American Cancer Society, pp. 1–12. https://onlinelibrary.wiley.com/doi/abs/10.1002/0471250570.spi036.

Merten O-W. 2015. Advances in cell culture: anchorage dependence. *Philos. Trans. R. Soc. B Biol. Sci.* **370**:20140040. https://doi.org/10.1098/rstb.2014.0040.

Montagnon BJ, Fanget B, Vincent-Falquet JC. 1984. Industrial-scale production of inactivated poliovirus vaccine prepared by culture of Vero cells on microcarrier. *Clin. Infect. Dis.* **6**:S341-4.

Nienow AW. 1998. Hydrodynamics of Stirred Bioreactors. *Appl. Mech. Rev.* **51**:3–32.

Nienow AW, Hewitt CJ, Heathman TRJ, Glyn VAM, Fonte GNGN, Hanga MP, Coopman K, Rafiq QA. 2016. Agitation conditions for the culture and detachment of hMSCs from microcarriers in multiple bioreactor platforms. *Biochem. Eng. J.* **108**:24–29. https://www.sciencedirect.com/science/article/pii/S1369703X15300309.

Nienow AW, Rafiq QA, Coopman K, Hewitt CJ. 2014. A potentially scalable method for the harvesting of hMSCs from microcarriers. *Biochem. Eng. J.* **85**:79–88. https://www.sciencedirect.com/science/article/pii/S1369703X14000278.

Parida S, Muniraju M, Mahapatra M, Muthuchelvan D, Buczkowski H, Banyard AC. 2015. Peste des petits ruminants. *Vet. Microbiol.* **181**:90–106.

Petiot E, El-Wajgali A, Esteban G, Gény C, Pinton H, Marc A. 2012. Real-time

monitoring of adherent Vero cell density and apoptosis in bioreactor processes. *Cytotechnology* **64**:429–441.

Placek J, Tavlarides LL. 1985. Turbulent flow in stirred tanks. Part I: Turbulent flow in the turbine impeller region. *AIChE J.* **31**:1113–1120.

Quesney S, Marc A, Gerdil C, Gimenez C, Marvel J, Richard Y, Meignier B. 2003. Kinetics and metabolic specificities of Vero cells in bioreactor cultures with serum-free medium. *Cytotechnology* **42**:1–11.

Rafiq QA, Ruck S, Hanga MP, Heathman TRJ, Coopman K, Nienow AW, Williams DJ, Hewitt CJ. 2018. Qualitative and quantitative demonstration of bead-to-bead transfer with bone marrow-derived human mesenchymal stem cells on microcarriers: Utilising the phenomenon to improve culture performance. *Biochem. Eng. J.* **135**:11–21.

Rappaport C. 2003. Review-progress in concept and practice of growing anchorage-dependent mammalian cells in three dimension. *Vitr. Cell. Dev. Biol. - Anim.* **39**:187–192.

Rourou S, van der Ark A, van der Velden T, Kallel H. 2007. A microcarrier cell culture process for propagating rabies virus in Vero cells grown in a stirred bioreactor under fully animal component free conditions. *Vaccine* **25**:3879–3889.

Serra M, Brito C, Sousa MFQQ, Jensen J, Tostões R, Clemente J, Strehl R, Hyllner J, Carrondo MJTT, Alves PM. 2010. Improving expansion of pluripotent human embryonic stem cells in perfused bioreactors through oxygen control. *J. Biotechnol.* **148**:208–215. https://www.sciencedirect.com/science/article/pii/S0168165610002750?via%3Dihub.

Silva AC, Delgado I, Sousa MFQQ, Carrondo MJTT, Alves PM. 2008. Scalable culture systems using different cell lines for the production of Peste des Petits ruminants vaccine. *Vaccine* **26**:3305–3311.

Singh RK, Balamurugan V, Bhanuprakash V, Sen A, Saravanan P, Pal Yadav M, Vinayagamurthy B, Veerakyathappa B, Sen A, Saravanan P, Yadav M. 2009. Possible control and eradication of peste des petits ruminants from India: technical aspects. *Vet. Ital.* **45**:449–462.

Sousa MFQ, Silva MM, Giroux D, Hashimura Y, Wesselschmidt R, Lee B, Roldão A, Carrondo MJTT, Alves PM, Serra M, Q. Sousa MF, M. Silva M, Roldão A, M. Alves P, Serra M, Giroux D, Hashimura Y, Wesselschmidt R, Lee B, Carrondo MJTT, Sousa MFQ, Silva MM, Giroux D, Hashimura Y, Wesselschmidt R, Lee B, Roldão A, Carrondo MJTT, Alves PM, Serra M. 2015. Production of oncolytic adenovirus and human mesenchymal stem cells in a single-use, Vertical-Wheel bioreactor system: Impact of bioreactor design on performance of microcarrier-based cell culture processes. *Biotechnol. Prog.* **31**:1600–12. http://doi.wiley.com/10.1002/btpr.2158.

Taylor W. 1979. The isolation of peste des petits ruminants virus from Nigerian sheep and goats. *Res. Vet. Sci.* **26**:94–6.

Varley J, Birch J. 1999. Reactor design for large scale suspension animal cell culture. *Cytotechnology* **29**:177. https://doi.org/10.1023/A:1008008021481.

Wang Y, Ouyang F. 1999. Bead-to-bead-transfer of vero cells in microcarrier culture. *Bioprocess Eng.* **31**:221–4.

Zeng AP, Hu WS, Deckwer WD. 1998. Variation of stoichiometric ratios and their correlation for monitoring and control of animal cell cultures. *Biotechnol. Prog.* **14**:434–441.

Chapter 4

New bioreactor design for the production of ATMPs

This chapter is adapted from:

Marcos F. Q. de Sousa, Marta M. Silva, Daniel Giroux, Yas Hashimura, Robin Wesselschmidt, Brian Lee, António Roldão, Manuel J. T. Carrondo, Paula M. Alves and Margarida Serra, 2015. Production of oncolytic adenovirus and human mesenchymal stem cells in a single-use, Vertical-Wheel bioreactor system: Impact of bioreactor design on performance of microcarrier-based cell culture processes. Biotechnology Progress, 31 (6) :1600-12. https://doi.org/10.1002/btpr.2158

Author's contribution to the chapter:

Marcos F. Q. de Sousa and Marta Silva participated equally on the experimental setup, design and performed the experiments and analyzed the data. **Marcos F. Q. de Sousa** wrote the chapter.

CONTENTS

SUMMARY

Anchorage-dependent cell cultures are used for the production of viruses, viral vectors, and vaccines, as well as for various cell therapies and tissue engineering applications. Most of these applications currently rely on planar, two-dimension (2D) technologies, for the generation of biological products. However, as new cell therapy product candidates move from clinical trials towards potential commercialization, 2D technologies have proven to be inadequate to meet large-scale manufacturing demand. Therefore, a new scalable platform for culturing anchorage-dependent cells at high cell volumetric concentrations is urgently needed. One promising solution is to grow cells on microcarriers suspended in single-use bioreactors (SUB). Toward this goal, a novel bioreactor system utilizing an innovative Vertical-Wheel™ technology was evaluated for its potential to support scalable cell culture process development. Two anchorage-dependent human cell types were used: human lung carcinoma cells (A549 cells) and human bone marrow-derived mesenchymal stem cells (hMSC). Key hydrodynamic parameters such as energy dissipation rate, mixing time, Kolmogorov eddy size and shear stress rate were estimated. The performance of Vertical-Wheel™ bioreactors (PBS-VW) was then evaluated for A549 cells growth and Oncolytic adenovirus type 5 production as well as for human Mesenchymal Stem Cell (hMSC) expansion. Regarding the first cell model, higher cell growth and number of infectious viruses per cell were achieved when compared with stirred-tank bioreactor (STB). For the hMSC model, although higher percentages of proliferative cells could be reached in the PBS-VW compared with STB, no significant differences in the cell volumetric concentration and expansion factor were observed. Noteworthy, the hMSC population generated in the PBS-VW showed a significantly lower percentage of apoptotic cells as well as reduced levels of HLA-DR positive cells. Overall, these results showed that process transfer from STB to PBS-

VW, and scale-up was successfully carried out for two different microcarrier-based cell cultures. Ultimately, the data herein generated demonstrate the potential of Vertical-Wheel™ bioreactors as a new scalable biomanufacturing platform for microcarrier-based cell cultures of complex biopharmaceuticals.

Key Words: anchorage-dependent cell cultures, scalability, microcarriers, single-use bioreactor, vertical-wheel bioreactor, OV-Ad5, hMSC

1. INTRODUCTION

Traditionally, stirred-tank bioreactor (STB) has been the most popular scalable platform for the production of biological therapeutics including monoclonal antibodies and other recombinant proteins (Matasci et al., 2008). Although STB was initially limited to cell types growing in suspension, in 1967 Van Wezel pioneered the use of microcarriers in STB to grow anchorage-dependent cells (Van Wezel, 1967). Large-scale, anchorage-dependent cell cultures are now used for the production of viruses, viral vectors, and vaccines for both human and animal use (Silva et al., 2008; Trabelsi et al., 2012). Previous and on-going clinical trials in cell therapies have used planar, two-dimensional (2D) technologies, such as cell stack to produce challenging cell-based products, but it has become clear that these methods are insufficient for scaling up to clinical manufacturing. Therefore, a new scalable platform to produce anchorage-dependent cells at high cell volumetric concentrations is still needed for the emerging cell therapy market Serra et al., 2012).

Recent findings indicate that microcarrier-based culture systems can increase therapeutic cell culture productivity in a cost-effective manner while ensuring culture homogeneity and strict process control (Simaria et al., 2014). However, developing and implementing microcarrier processes in conventional STB presents major challenges and limitations. Keeping microcarriers suspended and uniformly distributed in an STB vessel is difficult due to the fluid mixing properties of the propeller-like impeller. A potentially greater issue arises during scale-up; the impeller must spin faster to mix larger volumes and will likely affect the cells growing on microcarrier surfaces, as they are much more sensitive to shear forces than cells cultured in suspension (Croughan et al., 1987). Various types of single-use bioreactors (SUB) have recently been developed with features designed to

overcome these challenges. In particular, the Vertical-Wheel™ bioreactor (PBS-VW) incorporates a vertically rotating wheel inside a U-shaped vessel, resulting in faster and more efficient mixing at very low shear rates compared with STB designs across a range of working volumes from 0.1-500 L (Hashimura et al., 2012).

To investigate the potential applicability of PBS-VW on the performance of microcarrier-based cell culture processes, two anchorage-dependent human cell types with distinct biological features were used as models: A549 cells and human Mesenchymal Stem Cells (hMSC). The A549 cells have previously been used for the production of recombinant adenovirus vectors for human gene therapy such as oncolytic adenovirus type 5 (OV-Ad5) as well as for vaccination purposes (Alexander et al., 2013; Kovesdi and Hedley, 2010). Moreover, oncolytic viruses (OV) are natural or genetically modified viral species that selectively infect and kill cancer cells. This specificity has generated considerable interest around the possibility to employ OV as highly targeted agents that would mediate cancer cell autonomous anticancer effects (Pol et al., 2016). The cell therapy market is highly interested in hMSC due to their immunosuppressive, immunoregulating, migrating, and trophic properties, as well as their proliferative capacity and potential to differentiate into several cell types such as osteocytes, chondrocytes, and adipocytes. They also show great potential in numerous clinical applications for a wide range of medical disorders such as autologous and allogeneic therapies for diabetes mellitus, graft-versus-host disease, Crohn's Disease, myocardial infarction, orthopedic indications, and cancer (Wei et al., 2013).

In this study we evaluated (i) the growth performance of both A549 cells and hMSC on microcarriers using PBS-VW and STB and (ii) the impact of bioreactor design on the yield and quality of two challenging therapeutic

products, OV-Ad5 and hMSC.

2. MATERIALS AND METHODS

2.1. Bioreactor configuration and hydrodynamics

2.1.1. Vessel geometry and impellers

The geometry of Vertical-Wheel™ bioreactor (PBS-VW) is significantly different from stirred-tank bioreactor (STB) (**Table 4.1**).

Table 4.1. Comparison of Vertical-Wheel™ bioreactor (PBS-VW) and stirred-tank bioreactor (STB).

Characteristics	PBS/VW	STB
Vessel Geometry	U-shaped bottom and flat walls	Cylindrical
Baffles	Baffles not required	Baffles necessary for particle suspension and good mixing
Impeller position and rotation	Horizontal shaft and rotates in the vertical plane	Vertical (or nearly vertical) shaft and rotates in the horizontal (or nearly horizontal) plane
Impeller power source	Buoyancy of gas introduced under the impeller and caught in circumferential air cups	Rotating shaft and external motor
Impeller type	Combination of axial and radial flow features	Radial or axial flow impellers
Vertical fluid circulation and particle suspension	Comes from radial flow component of impeller interacting closely with vessel walls	Comes from axial flow component of impeller (especially in absence of baffles)
Mixing power	From turbulent dissipation and also “cut-and-fold” action generated by axial vanes arranged to pump in opposite directions	From turbulent dissipation
Power input	Dependent on and calculated from sparged gas flow rate	Usually estimated from engineering correlations
Impeller zone mass	22 % - 33 % of bioreactor mass, depending on scale	Typically, 5 % of bioreactor mass

The PBS-VW single-use vessel consists of four flat, vertical, baffle-less walls, and a U-shaped bottom (**Figure 4.1A**) whereas STB are cylindrically shaped with wall baffles. The Vertical-Wheel impeller itself is very large, accounting for almost 85 % of the width of the U-shaped bottom and rotates

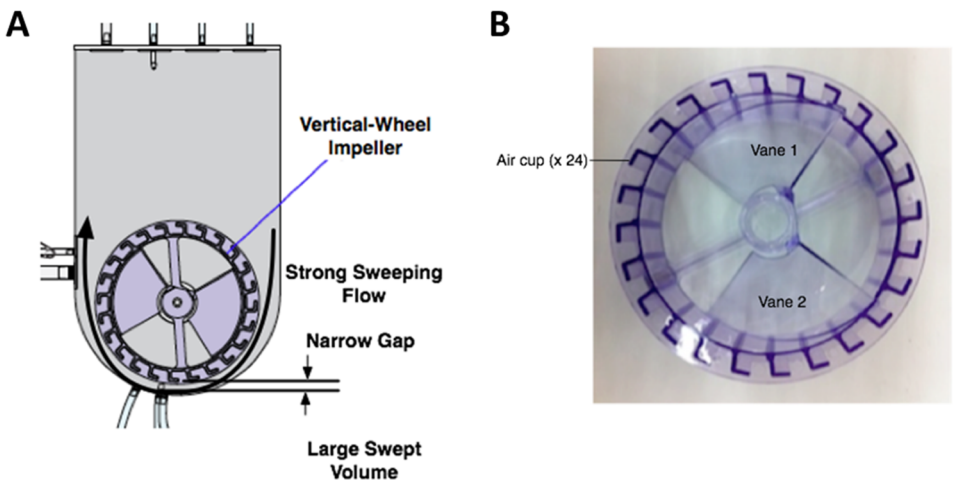

Figure 4.1. (A) Geometry of Vertical-Wheel™ bioreactor single-use vessel with enclosed vertical-wheel, U-shape round bottom and flat sides in the front and back. **(B)** Diagram of Vertical-Wheel impeller using AirDrive mixing mechanism.

in a vertical plane about a stationary horizontal axle, whereas impellers in STB bioreactors rotate in a horizontal plane. The PBS-VW can be thought of as a combination of radial and axial flow impellers, with the radial component in a vertical plane and the axial component in the horizontal one. The vanes in the impeller responsible for the axial flow component are positioned to generate flow in opposite directions, one pumping from front-to-back and the other from back-to-front (**Figure 4.1B**). This opposition creates a cut-and-fold action that leads to very efficient and fast mixing. The PBS-VW bioreactor used in these studies was powered by the buoyant energy of gas sparged from below the impeller whereas the STB, equipped with axial flow three- or four-blade pitched impeller 30º angled, were powered by the top drive motor or magnetic agitation (Biostat Qplus from Sartorius Stedim Biotech, Germany, and DasGip Cellfermpro from Eppendorf AG, Germany, respectively). Aeration in STB was promoted using the headspace of the bioreactor.

2.1.2. Mixing time and microcarrier suspension

Mixing time was measured in PBS-VW bioreactors using conductivity measurements and salt bolus additions. A conductivity probe was placed in the region of slowest mixing in the bioreactor, then a small volume of concentrated salt solution was added to the surface of the liquid and the conductivity signal recorded until equilibrium was reached, indicating complete mixing. The time for mixing to be 95 % complete was measured from the conductivity vs. time plots, with these measurements carried out in triplicates and the results averaged. In STB, mixing time (t_m) was quantified by means of simple engineering correlation (**Equation 4.1**) presented by Ruszkowski (Ruszkowski, 1994) and many others:

$$t_m = A.\left(\frac{1}{N}\right).\left(\frac{1}{P_0^{1/3}}\right).\left(\frac{D_i}{T}\right)^{-2} \qquad \text{Equation 4.1}$$

where A is a proportional factor, N (1/s) is the agitation rate, P_0 (-) is the power number (dimensionless) for the impeller, D_i (m) is impeller diameter, and T (m) the vessel diameter. The A proportional factor used was 8.7 as estimated by Kaiser et al. 2011 (Kaiser et al., 2011) for identical STB geometries used in our work and P_0 for the three-blade pitched impeller was also obtained in this study. $P_{0\ for}$ four-blade pitched impeller from Postmix Optimizaton and Solutions website (www.postmixing.com).

Microcarrier suspension experiments were performed using Cytodex™-1 (GE Healthcare Life Sciences, Sweden) and Synthemax™ II (Corning, USA) microcarriers to determine the minimum agitation rate for cell culture, $N_{c,min}$, that would fully suspend the microcarriers. This determination was made visually, with the criteria being the minimum agitation that kept all the microcarriers off the bottom of the vessel.

2.1.3. Hydrodynamics parameters

The estimation of shear stress rate (SSR, τ, N/m^2), under stirred conditions as result of flow through Kolmogorov eddies was performed using **Equation 4.2**, as described in the literature (Croughan et al., 1987; Cruz et al., 1998):

$$\tau = \left(\frac{\varepsilon}{\upsilon}\right)^{1/2} . \mu \qquad \text{Equation 4.2}$$

and the Kolmogorov eddy size (KES, λ, μm), was estimated by Equation 4.3:

$$\lambda = \left(\frac{\upsilon}{\varepsilon}\right)^{1/4} \qquad \text{Equation 4.3}$$

where υ (m^2/s) is the kinematic viscosity, ε (W/kg or m^2/s^3) is the specific energy dissipation rate in the impeller zone, and μ (N.s/m^2) is the viscosity of the fluid. For the microcarrier suspension studies using culture medium at 37º C, as well as the microcarrier cultures at the same temperature, the viscosity of the fluid was assumed to be 0.00071 N.s/m^2 and the kinematic viscosity used for the calculations was 7.0x10^{-7} m^2/s (Croughan et al., 1987).

The mean specific energy dissipation rate for PBS-VW, $\bar{\varepsilon}_{PBS}$, can be estimated by:

$$\bar{\varepsilon}_{PBS} = \frac{P_{VW}}{D_{VW}^2 . W_{VW} . \rho} \qquad \text{Equation 4.4}$$

where P_{VW} (W) is the power input and D_W (m) is the impeller (i.e., wheel) diameter for PBS-VW, respectively, and ρ (kg/m^3) is the density of the medium (Croughan et al., 1987). A characteristic of PBS-VW geometry is that using D_W^3 as an estimate of the impeller zone volume leads to a value greater than the actual culture volume of the present experiments. In the present experiments, the impeller zone volume measurement was estimated

by using D_W^2 multiplied by impeller width (W_{VW}, front-to-back). For the bioreactor used in this experiment, the Vertical-Wheel™ 3 L (PBS-3), D_{VW} = 13.5 cm and W_{VW} = 55.5 cm. The density of the medium was assumed to be 1.003 g/mL. The power input to the PBS-VW impeller, P_{VW} (W), is linearly dependent to the flow rate of the main sparged gas, similar to what is observed in a Pelton wheel (impulse type water turbine), and can be estimated by:

$$P_{VW} = \rho . \frac{Q}{60} . g . D_{VW} \qquad \text{Equation 4.5}$$

where Q (m^3/min) is the volumetric flow rate of the main sparged gas and g is the acceleration due to gravity (9.8 m/s^2). In Equation 4.5 the mixing power in PBS-VW is equal to the power input minus any solid-solid friction drag between the shaft and the wheel. The friction drag was experimentally estimated and considered negligible. For this reason, the mixing power can be considered equal to the power input.

The mean specific energy dissipation rate, $\bar{\varepsilon}_{STB}$, throughout an STB volume is commonly determined using the following equation:

$$\bar{\varepsilon}_{STB} = \frac{P_o . N^3 . D_i^5}{V} \qquad \text{Equation 4.6}$$

where V (m^3) the working volume and D_i (m) the impeller diameter of the STB. In 1985, Placek and Tavlarides reported that the energy dissipation near the impeller is much higher than estimated by the equation above, in a ratio of approximately (V/D_i^3) (Placek and Tavlarides, 1985). Assuming the impeller local power dissipation rate is the significant factor, the local energy dissipation rate around the impeller, $(\varepsilon_{STB})_{Max}$, can be estimated by:

$$(\varepsilon_{STB})_{Max} = P_o . N^3 . D_i^2 \qquad \text{Equation 4.7}$$

2.2. Cell culture under static conditions

2.2.1. Human lung carcinoma A549 cell line

The A549 cell was obtained from the National Institutes of Health. These cells were routinely propagated in tissue culture flasks at a cell inoculum density of $3x10^3$ cell/cm^2 using Ham's F-12K medium supplemented with 10 % (v/v) of FBS (both from Gibco, USA). A549 cells were cultured at 37 ºC in a humidified atmosphere of 5 % CO_2 in air. For bioreactor inoculum preparation, A549 cells were cultivated in roller-bottle with 1.750 cm^2 of available area for cell growth (Greiner Bio-One, Austria). At roughly 80 % cell confluence, cells were detached from the roller-bottles by rinsing with DPBS (Gibco, USA), adding TrypLE™ Select Enzyme (1x) (TrypLE Select) (Gibco, USA), and incubating for 5 min at 37 ºC. Cells were removed, pooled, and counted using Trypan Blue exclusion method to determine concentration and viability.

2.2.2. Human Mesenchymal Stem cells

The human Mesenchymal Stem Cell (hMSC) was obtained from STEMCELL™ Technologies (MSC-001F; STEMCELL™ Technologies). These hMSC were thawed and expanded to prepare working cell stocks following the manufacturer's instructions using the Mesencult-XF Kit (STEMCELL™ Technologies). Cryopreserved hMSC (passage 3 or 4) were thawed and plated at a cell density of $4x10^3$ cell/cm^2 on t-flask of 175 cm^2 or 225 cm^2 of available area for growth pre-coated with MesenCult™-SF attachment substrate (STEMCELL™ Technologies) using MesenCult™-XF medium (STEMCELL™ Technologies) supplemented with 2 mM L-glutamine (Life Technologies) cultured at 37 ºC in a humidified atmosphere of 5 % CO_2 in air. Fifty percent of the culture medium was exchanged on day 5. At roughly 70 % cell confluence, hMSC were detached from the flasks by rinsing

with DPBS, adding TrypLE Select, and incubating the flask for 5 min at 37 ºC. Cells were removed, pooled, and counted using Trypan Blue exclusion method to determine concentration and viability.

2.3. Cell culture in bioreactors

In this study, two different bioreactor systems were used: PBS-VW and glass STB. More specifically, A549 cells were cultured in PBS-3 (PBS Biotech, USA) and the DasGip Cellferm-pro bioreactor system equipped with four-blade pitched impeller (Eppendorf AG, Germany). hMSC were cultured in PBS-3 and Biostat Qplus bioreactor system equipped with three-blade segment impeller 30º angled (Sartorius Stedim Biotech, Germany). Data acquisition and process control were performed using Hello™ Software running on a Real-time OS (PBS Biotech, USA), DASGIP® Control (Eppendorf AG, Germany), and MFCS/Win (Sartorius Stedim Biotech, Germany) as described previously (Correia et al., 2014; Obom et al., 2014; Serra et al., 2010). In the following sections, we describe the operation parameters (**Table 4.2**) and methodology used (i) for A549 cell growth and oncolytic adenovirus type 5 (OV-Ad5) production and (ii) for the expansion of hMSC. It is important to highlight that the selection of the operation parameters for STB was based on previous data obtained by our group (Correia et al., 2014; Cunha et al., 2015a; Fernandes et al., 2012; Silva et al., 2008). For the PBS-VW, the same operation parameters (e.g., DO, pH, cell inoculum concentration, microcarrier type and concentration, temperature) were used and the agitation rate used was estimated experimentally having as criteria the minimum agitation to ensure that microcarriers are suspended ($N_{C.min}$).

2.3.1. A549 cell growth and oncolytic virus production in bioreactors

The PBS-3 (2.2 L working volume - wv) and DasGip Cellferm-pro STB (0.2 L

Table 4.2. Operational conditions used in PBS-3 and STB for A549 cells and hMSC.

Cell line	A549		hMSC	
Vessel Geometry	PBS-3	STB	PBS-3	STB
Temperature	37ºC		37ºC	
pH	7.2		7.2	
DO	40%		40%	
Aeration rate	0.1 vvm		0.1 vvm	
Agitation strategy and rate	20 rpm	90-110 rpm	0-7 h: 15 rpm, 1 min; off 20 min Day 1-6: 15 rpm Day 6-10: 15 rpm, 5 min; off 1 h Day 10-14: 17 rpm	0-6 h: 40 rpm, 1 min; off 20 min Day 1-6: 40 rpm Day 6-10: 40 rpm, 5 min; off 1 h Day 10-14: 45 rpm

hMSC - human Mesenchymal Stem Cells; PBS-3 - Vertical-Wheel™ bioreactor 3 L; STB - Stirred-tank bioreactor.
vvm - volume of gas per volume of culture per minute-

vw) were inoculated with A549 cells at a concentration of $1.5x10^5$ cell/mL using 3 g/L of Cytodex™-1 microcarriers (GE Healthcare Life Sciences, Sweden) prepared according to the manufacturer instructions. Cells were cultured in Ham's F-12K medium supplemented with 10 % (v/v) FBS (both from Gibco, USA) and 0.1 % (v/v) PF-68 (Sigma-Aldrich, USA). After 24 h, glucose (Merck, USA) and glutamine (Gibco, USA) was fed to each bioreactor to maintain glucose and glutamine concentrations above 6 and 2 mM, respectively. Infection of A549 cells with oncolytic adenovirus type 5 (OV-Ad5) was performed at 50 h post cell inoculation using multiplicity of infection (MOI) of 10 infectious particles (ip)/cell and EXCELL® 293 SFM (Sigma-Aldrich, USA) supplemented with 4 mM of Glutamax™ (Gibco, USA). Operational conditions used for A549 cells culturing are shown in **Table 4.2**. Cell growth, viability, and infection profiles were monitored daily according to the methodologies described below (see sections 2.4 and 2.5).

2.3.2. Expansion of hMSC in bioreactors

Human MSC were inoculated in the PBS-3 (2.2 L wv) and Biostat Qplus STB

(0.25 L wv) at a concentration of $2.5x10^4$ cell/mL using 16 g/L Synthemax™ II microcarriers (Corning, USA) prepared according to the manufacturer's instructions. For each bioreactor system, hMSC were cultured for 14 days in MesenCult™-XF medium supplemented with 2 mM L-glutamine and 0.025 % (v/v) antifoam C emulsion (Sigma-Aldrich, USA). On day 6 of culture, additional empty Synthemax™ II microcarriers were added at a 2:1 ratio, increasing the final concentration to 48 g/L. Fifty percent of culture medium was replaced every 2.5 days, starting at day 5. Operational parameters and culture conditions used for hMSC culturing are shown in **Table 4.2**. Sampling was performed daily and hMSC were characterized in terms of cell concentration, viability, morphology, proliferation capacity, and metabolism using the methodologies described below. The hMSC were harvested from the microcarriers using TrypLE Select solution according to the protocol described elsewhere (Cunha et al., 2015b).

2.4. Analytical methods

2.4.1. Cell growth and microcarrier colonization

Total cell concentration was determined using crystal violet staining. Cells were briefly disrupted using 0.1 M citric acid with 1 % (v/v) TritonX-100 at 37 ºC overnight and nuclei stained with 0.1 % (w/v) crystal violet as described elsewhere (Alves et al., 1996). Nuclei were counted in a Fuchs–Rosenthal hemocytometer chamber. Cell expansion in the bioreactors was characterized by assessing the specific growth rates, μ (1/day), as previously described (Serra et al., 2010). Fold increase in cell concentration was evaluated based on the ratio X_{MAX}/X_0, where X_{MAX} is the peak cell concentration and X_0 is the cell concentration at inoculum. Cell viability and microcarrier colonization were assessed by staining cells with fluorescein diacetate (FDA, green, viable cells) and propidium iodide (PI, red, dead cells) as described in Serra et al. (Serra et al., 2010). followed by visualization

under a fluorescence microscope (Leica Microsystems GmbH, Germany). The analysis of microcarrier colonization was performed by recording at least three representative images (with at least 300 microcarriers each) of cells on microcarriers. The percentage of colonized microcarriers was determined by dividing the number of colonized microcarriers with the total number of microcarriers (colonized and empty).

2.4.2. Metabolite Analysis

The consumption of glucose and glutamine, as well as the production of lactate and ammonia, were monitored throughout the culture period. Glucose, glutamine, and lactate concentrations were analyzed using YSI 7100MBS (YSI Life Sciences, USA) whereas the ammonia concentration was quantified enzymatically using a commercially available UV test (Roche Diagnostic, Germany). Specific metabolic rates, q_{Met} (mol/day/cell) and apparent yield of lactate-to-glucose ($Y_{Lac/Glc}$) were determined as described in the literature (Serra et al., 2010).

2.5. Quantification of oncolytic adenovirus type 5

2.5.1. Estimation of oncolytic adenovirus type 5 titers by end-point dilution method ($TCID_{50}$)

OV-Ad5 infectious titer was determined by Tissue Culture Infectious Dose 50 ($TCID_{50}$) method as described elsewhere (Darling et al., 1998). Briefly, 100 μL of A549 cells at a concentration of $0.5x10^6$ cell/mL was seeded onto a 96-well tissue culture plate (Sarstedt, USA) and incubated overnight at 37ºC in a humidified incubator at 5 % CO_2. The next day, the supernatant was removed and 100 μL of serially diluted virus (from 10^{-2} to 10^{-12}) was added to each well. After 10 days, the cytopathic effect on cell monolayer was observed using a Leica DM IRB inverted microscope (Leica Microsystems,

Germany). $TCID_{50}$ was calculated according to the statistical method of Spearman–Karber as described elsewhere (Darling et al., 1998). All samples were titrated in triplicates.

2.5.2. Estimation of oncolytic adenovirus type 5 by real time quantitative PCR (qPCR)

Titers were estimated within a couple of hours using real-time quantitative PCR (qPCR). Before to DNA extraction, samples were treated with DNase to eliminate unencapsulated viral DNA. DNA extraction from samples was briefly performed using the high pure viral nucleic acid kit (Roche Diagnostics, Germany). Purified adenovirus DNA was analyzed by real-time quantitative PCR in LightCycler® instrument (Roche Diagnostics, Germany) using TaqMan probe Technology (Roche Diagnostics, Germany). For each adenovirus sample, viral titers were estimated as viral genomes (vg) per mL (vg/mL) using the standard calibration curve of cross points vs. log concentrations of the purified DNA standard with known concentration.

2.6. hMSC characterization

2.6.1. Cell apoptosis and proliferation assays

The percentage of apoptotic hMSC was evaluated using the Apoptosis Assay Kit NucView™ 488 (Biotium, Inc., USA), following the manufacturer's instructions. This kit contains the green fluorescent NucView 488 caspase-3 substrate, which detects intracellular caspase-3. The percentage of proliferating hMSC was determined using Click-iT EdU Flow Cytometry Assay Kit according to the manufacturer's recommendation (Life Technologies, USA). All samples were analyzed in a CyFlow® space instrument (Partec GmbH, Germany). At least 10000 events were registered per sample.

2.6.2. Cell surface marker analysis by flow cytometry

Upon termination of each bioreactor culture, hMSC were dissociated from microcarriers using TrypLE Select solution and washed twice in DPBS. The hMSC were incubated with primary antibodies for 1 h at 48 ºC, washed with DPBS and analyzed in a CyFlow® space instrument (Partec GmbH) as reported elsewhere (Serra et al., 2009). Ten thousand events were registered per analysis. Conjugated antibodies used: CD90-PE, CD73-PE, CD105-PE, CD166-PE, CD44-PE, CD45-PE, CD34-PE, HLA-DR, and isotype control antibodies (all from BD Pharmingen™).

2.6.3. Immunocytochemistry.

The hMSC immobilized on microcarriers were fixed in 4 % (w/v) paraformaldehyde in DPBS for 20 min, then permeabilized for 20 min in 0.1 % (w/v) Triton X-100 (Sigma-Aldrich, USA) in DPBS. After 30 min of blocking with 0.2 % (w/v) fish skin gelatin (Sigma-Aldrich, USA) in DPBS, cells were incubated with phalloidin-FITC solution (1:100; Sigma-Aldrich, USA) for 2 h at room temperature (RT). Cells were washed three times in DPBS and then cell nuclei were counterstained with Hoechst 33342 (Sigma-Aldrich). The analysis of the cytoskeleton organization was performed both qualitatively and quantitatively. After staining, fixed cells were visualized using fluorescence microscopy (Leica Microsystems GmbH, Germany). One hundred cells were analyzed from each condition and the percentage of cells showing actin fibers and/or granular actin was quantified.

2.6.4. Multilineage differentiation assays

The hMSC multilineage differentiation assays were performed using the StemMACS™ AdipoDiff (Miltenyi Biotec, Germany), StemMACS™ OsteoDiff (Miltenyi Biotec) and StemPro® Chondrogenesis (Life Technologies, USA)

differentiation kits (Cunha et al., 2015b).

2.6.5. Colony Forming Unit (CFU) Assay

After hMSC cell detachment and separation from microcarriers, hMSC was inoculated in 100 mm Petri dishes in 10 mL of DMEM supplemented with 10% (v/v) FBS (250 cells/Petri dish). Fifty percent of the culture medium was replaced twice a week. After 15 days in culture, the number of colony forming unit (CFU) was measured. Briefly, cells were washed twice with DPBS and fixed with methanol for 20-40 min at -20 ºC. After fixation, cells were dried under the hood and then incubated with Giemsa solution (Sigma Aldrich, USA) diluted 1:20 in H_2O for 30 min at RT. After staining, cells were washed twice with DPBS and dried under the hood. The number of CFU was counted in each Petri dish. Colonies with less than 20 cells were not considered. At least four replicates were carried out. The number of CFU is presented as means ± standard error of all colonies in all Petri dishes.

2.7. Statistical analysis

All values presented in this work are mean ± standard error of the mean of two replicates (n=2). Student's t-tests (nonparametric test) were used to compare means. $P < 0.05$ was chosen as the level of significance. All comparisons were made using two-tailed statistical tests.

3. Results and Discussion

3.1. Bioreactors configuration, hydrodynamics parameters and operation

Although mixing and mass transfer in conventional stirred-tank bioreactor (STB) have been extensively characterized over the years (Chisti, 1993; Nienow, 1997), the performance of biological systems under specific

environmental conditions is still difficult to understand and predict. This is especially true for complex systems such as microcarrier-based cell cultures; highly sensitive to shear stresses, making it difficult to fine-tune the necessary mixing power in bioreactors during process scale-up while maintaining microcarriers uniformly suspended, shear stresses below a damaging level, and providing sufficient mass transfer to achieve high cell volumetric concentration.

The aim for many of the novel mixing regimes designed into single-use bioreactor (SUB), such as the Vertical-Wheel™ bioreactor (PBS-VW), STB, rocking-motion and orbitally shaken bioreactors, is to provide an environment that further enhances cellular productivity while maintaining mixing performance for optimal cell growth (van Eikenhorst et al., 2014). Löffelholz et al., 2010 showed that the size, geometry, and position of the PBS-VW bioreactor leads to a uniform distribution of the hydrodynamic forces (Löffelholz et al., 2010a). Consequently, maximum local energy dissipation rate ($2x10^3$ W/m^3), and maximum wall shear stress (1.7 N/m^2) calculated are within the range of values that animal cells can tolerate (Godoy-Silva et al., 2009a; Tramper et al., 1986; Vickroy et al., 2007). Furthermore, the power input generated by the Vertical-Wheel, P_{VW}, is significantly lower than a Rushton turbine, one of the types of impellers frequently used for the culture of animal cells in STB. In a different study, Löffelholz et al., 2010, showed that PBS-VW bioreactor exhibited a greater degree of fluid dynamic homogeneity and that the energy dissipation rate generated at higher wheel speeds is lower when compared with other SUB namely the Mobius™ CellReady® 3 L STB and rocking-motion bioreactor Cultibag RM (Löffelholz et al., 2010b). Vertical-Wheel bioreactors and orbitally shaken technology bioreactors are described as low shear stress bioreactors even under maximum agitation capacities (Löffelholz et al., 2010a; Tissot et al., 2011).

In order to evaluate the suitability of Vertical-Wheel™ bioreactor 3 L (PBS-3) for microcarrier applications, key hydrodynamic parameters were estimated, namely (1) energy dissipation rate (EDR, ε), (2) mixing time (t_m), (3) Kolmogorov eddy size (KES,λ) and (4) shear stress rate (SSR, τ) and compared with the values determined for STB (**Table 4.3**).

Table 4.3. Energy dissipation rate, mixing time, Kolmogorov eddy size and shear stress rate estimated for culturing A549 cells and hMSC in PBS-3 and STB.

Cell line	A549 Culture		hMSC culture	
Bioreactor	**PBS-3**	**STB**	**PBS-3**	**STB**
Agitation rate (rpm)	20	90-110	17	40-45
EDR (W/m^3)	0.5	Average: 0.4-0.8 Impeller: 3.6-6.6	0.3	Average: 0.1-0.2 Impeller: 0.6-0.8
t_m (sec)	16	26	18	56
KES (μm)	133	Average: 167-144 Impeller: 99-85	151	Average: 220-202 Impeller: 157-143
SSR (N/m^2)	0.07	Average: 0.022-0.041 Impeller: 0.050-0.068	0.021	Average: 0.008-0.010 Impeller: 0.019-0.024

EDR - Energy dissipation rate; KES - Kolmogorov eddy size; PBS-3 - Vertical-Wheel™ 3 L; SSR - Shear stress rate; STB - Stirred-tank bioreactor. t_m - mixing time.

To determine the minimum agitation rate for cell culture, $N_{c,min}$, in PBS-VW, suspension experiments with 3 g/L of Cytodex™-1, and 16 and 48 g/L of Synthemax™-II microcarriers were performed. From the $N_{c,min}$ values obtained, it was decided to run the culture of A549 cells at 20 rpm and hMSCs at 17 rpm, corresponding to an EDR of 0.5 and 0.3 W/m^3, respectively. These EDR values are within the range of those estimated for STB, except for the EDR in impeller estimated for A549 cell culture (3.6-6.6 W/m^3). This may be due to particular characteristics of vessel design and impeller geometry leading to high dissipation of energy to the culture. Nonetheless, the EDR in

impeller estimated for A549 cell culture is within the non-detrimental range of values of cell growth (Chalmers and Ma, 2015). The mixing studies were performed in the PBS-VW using conductivity measurements and salt bolus additions. In fact, the mixing characterization of one bioreactor is normally performed by investigating the fluid flows of an inert tracer inside the vessel aiming to establish numerical correlations to predict the time needed to reach homogeneity inside an STB. In the last decades, numerical correlations have been established (Grenville and Ruszkowski, 1995; Ruszkowski, 1994) and have been shown to correlate well with the t_m predicted by CFD data (Kaiser et al., 2011). Based on such results and since no experimental data was generated to estimate the t_m in the STB, it was decided to use a numerical correlation for this purpose. For both cultures, the t_m estimated for PBS-3 (16 s and 18 s for A549 cells and hMSC, respectively) was lower than for STB (26 s and 56 s for A549 cells and hMSC, respectively). The reason for this observation may lie on the greater degree of fluid dynamic homogeneity observed in PBS-3 when compared with STB as described by others (Löffelholz et al., 2010b). To provide engineering correlations to guide the design of STB for microcarrier cultures, Croughan et al. (1987) have established a relationship between Kolmogorov length scale (KLS) and cell growth inhibition and death rates (Croughan et al., 1987) identifying a critical threshold for KES above which no harm to cells occurs. For cell culture on microcarriers, this threshold corresponds to approximately 130 μm (Croughan et al., 1987). The estimated KES values for PBS-3 and average KES in STB are above that critical length: the lowest value estimate was 133 μm for PBS-3 (**Table 4.3**). On the other hand, the estimated impeller KES for A549 cell cultures in STB is below this value. This is an expected value that can be justified by the high dissipation of energy to the culture in such STB used; high EDR leads to the formation of eddies with small size in the impeller region that can interfere with cell growth extent. Nonetheless, the volume

occupied by the impeller in STB is small thus making the average KES the most appropriate correlation for hydrodynamic characterization of the cell culture. In contrast, since the Vertical-Wheel™ accounts for almost 85 % of the width of the U-shaped bottom of PBS-VW, impeller KES is the most appropriate value to characterize cell culture in this bioreactor. Shear stress is an essential parameter for the design and operation of STB used for cultivations involving shear-sensitive cells. This is an important engineering correlation since it is a function not only of the impeller speed or EDR but also of the density and rheological properties of culture medium. From the several descriptions available in the literature for microcarrier cultures, Croughan et al. (1987) reported shear stress levels detrimental for cell growth roughly an order-of-magnitude higher than those estimated in our study for the culture conditions used (**Table 4.3**) (Croughan et al., 1987).

Although different bioreactor scales of PBS-3 (2.2 L wv) and STB (0.2 and 0.25 L wv) were used in this study, we believe that the results reported in the following sections can be directly compared. STB has been used for decades and during this period, engineering/hydrodynamic parameters have been extensively explored and used to assist the transfer of processes from the lab (e.g., 2 L) to manufacturing scale (e.g., > 500 L). Importantly, in all these scaling-up processes, the main objective is to maintain constant as much many hydrodynamic parameters as possible. Translating this concept to our study, the results obtained with a 0.2 L can be comparable to a 2 L scale as long as the hydrodynamic conditions are kept similar.

3.2. A549 cells growth and oncolytic adenovirus 5 production

The performance of PBS-VW and STB for A549 cells and oncolytic adenovirus type 5 (OV-Ad5) was evaluated based on the following parameters: cell attachment, microcarrier colonization, cell growth, maximum cell concentration, infection kinetics, OV-Ad5 production, ratio of viral

genomes (vg) to infectious particles (ip) (ratio vg/ip), and metabolite consumption/production.

The kinetic of cell attachment to the microcarriers was assessed at 0, 2, 6, 24, and 48 h (**Figures 4.2A and B**). The highest cell attachment rate was observed for the PBS-3 with approximately 100 % of microcarriers being colonized at 6 h compared with 85 % in the STB (**Figure 4.2B**). After 12 h, many cells in the PBS-3 were already flattening onto the substrate while it took 24 h before flattening of the cells was observed in STB (**Figure 4.2A**). This enhanced performance might be explained by the efficient homogeneous mixing inherent to PBS-VW (**Table 4.3**). Although low shear stress is beneficial throughout the culture process, it can be particularly advantageous during the cell-microcarrier attachment phase, as this is the period when attachment forces are weakest. As expected, the better microcarrier colonization observed in the PBS-3 resulted in faster cell growth, 0.037 1/h vs. 0.018 1/h for STB, and higher maximum cell density at the time of infection, $1.0x10^6$ cell/mL vs. $0.6x10^6$ cell/mL for STB (**Figure 4.2C**).

A549 cells were infected with OV-Ad5 viruses at 50 h with multiplicity of infection (MOI) of 10 ip/cell. After infection, cell growth was arrested (**Figure 4.2C**). The cell concentration decrease observed 24 h after the infection is a consequence of the infection process itself, as reported previously by our group and others (Altaras et al., 2005; Silva et al., 2015).

The specific rates of glucose consumption and lactate production were estimated. In both bioreactor types, no depletion of glucose was observed and the build-up of lactate never achieved toxic values as defined elsewhere (Cruz et al., 2000) (**Supporting information Figure S4.1**). The specific rates of glucose consumption and lactate production were estimated. In both bioreactor types, no depletion of glucose was observed and the build-up

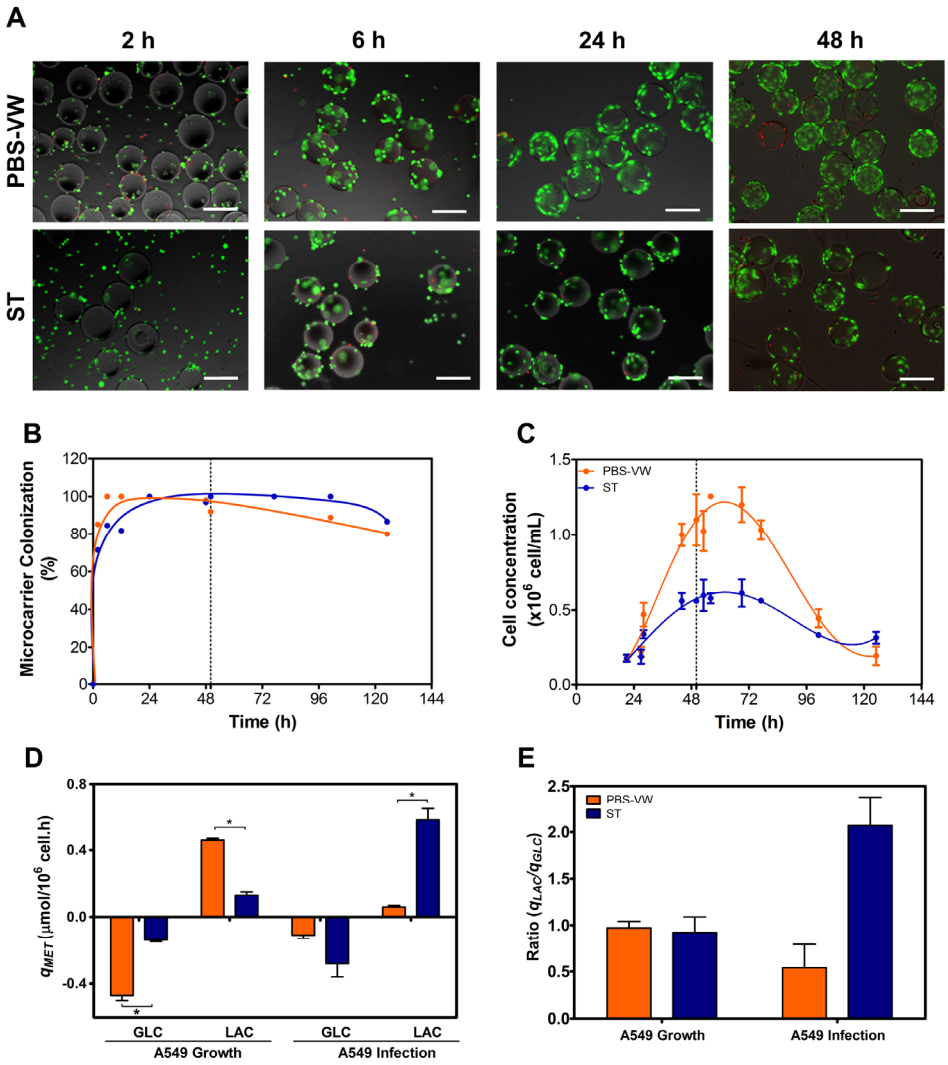

Figure 4.2. A549 cell culture in PBS-3 and STB. **(A)** Representative images of A549 cells at 2, 6, 24, and 48 h of culture (green: live cells stained with FDA; red: dead cells stained with PI; scale bars: 200 µm). **(B)** Percentage of colonized microcarriers and **(C)** cell growth curves, expressed in terms of cell concentration per volume of medium, in PBS-3 (orange circles) and STB (blue circles) with dashed lines denoting the time of A549 cells infection with OV-Ad5. **(D)** Specific rates of glucose (GLC) consumption and lactate (LAC) production as well as **(E)** apparent yields of lactate-to-glucose estimated during A549 cells growth and infection phases in PBS-3 (orange bars) and STB (blue bars). Data are mean ± standard deviation of two replicates. Asterisks indicate significant difference (*P<0.05). PBS-VW - Vertical-Wheel™ bioreactor. PBS-3 - Vertical-Wheel™ bioreactor 3 L. ST - Stirred-tank (bioreactor).

of lactate never achieved toxic values as defined elsewhere (Cruz et al., 2000) (**Supporting information Figure S4.1**). During cell growth, these specific rates were significantly higher in the PBS-3 (~3.5 times) than in STB (**Figure 4.2D**). This can be explained by the faster cell growth observed in the PBS-3. Despite the differences in specific production/consumption rates, similar Lac/Glc yields were obtained in both bioreactors, 0.97 ± 0.07 in PBS-3 and 0.92 ± 0.17 in STB (**Figure 4.2E**), indicating that cells have similar metabolic fingerprints. After infection, an increase in glucose consumption and lactate production specific rates ($q_{Glc} = 0.28 \pm 0.08$ μmol/(10^6 cell.h)) and ($q_{Lac} = 0.58 \pm 0.07$ μmol/(10^6 cell.h)) was observed in STB, which also resulted in a 2-fold increase in the Lac/Glc yield when compared with the cell growth phase (**Figures 4.2D and E**). In contrast, the specific rates of glucose consumption and lactate production estimated in the PBS-3 were lower after infection than during cell growth, leading to a decrease in the Lac/Glc yield (**Figure 4.2E**). The metabolic shift observed after infection is a very well described phenomenon in processes involving cells infection by viruses (Carinhas et al., 2010). Although we may speculate that the metabolic differences observed between PBS-3 and STB are related with the hydrodynamics of the system used, further studies should be done to confirm this (e.g., analysis of intracellular metabolites and metabolic flux analysis).

The production of OV-Ad5 was estimated at 72 h post-infection (pi) by $TCID_{50}$ (infectious particles) and real-time quantitative PCR (qPCR) (viral genomes). The number of infectious viruses generated per cell is slightly higher in PBS-3 ($6.3 \pm 3.1 \times 10^2$ ip/cell) than in STB ($4.3 \pm 0.9 \times 10^2$ ip/cell). Likewise, the volumetric concentration achieved in the PBS-3 is higher ($6.3 \pm 3.0 \times 10^8$ ip/mL) when compared with STB ($2.6 \pm 0.5 \times 10^8$ ip/mL) (**Figure 4.3A**). This is correlated with the higher cell density achieved in the PBS-3. The scenario changes when looking at the data for viral genomes, with the

number of viral genomes generated per cell higher in STB (6.5 ± 1.2x10^4 vg/cell) than in the PBS-3 (4.0 ± 0.5x10^4 vg/cell). In addition, the volumetric concentrations achieved in both bioreactor types are quite similar (4.0 ± 0.2x10^{10} in PBS-3 and 3.9 ± 0.6x10^{10} vg/mL in STB) (**Figure 4.3B**). Importantly, apart from the difference observed, those concentrations of viral genomes generated per cell are within the range of values reported in the literature using both A549 and HEK293 cells (10^4 and 10^5 vg/cell) (Vellinga et al., 2014).

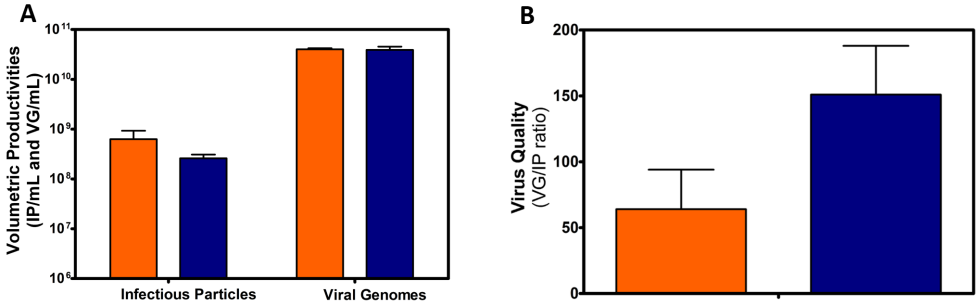

Figure 4.3. Characterization of OV-Ad5 production in PBS-3 and STB. **(A)** Volumetric productivities of infectious particles and viral genomes as well as **(B)** viral genomes per infectious particles ratio obtained in PBS-3 (orange bars) and STB (blue bars). Data are mean ± standard deviation of 2 replicates.

A key parameter in processes related to the production of vectors for gene therapy is the ratio of viral genomes per infectious particles (vg/ip). For this type of application, an Food and Drug Administration Advisory Committee recommended a targeted vg/ip ratio below 30 (Simek et al., 2002). In this study, the ratios vg/ip estimated for the STB and PBS-3 were 151 ± 37 and 64 ± 30 vg/ip, respectively (**Figure 4.3B**). Although these values are well above the recommended target, it is important to highlight that the PBS-3 induced a vg/ip ratio 2.5 times lower than the STB. In terms of downstream processing, this represents a significant advantage as the separation of non-infectious viruses from infectious viruses is difficult.

3.2. hMSC production

The impact of bioreactor design on the growth, metabolism, and quality of hMSC derived from bone marrow was evaluated based on the following parameters: seeding efficiency and microcarrier colonization, growth rate and expansion factor, actin organization, apoptosis, metabolite consumption/production, and hMSC phenotype.

An intermittent agitation scheme was used to promote cell attachment during the first hours after inoculation (**Table 4.2**). Using this strategy, more than 95 % of seeded hMSC attached to microcarriers 12 h after inoculation in both types of bioreactor cultures. Despite these similar seeding efficiencies, a higher percentage of colonized beads were attained in the PBS-3 (68 $\pm$ 6 %) when compared with STB (48 $\pm$ 16 %) (**Figures 4.4A and B**). These results might be a direct consequence of the more efficient and gentle mixing characteristics of PBS-3 (**Table 3.3**). At day 6, empty microcarriers were added to the cultures to provide additional area available for cell growth, as described previously (Hervy et al., 2014). In both bioreactor systems, hMSC were able to migrate to empty microcarriers and proliferate (**Figures 4.4B,C and 4.5A**). Again, the percentage of colonized microcarriers was higher in the PBS-3 from day 7 to day 12 (**Figure 4.4B**), confirming that cell migration was more efficient in this system. The more homogenous microcarrier colonization and better migration efficiency observed in the PBS-3 bioreactor resulted in higher percentages of proliferative cells and were significantly different at days 3 and 9 of culture when compared with STB (**Figure 4.4A**). However, the differences observed in cell volumetric concentrations between PBS-3 and STB throughout culture time (**Figure 4.4C**) were not statistically significant; in both bioreactor systems hMSC displayed similar maximum growth rates (0.012 1/h in PBS-3 vs. 0.010 1/h in STB) and expansion factors (12 and 11, respectively). The

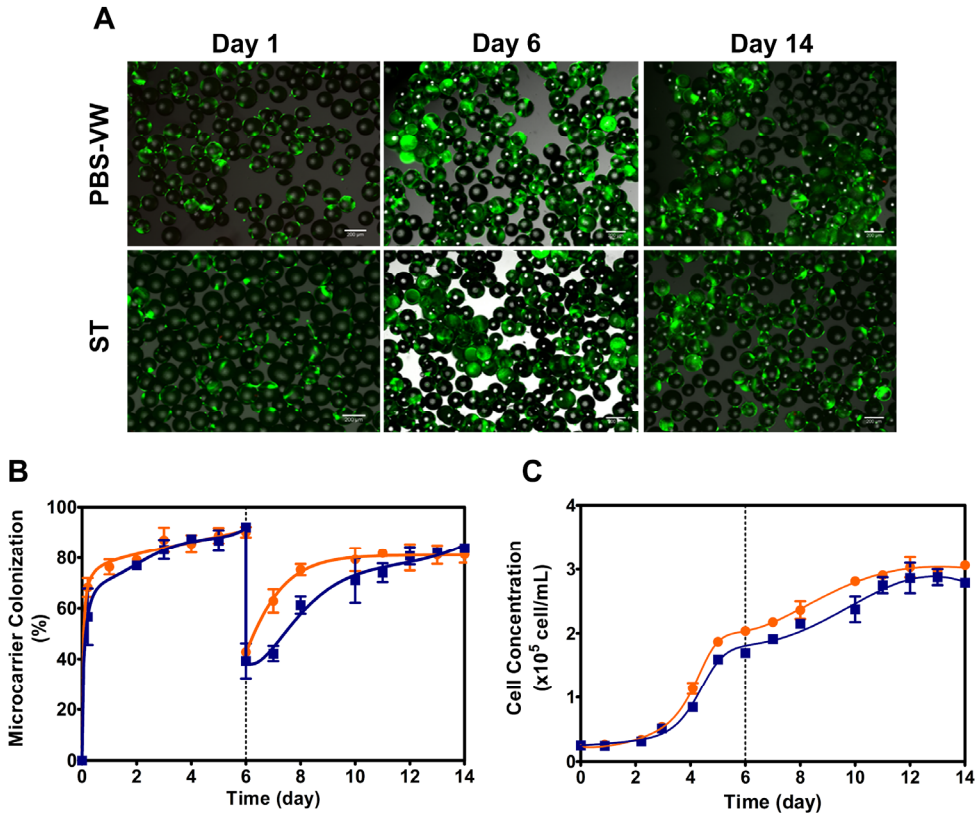

Figure 4.4. Human Mesenchymal Stem Cells expansion in PBS-3 and STB. **(A)** Representative images of hMSC at day 1 of culture (green: live cells stained with FDA; red: dead cells stained with PI; scale bars: 200 μm). (B) Percentage of colonized microcarriers and (C) cell growth curves, expressed in terms of cell concentration per volume of medium, in PBS-3 (orange circles) and STB (blue circles). Data are mean ± standard deviation of two replicates. PBS-VW - Vertical-Wheel™ bioreactor. PBS-3 - Vertical-Wheel™ bioreactor 3 L. ST - Stirred-tank (bioreactor).

maximum cell concentration achieved in both bioreactor systems (~ $3x10^5$ cell/mL) was lower than other reports in the literature (Caruso et al., 2014; Goh et al., 2013; Dos Santos et al., 2014). The difference in the cell growth profile may reflect the distinct cell origins (hMSC were isolated from the bone marrow of different donors), and the different culture conditions such as the microcarrier type, medium formulation, culture system, and operation mode.

It is important to highlight that in our study, hMSC were cultured under well-defined conditions using synthetic microcarriers and xeno- and serum-free culture medium, which facilitates process transfer to a cGMP compliant environment. Further studies should be carried out in the future to test hMSC derived from different tissue origins and isolated from different donors to confirm the robustness of the PBS-3 process implemented in this study and integrate biological variability.

Actin organization is believed to play a pivotal role in hMSC phenotype (Mammoto and Ingber, 2009) and proliferation capacity (Sart et al., 2013). Bioreactor design did not impact the actin organization since the hMSC displaying organized actin fibers were observed in both culture systems at days 6 and 14 (**Figures 4.5B and C**). The percentage of apoptotic cells was also assessed at these time points. Although no differences were observed at day 6, a significantly higher percentage of apoptotic cells were observed in STB at day 14 (**Figure 4.5D**). These results might be explained by the lower shear stress and more efficient mixing environment of PBS-3 (**Table 3.3**). The consumption of glucose and glutamine, as well as the production of lactate and ammonia, were monitored throughout the culture period (**Figure 4.5E**). Results show that bioreactor design did not impact cell metabolism since similar consumption and production rates were observed. The yield Lac/Glc ($Y_{LAC/GLC}$) was approximately 2 for both bioreactor types, which is in accordance with results described in the literature for various types of stem cells during the self-renewal process (Zhang et al., 2012). Measurements of the concentrations of glucose and glutamine showed no complete depletion of these nutrients during the culture period (**Supporting information Figure S4.2**). Moreover, the accumulation of lactate and ammonia was always below the growth-inhibitory concentrations (Schop et al., 2010) (< 8 and < 1 mM, respectively). It is well known that the cellular and immunophenotype of hMSC depend on the isolation protocol and on the

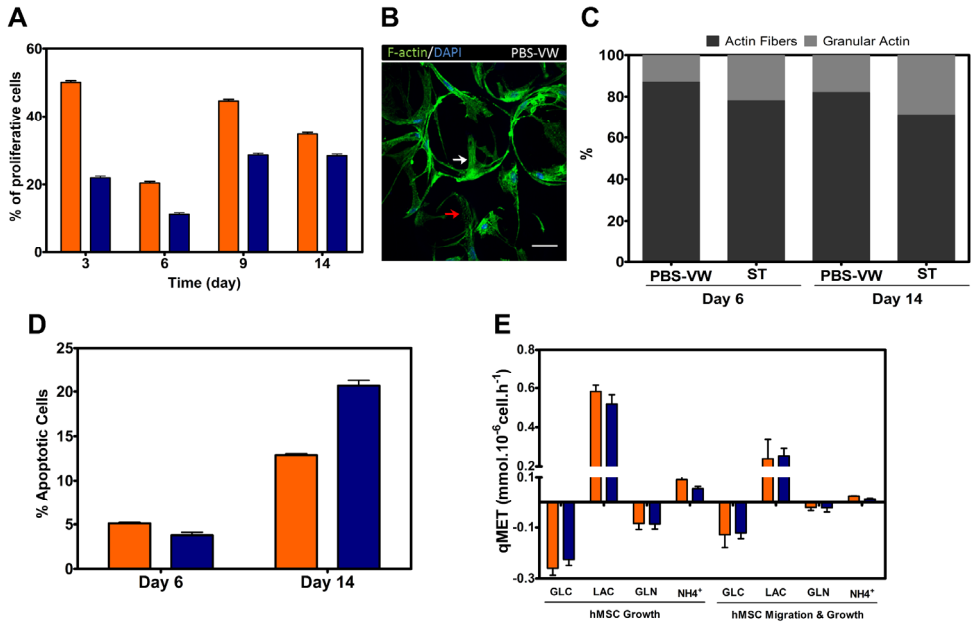

Figure 4.5. Characterization of hMSC during expansion in PBS-3 and STB. **(A)** Percentage of proliferative cells evaluated at days 3, 6, 9, and 14 of culture in PBS-3 (orange bars) and ST B(blue bars) using Click-iT EdU flow cytometry assay kit. **(B)** Representative image of actin organization of hMSC attached to microcarriers in PBS-3 at day 6, assessed by cell staining with phalloidin FITC (green; nuclei stained in blue); white arrows show cortical actin and red arrows show globular actin (scale bar: 50 mm). **(C)** Percentage of hMSC with actin fibers (dark gray bars) or granular actin (light gray bars) organization estimated by microscopic evaluation. **(D)** Percentage of apoptotic cells assessed by NucView^{TM} dye and flow cytometry at days 6 and 14. Data are mean ± standard deviation of two measurements. **(E)** Specific rates of glucose (GLC) and glutamine (GLN) consumption and lactate (LAC) and ammonia (NH_3) production for hMSC growth and migration and growth phases in PBS-3 (orange bars) and STB (blue bars). Data of hMSC growth phase are mean ± standard deviation of the mean of two independent experiments; data of hMSC growth and migration phase are mean ± standard deviation of two replicates. Asterisks indicate the significant difference (*P<0.05). PBS-VW - Vertical-Wheel^{TM} bioreactor. PBS-3 - Vertical-Wheel^{TM} bioreactor 3 L. ST - Stirred-tank (bioreactor).

culture conditions (Bocelli-Tyndall et al., 2015; Sotiropoulou et al., 2006). Our results showed that both bioreactor types were able to maintain the hMSC cellular phenotype; hMSC were negative for hematopoietic CD34 and CD45

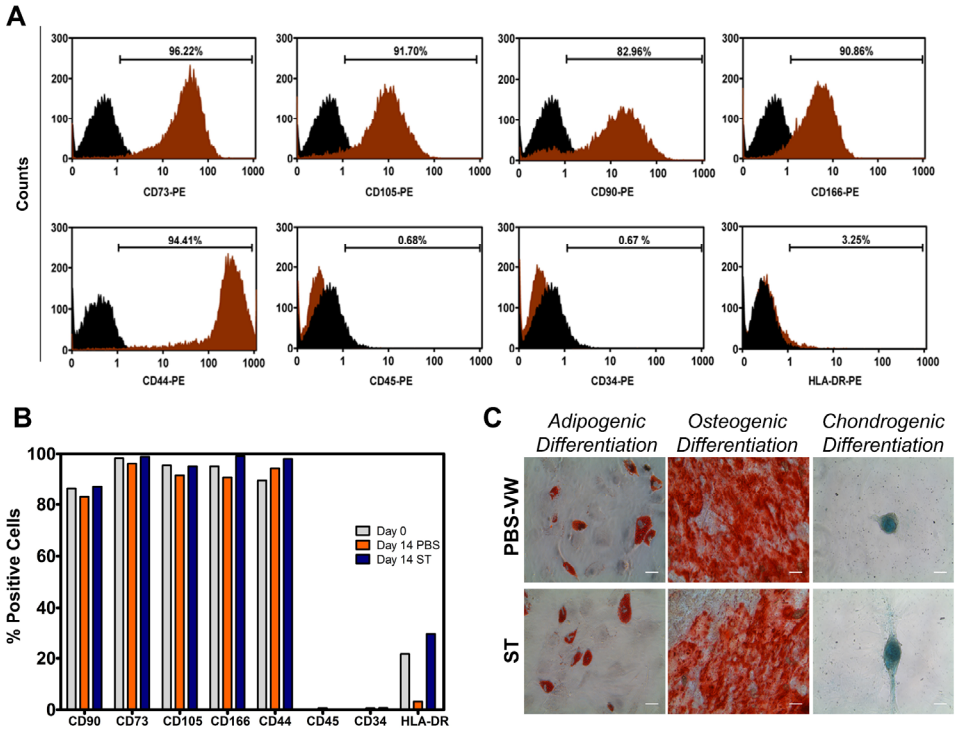

Figure 4.6. Quality control assays of hMSC expanded in PBS-3 and STB. **(A,B)** Flow cytometry analysis of percentages of hMSC markers CD90, CD73, CD105, CD166, CD44, and non-hMSC markers CD45, CD34, as well as HLA-DR at day 0 (grey bars) and day 14 after expansion in PBS-3 (orange bars) and STB (blue bars). Representative histograms from flow cytometry analysis of hMSC after expansion in PBS-3 are included in **(A)**. **(C)** Multilineage differentiation potential of hMSC expanded in each bioreactor; cell differentiation was induced for up to 21 days then assessed by staining for adipogenesis (Oil Red-O), osteogenesis (Alizarin red), and chondrogenesis (Alcian blue); (Scale bar: 100 μm). Asterisks indicate significant difference (* $P < 0.05$). PBS-VW or PBS - Vertical-Wheel^{TM} bioreactor. ST - Stirred-tank (bioreactor).

markers and displayed high levels of CD44, CD73, CD105, CD90, and CD166 mesenchymal stem markers (**Figures 4.6A and B**). According to the International Society for Cellular Therapy, hMSC are also considered HLA-DR-negative with no/reduced (below 5 %) expression of HLA-DR surface molecules (Dominici et al., 2006). Importantly, in our work, we demonstrated

that the percentage of HLA-DR positive cells was significantly reduced when hMSC were cultured in PBS-3 (from 22 % at the inoculum time to 3 % at day 14) than the cells expanded in STB (30% at day 14) (**Figure 4.6B**), suggesting that it might be the consequence of the different bioreactor design and hydrodynamics. Finally, in both bioreactor strategies, expanded hMSC were able to reattach on plastic surfaces and presented the ability to form colony forming units colony forming unit (CFU), showing similar number of colonies (83 $\pm$9 in PBS-VW and 83 $\pm$5 in STB). The multipotent differentiation potential of hMSC was similar in both PBS-3 and STB since they could successfully differentiate into adipocytes, osteocytes, and chondrocytes (**Figure 4.6C**). No spontaneous differentiation was observed (data not shown). In future studies it will also be important to evaluate whether the gene expression profile and the paracrine activity of hMSC are affected by the expansion process using different bioreactor systems. It has been described in the literature that the cell culture system (planar technologies vs. microcarrier-based stirred systems) and operation conditions (e.g., hypoxia) greatly impacts and regulates the secretion of bioactive molecules such as growth factors, immune-modulating and anti-inflammatory molecules, and anti-cancer factors (Hupfeld et al., 2014; Madrigal et al., 2014).

4. CONCLUSION

This study demonstrates the applicability of Vertical-Wheel™ bioreactor (PBS-VW) for microcarrier-based cell culture processes. Hydrodynamic studies and calculations were performed in this bioreactor, allowing for the estimation of key hydrodynamic parameters such energy dissipation rate (EDR), mixing time (t_m) and Kolmogorov eddy size. The performance of a Vertical-Wheel™ bioreactor 3 L (PBS-3) was then evaluated for (i) A549 cells growth and production of oncolytic adenovirus type 5 (OV-Ad5) and (ii)

human Mesenchymal Stem Cells (hMSC) expansion.

For the first cell model, faster cell attachment, more homogeneous microcarrier colonization, faster cell growth and higher maximum cell concentration were achieved with the PBS-3 when compared with stirred-tank bioreactor (STB). Regarding OV-Ad5 production, the number of infectious viruses generated per cell or per mL was slightly higher in PBS-3 than in the STB. In terms of cell metabolism, both the PBS-3 and STB show similar metabolic fingerprints (q_{Glc} and yield Lac/Glc) before infection. However, upon infection the scenario changes, with the STB showing Lac/Glc yields 2.5-fold higher when compared with the PBS-3. Although this may indicate a more rational utilization of nutrients by the cells upon infection in the PBS-VW, further studies are required to validate such a hypothesis.

In hMSC cultures, a higher percentage of proliferative cells were observed in PBS-3 when compared with STB. However, this does not translate into significant differences in cell volumetric concentration, expansion factor, or metabolic performance. Both bioreactor system types investigated here were able to maintain the hMSC phenotype and multipotent differentiation potential. Noteworthy, the hMSC population generated in the PBS-3 showed a significantly lower percentage of apoptotic cells as well as reduced levels of HLA-DR positive cells when compared with the cells produced in the STB, which may be an important finding for the clinical application of these cells. Further studies are required to understand the effect of bioreactor hydrodynamics and culture conditions in modulating HLA-DR surface expression of hMSC.

Overall, these results show that process transfer from STB to PBS-3 and scale-up was successfully carried out for two different microcarrier-based cell cultures. Concerning a new three-dimensional manufacturing platform for gene and cell therapy process development, PBS-VW bioreactors offer

benefits over STB. In particular, the low shear stress mixing environment of PBS-VW address the key scalability limitation of existing platforms and thus they are positioned to become a potential boon for the needs of emerging cell therapy applications.

5. ACKNOWLEDGMENTS

The authors acknowledge João Sá and Dr Manuel Garrido for technical support. We thank Marie-Maud Bear, Sebastien P. Chauvel and Stephen J. Caracci (from Corning Inc.) for providing the Synthemax™-II microcarriers used in this work. Conflicts of interest: Brian Lee is CEO and Co-Founder of PBS Biotech. Daniel Giroux, Yas Hashimura and Robin Wesselschmidt are employees of PBS Biotech. Manuel J. T. Carrondo and Paula M. Alves are members of the Advisory Board of PBS Biotech. This does not alter the authors' adherence to all the policies of the journal on sharing data and materials.

6. SUPPORTING INFORMATION

6.1. Supplementary material

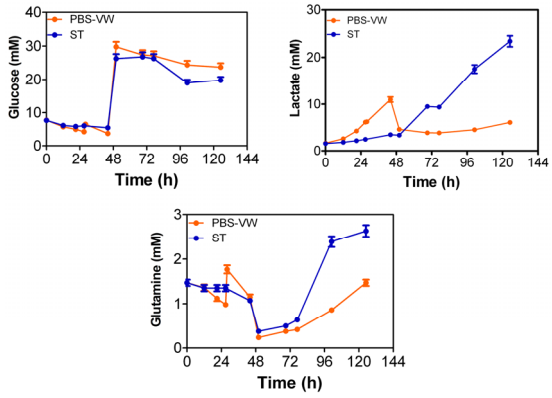

Supplementary Figure S4.1. Metabolite concentration profiles during A549 growth and infection with oncolytic adenovirus type 5 for glucose, lactate and glutamine. PBS-VW - Vertical-Wheel™ bioreactor. ST - Stirred-tank (bioreactor).

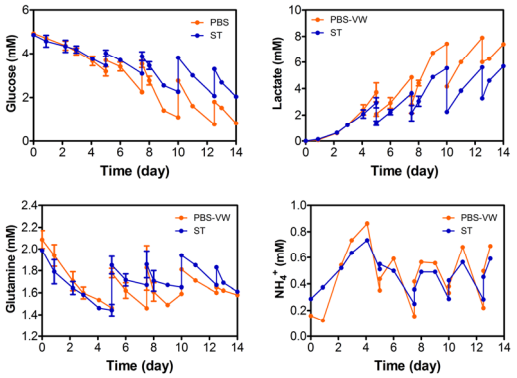

Supplementary Figure S4.2. Metabolite concentration profiles during human Mesenchymal Stem Cells growth (expansion and migration) for glucose, lactate, glutamine, and ammonia (NH_4^+). PBS-VW - Vertical-Wheel™ bioreactor. ST - Stirred-tank (bioreactor).

7. REFERENCES

Alexander J, Mendy J, Vang L, Avanzini JB, Garduno F, Manayani DJ, Ishioka G, Farness P, Ping L-H, Swanstrom R, Parks R, Liao H-X, Haynes BF, Montefiori DC, LaBranche C, Smith J, Gurwith M, Mayall T. 2013. Pre-clinical development of a recombinant, replication-competent adenovirus serotype 4 vector vaccine expressing HIV-1 envelope 1086 clade C. *PLoS One* **8**:e82380.

Altaras NE, Aunins JG, Evans RK, Kamen A, Konz JO, Wolf JJ. 2005. Production and formulation of adenovirus vectors. *Adv. Biochem. Eng. Biotechnol.* **99**:193–260.

Alves PM, Moreira JL, Rodrigues JM, Aunins JG, Carrondo MJ. 1996. Two-dimensional versus three-dimensional culture systems: Effects on growth and productivity of BHK cells. *Biotechnol. Bioeng.* **52**:429–432.

Bocelli-Tyndall C, Trella E, Frachet A, Zajac P, Pfaff D, Geurts J, Heiler S, Barbero A, Mumme M, Resink TJ, Schaeren S, Spagnoli GC, Tyndall A. 2015. FGF2 induces RANKL gene expression as well as IL1β regulated MHC class II in human bone marrow-derived mesenchymal progenitor stromal cells. *Ann. Rheum. Dis.* **74**:260–266.

Carinhas N, Bernal V, Monteiro F, Carrondo MJT, Oliveira R, Alves PM. 2010. Improving baculovirus production at high cell density through manipulation of energy metabolism. **12**:39–52.

Caruso SR, Orellana MD, Mizukami A, Fernandes TR, Fontes AM, Suazo CAT, Oliveira VC, Covas DT, Swiech K. 2014. Growth and functional harvesting of human mesenchymal stromal cells cultured on a microcarrier-based system.

Biotechnol. Prog. **30**:889–895.

Chalmers J, Ma N. 2015. Hydrodynamic Damage to Animal Cells. In: . *Anim. Cell Cult. Cell Eng. vol 9. Springer, Cham*, Vol. 9, pp. 168–183.

Chisti Y. 1993. Animal cell culture in stirred bioreactors: observations on scale-up. *Process Biochem.* **28**:511–517. http://www.sciencedirect.com/science/article/pii/0032959293850125.

Correia C, Serra M, Espinha N, Sousa M, Brito C, Burkert K, Zheng Y, Hescheler J, Carrondo MJT, Šarić T, Alves PM. 2014. Combining Hypoxia and Bioreactor Hydrodynamics Boosts Induced Pluripotent Stem Cell Differentiation Towards Cardiomyocytes. *Stem Cell Rev. Reports* **10**:786–801.

Croughan MS, Hamel JF, Wang DI. 1987. Hydrodynamic effects on animal cells grown in microcarrier cultures. *Biotechnol. Bioeng.* **29**:130–41. http://www.ncbi.nlm.nih.gov/pubmed/18561137.

Croughan MS, Hamel JPJP, Wang DIC. 1988. Effects of microcarrier concentration in animal cell culture. *Biotechnol. Bioeng.* **32**:975–982.

Cruz HJ, Freitas CM, Alves PM, Moreira JL, Carrondo MJ. 2000. Effects of ammonia and lactate on growth, metabolism, and productivity of BHK cells. *Enzyme Microb. Technol.* **27**:43–52.

Cruz PE, Cunha A, Peixoto CC, Clemente J, Moreira JL, Carrondo MJT. 1998. Optimization of the production of virus-like particles in insect cells. *Biotechnol. Bioeng.* **60**:408–418.

Cunha B, Aguiar T, Silva MM, Silva RJS, Sousa MFQ, Pineda E, Peixoto C, Carrondo MJT, Serra M, Alves PM. 2015a. Exploring continuous and integrated strategies for the up- and downstream processing of human mesenchymal stem cells. *J. Biotechnol.*

Cunha B, Peixoto C, Silva MM, Carrondo MJT, Serra M, Alves PM. 2015b. Filtration methodologies for the clarification and concentration of human mesenchymal stem cells. *J. Memb. Sci.* **478**:117–129. http://www.sciencedirect.com/science/article/pii/S0376738814009442.

Darling AJ, Boose JA, Spaltro J. 1998. Virus Assay Methods: Accuracy and Validation. *Biologicals* **26**:105–110. http://www.sciencedirect.com/science/article/pii/S1045105698901348.

Dominici M, Le Blanc K, Mueller I, Slaper-Cortenbach I, Marini F, Krause D, Deans R, Keating A, Prockop D, Horwitz E. 2006. Minimal criteria for defining multipotent mesenchymal stromal cells. The International Society for Cellular Therapy position statement. *Cytotherapy* **8**:315–317.

van Eikenhorst G, Thomassen YE, van der Pol LA, Bakker WAM. 2014. Assessment of mass transfer and mixing in rigid lab-scale disposable bioreactors at low

power input levels. *Biotechnol. Prog.* **30**:1269–1276.

Fernandes P, Peixoto C, Santiago VM, Kremer EJ, Coroadinha AS, Alves PM. 2012. Bioprocess development for canine adenovirus type 2 vectors. *Gene Ther.* **20**:353–360. https://doi.org/10.1038/gt.2012.52.

Godoy-Silva R, Chalmers JJ, Casnocha SA, Ma N, Bass LA, Ma N. 2009a. Quantitative Study of physiological responses of CHO cells to repetitive hydrodynamic stress. *Biotechnol. Bioeng.* **103**:1103–1117.

Goh TK-P, Zhang Z-Y, Chen AK-L, Reuveny S, Choolani M, Chan JKY, Oh SK-W. 2013. Microcarrier culture for efficient expansion and osteogenic differentiation of human fetal mesenchymal stem cells. *Biores. Open Access* **2**:84–97.

Grenville K, Ruszkowski S. 1995. Blending of miscible liquids in the turbulent and transional regimes. In: . *15th NAMF Mix. Conf. Canada*.

Hashimura Y, Giroux D, Lee B. 2012. Designing the ideal bioreactor with single-use technology. *Bioprocess Int.* **10**.

Hervy M, Weber JL, Pecheul M, Dolley-Sonneville P, Henry D, Zhou Y, Melkoumian Z. 2014. Long term expansion of bone marrow-derived hMSCs on novel synthetic microcarriers in xeno-free, defined conditions. *PLoS One* **9**:e92120.

Hupfeld J, Gorr IH, Schwald C, Beaucamp N, Wiechmann K, Kuentzer K, Huss R, Rieger B, Neubauer M, Wegmeyer H. 2014. Modulation of mesenchymal stromal cell characteristics by microcarrier culture in bioreactors. *Biotechnol. Bioeng.* **111**:2290–2302.

Kaiser SC, Loffelholz C, Werner SS, Eibl D, Kaiser S, Löffelholz C, Werner SS, Eibl D, C. S, Loffelholz C, Werner SS, Eibl D. 2011. CFD for Characterizing Standard and Single-use Stirred Cell Culture Bioreactors. In: . *Comput. Fluid Dyn. Technol. Appl.*, pp. 97–122.

Kovesdi I, Hedley SJ. 2010. Adenoviral producer cells. *Viruses* **2**:1681–703.

Löffelholz C, Kaiser S, Werner S. 2010a. Single-Use Technology in Biopharmaceutical Manufacture. *Hoboken, NJ John Wiley Sons, Inc*.

Löffelholz C, Kaiser SC, Werner S, Eibl D. 2010b. CFD as a Tool to Characterize Single-Use Bioreactors. *Single-Use Technol. Biopharm. Manuf.* Wiley Online Books. https://doi.org/10.1002/9780470909997.ch22.

Madrigal M, Rao KS, Riordan NH. 2014. A review of therapeutic effects of mesenchymal stem cell secretions and induction of secretory modification by different culture methods. *J. Transl. Med.* **12**:260.

Mammoto A, Ingber DE. 2009. Cytoskeletal control of growth and cell fate switching. *Curr. Opin. Cell Biol.* **21**:864–870.

Matasci M, Hacker DL, Baldi L, Wurm FM. 2008. Recombinant therapeutic protein production in cultivated mammalian cells: current status and future prospects. *Drug Discov. Today. Technol.* **5**:e37-42.

Nienow AW. 1997. On impeller circulation and mixing effectiveness in the turbulent flow regime. *Chem. Eng. Sci.* **52**:2557–2565. http://www.sciencedirect.com/science/article/pii/S0009250997000729.

Obom KM, Cummings PJ, Ciafardoni JA, Hashimura Y, Giroux D. 2014. Cultivation of Mammalian Cells Using a Single-use Pneumatic Bioreactor System. *JoVE*:e52008. https://www.jove.com/t/52008.

Placek J, Tavlarides LL. 1985. Turbulent flow in stirred tanks. Part I: Turbulent flow in the turbine impeller region. *AIChE J.* **31**:1113–1120.

Pol J, Buqué A, Aranda F, Bloy N, Cremer I, Eggermont A, Erbs P, Fucikova J, Galon J, Limacher J-M, Preville X, Sautès-Fridman C, Spisek R, Zitvogel L, Kroemer G, Galluzzi L. 2016. Trial Watch-Oncolytic viruses and cancer therapy. *Oncoimmunology* **5**:e1117740.

Ruszkowski S. 1994. Rational method for measuring blending performance and comparison of different impeller types. *Proc. 8th Eur. Mix. Conf. I Chem E, Rugby, UK*:283–291.

Dos Santos F, Campbell A, Fernandes-Platzgummer A, Andrade PZ, Gimble JM, Wen Y, Boucher S, Vemuri MC, da Silva CL, Cabral JMS. 2014. A xenogeneic-free bioreactor system for the clinical-scale expansion of human mesenchymal stem/stromal cells. *Biotechnol. Bioeng.* **111**:1116–1127.

Sart S, Errachid A, Schneider Y-J, Agathos SN. 2013. Modulation of mesenchymal stem cell actin organization on conventional microcarriers for proliferation and differentiation in stirred bioreactors. *J. Tissue Eng. Regen. Med.* **7**:537–551.

Schop D, van Dijkhuizen-Radersma R, Borgart E, Janssen FW, Rozemuller H, Prins H-J, de Bruijn JD. 2010. Expansion of human mesenchymal stromal cells on microcarriers: growth and metabolism. *J. Tissue Eng. Regen. Med.* **4**:131–140.

Serra M, Brito C, Correia C, Alves PM. 2012. Process engineering of human pluripotent stem cells for clinical application. *Trends Biotechnol.* **30**:350–359.

Serra M, Brito C, Costa EM, Sousa MFQ, Alves PM. 2009. Integrating human stem cell expansion and neuronal differentiation in bioreactors. *BMC Biotechnol.*

Serra M, Brito C, Sousa MFQQ, Jensen J, Tostões R, Clemente J, Strehl R, Hyllner J, Carrondo MJTT, Alves PM. 2010. Improving expansion of pluripotent human embryonic stem cells in perfused bioreactors through oxygen control. *J. Biotechnol.* **148**:208–215. https://www.sciencedirect.com/science/article/pii/S0168165610002750?via%3Dihub.

Silva AC, Delgado I, Sousa MFQQ, Carrondo MJTT, Alves PM. 2008. Scalable culture systems using different cell lines for the production of Peste des Petits ruminants vaccine. *Vaccine* **26**:3305–3311.

Silva AC, Simão D, Küppers C, Lucas T, Sousa MFQ, Cruz P, Carrondo MJT, Kochanek S, Alves PM. 2015. Human amniocyte-derived cells are a promising cell host for adenoviral vector production under serum-free conditions. *Biotechnol. J.* **10**:760–771.

Simaria AS, Hassan S, Varadaraju H, Rowley J, Warren K, Vanek P, Farid SS. 2014. Allogeneic cell therapy bioprocess economics and optimization: Single-use cell expansion technologies. *Biotechnol. Bioeng.* **111**:69–83.

Simek S, Byrnes A, Bauer S. 2002. FDA Perspectives on the Use of the Adenovirus Reference Material. *BioProcess J* **1**:40–42.

Sotiropoulou PA, Perez SA, Salagianni M, Baxevanis CN, Papamichail M. 2006. Characterization of the optimal culture conditions for clinical scale production of human mesenchymal stem cells. *Stem Cells* **24**:462–471.

Tissot S, Reclari M, Quinodoz S, Dreyer M, Monteil DT, Baldi L, Hacker DL, Farhat M, Discacciati M, Quarteroni A, Wurm FM. 2011. Hydrodynamic stress in orbitally shaken bioreactors. *BMC Proc.* **5 Suppl 8**:P39.

Trabelsi K, Majoul S, Rourou S, Kallel H. 2012. Development of a measles vaccine production process in MRC-5 cells grown on Cytodex1 microcarriers and in a stirred bioreactor. *Appl. Microbiol. Biotechnol.* **93**:1031–1040. https://doi.org/10.1007/s00253-011-3574-y.

Tramper J, Williams JB, Joustra D, Vlak JM. 1986. Shear sensitivity of insect cells in suspension. *Enzyme Microb. Technol.* **8**:33–36.

Vellinga J, Smith JP, Lipiec A, Majhen D, Lemckert A, van Ooij M, Ives P, Yallop C, Custers J, Havenga M. 2014. Challenges in manufacturing adenoviral vectors for global vaccine product deployment. *Hum. Gene Ther.* **25**:318–327.

Vickroy B, Lorenz K, Kelly W. 2007. Modeling Shear Damage to Suspended CHO Cells during Cross-Flow Filtration. *Biotechnol. Prog.* **23**:194–199. https://aiche.onlinelibrary.wiley.com/doi/abs/10.1021/bp060183e.

Wei X, Yang X, Han Z, Qu F, Shao L, Shi Y. 2013. Mesenchymal stem cells: a new trend for cell therapy. *Acta Pharmacol. Sin.* **34**:747–754.

Van Wezel AL. 1967. Growth of Cell-strains and Primary Cells on Micro-carriers in Homogeneous Culture. *Nature* **216**:64–65. https://doi.org/10.1038/216064a0.

Zhang J, Nuebel E, Daley GQ, Koehler CM, Teitell MA. 2012. Metabolic regulation in pluripotent stem cells during reprogramming and self-renewal. *Cell Stem Cell* **11**:589–595.

Chapter 5

Discussion and Future Directions

Author's contribution to the chapter:

Marcos F. Q. de Sousa wrote the chapter based on the referred bibliography

CONTENTS

1. DISCUSSION

In this PhD thesis, bioengineering tools such as bioreactors and microcarriers technology, perfusion and integrated biomanufacturing were used to optimize upstream processing of four complex biopharmaceuticals: human recombinant Bone Marrow Tyrosine kinase on the chromosome X (hrBMX) to support high-throughput screening of covalent inhibitors, Peste des Petites ruminants virus (PPRV) vaccine candidate to support the eradication program of Peste des Petites ruminants (PPR), oncolytic adenovirus type 5 (OV-Ad5) for cancer therapy and human Mesenchymal Stem Cells (hMSC) for cell therapy. The work herein developed was done in scale-down bioreactor models from 0.5 L to 20 L of working volume, allowing us to explore key topics in bioprocess development and optimization:

- Expression platforms for the rapid production of recombinant proteins (**Chapter 2**),
- Microcarriers-based cultures in bioreactors (**Chapter 3 and 4**),
- Bioengineering correlations for process operation and scale-up (**Chapter 3 and 4**),
- Bioprocess intensification: perfusion and integration Upstream processing (USP) and Downstream processing (DSP) (**Chapter 3**),
- Integration of USP and DSP to generate a continuous biomanufacturing scheme for production of virus-based vaccines (**Chapter 3**),
- New bioreactor designs for Advanced Therapy Medicinal Products (ATMPs) production (**Chapter 4**).

The specific aims and major achievements obtained in **Chapters 2-4** of this thesis are summarized in **Figure 5.1**.

Figure. 5.1. Schematic view of the work developed in thesis including aims and goals based on the existing background and major achievements.

In **Chapter 2**, we developed a platform for rapid production of hrBMX, an important kinase involved in inflammatory cell pathways (Chen et al., 2014). The recent decision from Food and Drug Administration to boost the use of covalent inhibitors validates the potential of these small molecules that temporarily or permanently (Ghosh et al., 2019) bind to enzymes. Implementing a rapid production platform capable of obtaining high quantities of highly pure hrBMX in a cost-effectively manner is thus critical to accelerating the development of new drugs against diseases such as cancer.

PPR is one of the deadliest diseases for cattle of poor farmers and is targeted for eradication by Food and Agriculture of the United Nations (FAO) in 2030 (Dhinakar Raj et al., 2015). Vaccines to be used in such program are based on tissue culture attenuated wild-type PPR isolates (Diallo, 2004) and rely on planar technologies for their production. In **Chapter 3**, we developed a flexible and scalable seed-train strategy using microcarriers to produce a PPRV vaccine candidate to support the disease eradication program.

Oncolytic viruses based on adenovirus type 5 backbone have been considered a promising anticancer therapy. However, they are only clinically efficient at high concentrations (Machiels et al., 2019). **In Chapter 4**, we explored the potential of a new bioreactor design to improve production yields (volumetric titers) and product quality attributes for clinical efficiency intending to support such clinical demand.

hMSC are frequently used in tissue engineering and seem to be a promising vehicle for anticancer therapy (Scherzad et al., 2015). Despite the significant developments made so far, cell availability remains one of the main limitations of this therapeutic approach. In **Chapter 4**, we addressed this issue by assessing the potential of a new bioreactor design to improve hMSC quantity and quality.

1.1. Bioprocess Development and Optimization

1.1.1. Expression platforms for rapid production of recombinant proteins

Robust expression platforms capable of delivering substantial quantities of high-quality proteins in a fast, cost-effective way is fundamental for drug development (Andréll and Tate, 2013; Tripathi and Shrivastava, 2019). Within the hosts traditionally used for recombinant protein production, insect cells have emerged as one of the most efficient expression systems (Kost and Kemp, 2016). In combination with the baculovirus expression vector system (BEVS), they have been successfully used for the production of a myriad of biological entities ranging from viruses to multimeric protein structures such as virus-like particles (Cox, 2012). Within insect cells, Sf-9 cells have been used for both virus generation and protein production whereas Hi5 cells have been used in the majority of cases for protein production due to its low virus production yields. **In Chapter 2**, Sf-9 cells in combination with the BEVS were used for the production of hrBMX.

System predictability is of enormous importance for reliable implementation of any expression platform at large-scale (Maranga et al., 2003; Sequeira et al., 2018). In our case, a small-scale screening platform was implemented for the selection of the best conditions for scale-up and production of hrBMX in stirred-tank bioreactor (STB). The reproducible results obtained during screening (15 mL in shake flasks) and production (5 L in STB) demonstrates the scalability of the expression platform. Regarding purification, by remodeling the standard purification setup for tyrosine kinases (Muckelbauer et al., 2011) into a 2-step chromatographic train, protein quantity and stability was substantially improved. The yields of purified hrBMX were in-line with what is reported for tyrosine kinases produced in non-animal (Albanese et al., 2018; Cui and Sun, 2019; Díaz

Galicia et al., 2019; Seeliger et al., 2005) and animal (Muckelbauer et al., 2011) cells. Most importantly, the high quality of hrBMX produced enabled subsequent studies related with anti-cancer pharmacological applications (Seixas et al., 2020).

1.1.2. Microcarriers-based cultures in bioreactors

Microcarriers-based cultures are the most advanced system for growing anchorage-dependent cells in suspension conditions. They are well adapted to large-scale production (STB 6 000 L) (Barrett et al., 2009) and have been used for viruses and virus-based vaccines production (Genzel, 2015) and stem cells expansion (Serra et al., 2018).

One of the major challenges of microcarriers-based cultures is the use of serum-free medium (SFM) and its impact on both cell attachment and detachment from microcarriers (Gallo-Ramírez et al., 2015) during cell growth and virus infection. Although existing, very few (if any) commercial SFM and protein-free medium have proven efficacious for culture of anchorage-dependent cells in microcarriers. In **Chapter 3**, we adapted Vero cells to a commercial SFM formulation under similar cell-yields as described by others (Petiot et al., 2012). Vero cells cultured in SFM conditions revealed challenging given the poor yields obtained using traditional microcarrier cell-detachment procedures; which led us to revise the basis of cell attachment/detachment to microcarriers under SFM conditions. Improvement of the global yield was possible after removing specific, unnecessary steps such as PBS washing and, most importantly, introducing the parameter “agitation” as a detachment enhancer. This strategy was inspired by the work of Nienow and co-workers (Nienow et al., 2014), and it is based on the theory that short periods of intense agitation in the presence of a suitable enzyme should enhance cell detachment from relatively large microcarriers. The method was developed for hMSC and successfully

adapted for Vero cells herein used. In addition to the promising data obtained for cell growth, the yields obtained for PPRV production in SFM were in-line with data available in the literature for serum-containing medium (SCM) (Silva et al., 2008). Noteworthy, we were able to demonstrate that SFM and in-situ detachment do not impact on PPRV productivities at both 2L and 20 L scale, contrasting with what has been previously reported (Gallo-Ramírez et al., 2015). The impact of SFM was also assessed for the production of OV-Ad5 in A549 cells grown on microcarriers in **Chapter 4**. A549 cells were grown up to infection in SCM while the oncolytic virus was produced in SFM. The medium exchange strategy aimed at evaluating the impact of SFM on virus infection kinetics, cell detachment process and cell-specific productivity. No significant differences were observed when compared with SCM (in-house data - not published due to the nature of the work carried out) and in-line with previous reports (Longley Jr et al., 2005). Recent studies describe the development of SFM for anchorage-dependent cells (Genzel, 2015), but most are proprietary non-commercial formulations and thus difficult to access and evaluate.

1.1.3. Bioengineering correlations for process operation and scale-up

Transferring processes from laboratory to manufacturing scale is a complex and challenging task as commonly the mixing regimes in both settings differ significantly (Tescione et al., 2015). Therefore, it is critical to select appropriate scale-down models that mimic the culture and operational conditions that animal cells experience at large-scale (Janakiraman et al., 2015). In this thesis, the STB was used as scale-down model for bioprocess development given the wide utilization and proof-of-concept in biopharmaceuticals production (Catapano et al., 2009). To fit the process development needs in a representative manner of manufacturing scale (Neubauer and Junne, 2016), a scale range of 2 to 20 L was used.

The major challenge in scaling-up animal cell cultures is the shear sensitivity of the cells. In stirred culture systems, shear stress results from the mean energy dissipation rate (Nienow, 2006) imposed by agitation (Cherry and Papoutsakis, 1988; Cherry and Papoutsakis, 1989; Tramper et al., 1986), aeration (King et al., 1992; Murhammer and Goochee, 1990) or both (Cruz et al., 1998; Maranga et al., 2004). The critical hydrodynamic parameters considered in this thesis were energy dissipation rate (EDR, ε) and Kolmogorov eddy size (KES, λ). Although substantial data is already known for flow and turbulence levels in STB, estimating ε remains challenging given the myriad of existing bioengineering correlations. In **Chapters 2-4**, $(\varepsilon_{\mathrm{STB}})_{\mathrm{Max}}$ was determined for the impeller region assuming that the volume into which the energy is dissipated is equivalent to $\mathrm{D_i^3}$, where $\mathrm{D_i}$ is the impeller diameter. This relation was described by Placek and Tavlarides (1985) for turbine (radial) impeller discharge flow (Placek and Tavlarides, 1985) and used by several authors in the last decades (Cruz et al., 1998; Maranga et al., 2004). The ε values obtained in this thesis are in-line with what is described for suspension (Cruz et al., 1998; Maranga et al., 2004) and microcarrier-based (Croughan et al., 1987) cultures. In **Chapter 3**, $(\varepsilon_{\mathrm{STB}})_{\mathrm{Max}}$ was estimated following the assumption that the volume into which the energy is dissipated is equal to the volume swept out by the impeller as it rotates (McManamey, 1979; Nienow, 1998; Nienow et al., 2016a; Pacek et al., 1999). Interestingly, the ensuing KES value was significantly different from that estimated based on ε, thus indicating that the most used threshold for maximum energy dissipation (Croughan et al., 1987) may be overestimated. The experimental setup of Croughan and colleagues was based in agitation with cylindrical bars producing radial flow patterns, expected to impose relatively high values of ε to microcarriers. Recently, the work of Nienow and co-workers (Nienow et al., 2016b) showed that hMSC can grow successfully at ε corresponding to KES values as small as 30 % of

the microcarrier size. There is certainly no reason to think that hMSC are more resistant to fluid dynamic stress than Vero (or other) cells used in much earlier works (Cherry and Papoutsakis, 1988; Cherry and Papoutsakis, 1989; Croughan et al., 1987). Nevertheless, the KES was kept as the main criteria for setting the agitation requirements above 20 μm (single-cell suspension) (**Chapter 2**) and 126 μm (Cytodex™-1 microcarrier-based cultures) (**Chapter 3 and 4**). From the available literature and based on these hydrodynamic thresholds similar or even higher yields for cell (Rasey et al., 1996; Rourou et al., 2007; Sequeira et al., 2018) and product (Lawson et al., 2017; Muckelbauer et al., 2011; Sequeira et al., 2018; Silva et al., 2008) were obtained in this thesis indicating that the scale-up strategy applied is adequate to develop processes.

In **Chapter 3**, two agitation rate concepts for microcarrier-based cultures were added to the classical N (agitation needed to keep microcarriers in suspension under homogenous conditions with no impact on cell viability). These were the N_{FS}, the agitation rate needed to fully suspend microcarriers under reduced shear stress to the cells and the N_{Detach}, the agitation rate needed to promote cell detachment from microcarriers. Few papers describe N_{FS} from the impellers/vessel geometries configurations perspective (Collignon et al., 2010), and the most used engineering correlation for N_{FS} estimation (Ibrahim and Nienow, 2004) commonly overestimates its value (George et al., 2010). The latter is confirmed in our findings, suggesting that visual inspection/experimental determination is still the best option for N_{FS} determination. As to N_{Detach}, its correct estimation is critical for processes using SFM given the low yields achieved for cell sub-culturing when compared with processes using serum-containing medium (Aunins, 2003). The N_{Detach} values estimated in this thesis are in-line with those reported in literature (Nienow et al., 2014). Noteworthy, in **Chapters 3 and 4** the ensuing shear stress rate imposed by the three types of agitation is below the

hydrodynamic limit described to critically affect cells (> 0.5 N/m^2) (Czermak et al., 2009): 0.1-0.2, 0.2-0.3 and 0.40 N/m^2 for N_C, N_{FS} and N_{Detach}, respectively.

1.1.4. Bioprocess intensification: perfusion and integration of Upstream and Downstream processing

The biopharmaceutical industry is moving towards process intensification given the possibility to improve product quality while reducing process scale and number of unit operations.

One of the target areas for process intensification is improving the seed-train. In **Chapter 3**, seed-train intensification for Vero cells grow on microcarriers in STB was successfully performed using perfusion operation mode. This required the use of a perfusion apparatus composed by internal spin-filter and, most importantly, the development of in-house gravimetric control software (VBA-based in-house developed at iBET, not published) for controlling perfusion flows. The implemented process design entailed significant operational risk due to the complex peripheral equipment and additional operation steps (namely, medium addition to inlet flasks). Nonetheless, the benefits it induced (i.e. reduction of mid-scales by achieving higher cell concentrations) overcame the risks involved. Noteworthy, robust perfusion systems assured efficient and automated operation management, overcoming the major drawbacks of semi-continuous strategies which require repeated manipulation. Expanding Vero cells in perfusion has been reported (Rourou et al., 2007). However, these processes rely on either proprietary medium formulations (Trabelsi et al., 2012), modified versions of commercial medium formulations (Trabelsi et al., 2005) or SFM (De Oliveira Souza et al., 2005). In our work, we used a commercially available SFM for Vero cells grow on microcarriers and production of PPRV with positive results. The robustness and scalability of the perfusion strategy reported in

Chapter 3 may be essential to support the PPR global eradication program. Moreover, the flexibility of the ensuring process may as well support the growth of other anchorage-dependent cell lines and the production of other viruses such as influenza vaccines in MDCK cells (George et al., 2010) or coronavirus in MRC-5 cells (Stacey et al., 2007).

Another target area for process intensification is USP and DSP integration. In **Chapter 3** the benefits of designing a closed and scalable process for clarification integrated with bioreactor in a single flow operation were highlighted. Besides reducing process time and costs, and increasing product recovery, integration of USP (i.e. STB) and DSP (i.e. single-use depth filters for clarification) allowed to remove Vero cell contaminants in a single step. Reducing clarification time was important since PPRV is a live-attenuated vaccine known to be particularly unstable at relatively high temperatures (Silva et al., 2011). Significant value can be obtained by implementing multiple-operations system combining perfusion and USP-DSP process integration; it will improve the global yield of the manufacturing process of a biopharmaceutical.

High-density cell banking is another target area for process intensification. The use of highly concentrated cell banks may allow direct inoculation of the N-1 bioreactor, thus further intensifying the process. Such procedure was described before for CHO-based processes (Wright et al., 2015) but, to our knowledge, no report has demonstrated its feasibility for microcarrier-based cultures as achieved here.

1.1.5. New bioreactor designs for ATMPs production

STB is the most “universal” bioreactor design in use given its well-characterized hydrodynamics, enabling seamless process transfer to several scales. STB facilitates not only scale-down approaches for optimization

studies and later implementation of identified parameters at larger scales but also translation to other bioreactor technologies as shown in **Chapter 3 and 4** for microcarrier-based processes. STB are traditionally operated under low impeller speed and low aeration rate. In some cases, these conditions are insufficient for an optimal supply of oxygen and nutrient to the cells. Increasing agitation and aeration to guarantee optimal mixing conditions for cell culture is thus necessary; however, this will promote an increase in shear and cell death. During the last decades, several bioreactor designs have been developed considering, primarily, the shear sensitivity of animal cells but also other aspects such as operation mode, ease of handling, regulatory considerations, and easiness of scale-up. Interestingly, for microcarrier-based cultures, these are based on new or revamped bioreactor designs such as immobilized or fixed-bed (Catapano et al., 2009). Such solutions have been reported for Vero cells (Han and Sha, 2017; Patel et al., 2019) and stem cells expansion (Osiecki et al., 2018) as well as for virus-based vaccines production (Drugmand et al., 2018; Lennaertz et al., 2013). Nonetheless, large-scale utilization has not yet been reported; these concepts are still in their infancy and ensuring manufacturing suitability from lab- to full-scale production is still the role played by the STB.

In **Chapter 4**, we implemented two scalable bioprocess approaches using a single-use and low shear-stress bioreactor, the Vertical-Wheel™ (PBS-VW). The U-shape vessel geometry combined with vertical wheel impeller provides homogeneous energy dissipation resulting in efficient mixing under low shear conditions. The impact of the new bioreactor design and hydrodynamics on (i) cell A549 cell growth and OV-Ad5 production, and (ii) hMSC expansion and quality were evaluated. The strategy relied on cell growth under agitation conditions comparing this new bioreactor design to the STB. For the first time, we demonstrated that an OV-Ad5 vector and hMSC expansion under such new bioreactor hydrodynamics may play a role

in the product quality. OV-Ad5 quality ratio based on the total per infectious virus ratio was higher in new design bioreactor impacting in later DSP stages of the production process. hMSC proliferative capacity and immunomodulatory surface marker expression was higher in PBS-VW when compared with STB. Similar hMSC cell expansion results were reported for another single-use bioreactor in large-scale (Lawson et al., 2017).

2. CONCLUSIONS

Based on the work presented in this thesis and the above discussion, the following set of conclusions can be outlined:

- The Sf-9 and baculovirus expression vector system (BEVS) platform can be used for fast production of Bone Marrow Tyrosine kinase in the chromosome X (hrBMX) towards drug discovery studies (**Chapter 2**).
- Optimizing upstream (e.g. infection strategy) and downstream (e.g. number of operation units) processes was essential to maximize the quantity and stability of hrBMX produced (**Chapter 2**).
- Defining the maximum agitation conditions that can be achieved in stirred-tank bioreactor (STB) without negatively impacting cell growth, expansion and/or infection is important for maximizing production yields and for process scale-up (**Chapter 2-4**).
- Bioprocess intensification was successfully achieved using perfusion and integration of upstream processing (USP) and downstream processing (DSP) (**Chapter 3**).
- Integrating USP and DSP generated a continuous biomanufacturing scheme for production of virus-based vaccines with high virus recovery yields after filtration (**Chapter 3**).

- Serum-free medium (SFM) enables Peste des Petites ruminant virus (PPRV) vaccine production yields similar to those achieved in serum-containing formulations (**Chapter 3**).

- The use of SFM required the redesign of the Vero cell detachment method from microcarriers for efficient subculturing (**Chapter 3**).

- A scalable seed-train strategy for the production of PPRV vaccine candidate was developed combining perfusion with an efficient enzymatic/mechanical method for Vero cell detachment from microcarriers and integration with DSP based in the clarification step (**Chapter 3**).

- The new PPRV production process herein designed allows the generation of a high number of vaccine doses in a short period of time, thus having the potential to support the Peste des Petites ruminants global eradication program (**Chapter 3**).

- New bioreactor designs (the Vertical-Wheel™ bioreactor) have the potential to improve the quality of complex biopharmaceuticals such as those herein targeted (oncolytic adenovirus type 5 – OV-Ad5 – and human Mesenchymal Stem Cells – hMSC) (**Chapter 4**).

This PhD thesis addresses several challenges in bioprocess development and optimization of complex biopharmaceuticals, from the selection of expression platform (**Chapter 2**) and bioreactors type (**Chapter 4**), to the definition of bioreactors operating conditions (**Chapter 2-4**) and process scale-up criteria (**Chapter 3-4**) and implementation of bioprocess intensification and integration designs (**Chapter 3**). The work herein developed contributed to advance the state of the art on UPS of four biologics (hrBMX, PPRV vaccine, Onco-Ad5 and hMSC) providing a set of novel and improved optimization schemes for their production.

3. FUTURE DIRECTION

The global complex biopharmaceuticals market is expected to grow in the next years and with it the demand for continued process development and intensification. This thesis contributes to the clarification of some critical aspects of complex biopharmaceuticals production and, most importantly, for the design of novel and improved optimization schemes for their production. Still, some key issues need further investigations and other technologies could be applied, namely:

- Validate the manufacturing platform implemented in **Chapter 2** for other insect cell line than Sf-9 with better protein expression capacity (e.g. Hi5 cells) or for other cell lines with mammalian-like cellular machinery (e.g. HEK 293-E6). Regarding the latter, re-evaluation of the upstream phase would be required as transient expression would be changed from an infection to a transfection process,
- Implement a “push-to-low” perfusion strategy based on the stepwise reduction of cell-specific perfusion rate (CSPR) to increase robustness of the Vero cell perfusion process proposed in **Chapter 3**. Reducing perfusion rate maintaining cell growth and viability will significantly enhance the economic potential of perfusion platforms,
- Integration of a virus purification step to the established platform proposed in **Chapter 3** for Peste des Petites ruminants virus (PPRV) production to improve vaccine quality. Assessing PPRV vaccine efficacy for such new production process will be essential,
- Proof-of-concept of the scalability of the new bioreactor design proposed in **Chapter 4** for volumes above 2 L working volume. Demonstration of robustness at higher volumes would be required if

the new bioreactor concept herein evaluated is to be implemented at manufacturing scale.

4. REFERENCES

Albanese SK, Parton DL, Işlk M, Rodríguez-Laureano L, Hanson SM, Behr JM, Gradia S, Jeans C, Levinson NM, Seeliger MA, Chodera JD. 2018. An Open Library of Human Kinase Domain Constructs for Automated Bacterial Expression. *Biochemistry* **57**:4675–4689.

Andréll J, Tate CG. 2013. Overexpression of membrane proteins in mammalian cells for structural studies. *Mol. Membr. Biol.* **30**:52–63. https://doi.org/10.3109/09687688.2012.703703.

Aunins JG. 2003. Viral Vaccine Production in Cell Culture. In: . *Encycl. Cell Technol.*

Barrett PN, Mundt W, Kistner O, Howard MK. 2009. Vero cell platform in vaccine production: moving towards cell culture-based viral vaccines. *Expert Rev. Vaccines* **8**:607–18. http://informahealthcare.com/doi/abs/10.1586/erv.09.19.

Catapano G, Czermak P, Eibl R, Eibl D, Pörtner R. 2009. Bioreactor Design and Scale-Up. In: . *Cell Tissue React. Eng. Princ. Pract.*, pp. 173–259.

Chen X-L, Qiu L, Wang F, Liu S. 2014. Current understanding of tyrosine kinase BMX in inflammation and its inhibitors. *Burn. Trauma* **2**:121–124.

Cherry RS, Papoutsakis ET. 1989. Growth and death rates of bovine embryonic kidney cells in turbulent microcarrier bioreactors. *Bioprocess Eng.* **4**:81–89.

Cherry RS, Papoutsakis ET. 1988. Physical mechanisms of cell damage in microcarrier cell culture bioreactors. *Biotechnol. Bioeng.* **32**:1001–14.

Collignon ML, Delafosse A, Crine M, Toye D. 2010. Axial impeller selection for anchorage dependent animal cell culture in stirred bioreactors: Methodology based on the impeller comparison at just-suspended speed of rotation. *Chem.*

Eng. Sci. **65**:5929–5941.

Cox MMJ. 2012. Recombinant protein vaccines produced in insect cells. *Vaccine* **30**:1759–66.

Croughan MS, Hamel JF, Wang DI. 1987. Hydrodynamic effects on animal cells grown in microcarrier cultures. *Biotechnol. Bioeng.* **29**:130–41. http://www.ncbi.nlm.nih.gov/pubmed/18561137.

Cruz PE, Cunha A, Peixoto CC, Clemente J, Moreira JL, Carrondo MJT. 1998. Optimization of the production of virus-like particles in insect cells. *Biotechnol. Bioeng.* **60**:408–418.

Cui Y, Sun G. 2019. Structural versatility that serves the function of the HRD motif in the catalytic loop of protein tyrosine kinase, Src. *Protein Sci.* **28**:533–542.

Czermak P, Pörtner R, Brix A. 2009. Special Engineering Aspects. In: . *ell Tissue React. Eng. Princ. Pract.*, pp. 83–172.

Dhinakar Raj G, Thangavelu A, Munir M. 2015. Strategies and Future of Global Eradication of Peste des Petits Ruminants Virus. In: Munir, M, editor. *Peste des Petits Ruminants Virus*. Berlin, Heidelberg, Heidelberg: Springer Berlin Heidelberg, pp. 227–254. https://doi.org/10.1007/978-3-662-45165-6_13.

Diallo A. 2004. Peste des Petits ruminants. Manual of Diagnostic Tests and Vaccines for Terrestrial Animals, vols. I and II. *OIE* **I and II**.

Díaz Galicia ME, Aldehaiman A, Hong SB, Arold ST, Grünberg R. 2019. Methods for the recombinant expression of active tyrosine kinase domains: Guidelines and pitfalls. In: Shukla, AKBT-M in E, editor. *Methods Enzymol.* Academic Press, Vol. 621, pp. 131–152. http://www.sciencedirect.com/science/article/pii/S0076687919300461.

Drugmand JC, Dubois S, Reniers A, Forte J, Deleau A, Herbiniat D, Dohogne Y, Castillo J. 2018. Disruptive micro-facility for affordable vaccine manufacturing.

Vaccine Technol. VII Conf.

Gallo-Ramírez LE, Nikolay A, Genzel Y, Reichl U, Gallo–Ramírez LE, Nikolay A, Genzel Y, Reichl U, Gallo-Ramírez LE, Nikolay A, Genzel Y, Reichl U. 2015. Bioreactor concepts for cell culture-based viral vaccine production. *Expert Rev. Vaccines* **14**:1181–1195. https://doi.org/10.1586/14760584.2015.1067144.

Genzel Y. 2015. Designing cell lines for viral vaccine production: Where do we stand? *Biotechnol. J.*

George M, Farooq M, Dang T, Cortes B, Liu J, Maranga L. 2010. Production of cell culture (MDCK) derived Live Attenuated Influenza Vaccine (LAIV) in a fully disposable platform process. *Biotechnol. Bioeng.* **106**:906–17.

Ghosh AK, Samanta I, Mondal A, Liu WR. 2019. Covalent Inhibition in Drug Discovery. *ChemMedChem* **14**:889–906. https://doi.org/10.1002/cmdc.201900107.

Han X, Sha M. 2017. High-Density Vero Cell Perfusion Culture in BioBLU® 5p Single-Use Vessels. *Apllication Note* **359**:1–8.

Ibrahim S, Nienow AW. 2004. Suspension of microcarriers for cell culture with axial flow impellers. *Chem. Eng. Res. Des.* **82**:1082–1088. https://www.sciencedirect.com/science/article/pii/S0263876204725940.

Janakiraman V, Kwiatkowski C, Kshirsagar R, Ryll T, Huang YM. 2015. Application of high-throughput mini-bioreactor system for systematic scale-down modeling, process characterization, and control strategy development. *Biotechnol. Prog.* **31**:1623–32.

King GA, Daugulis AJ, Faulkner P, Goosen MFA. 1992. Recombinant β-Galactosidase Production in Serum-Free Medium by Insect Cells in a 14-L Airlift Bioreactor. *Biotechnol. Prog.* **8**:567–571.

Kost TA, Kemp CW. 2016. Fundamentals of baculovirus expression and

applications. *Adv. Exp. Med. Biol.* **896**:187–197.

Lawson T, Kehoe DE, Schnitzler AC, Rapiejko PJ, Der KA, Philbrick K, Punreddy S, Rigby S, Smith R, Feng Q, Murrell JR, Rook MS. 2017. Process development for expansion of human mesenchymal stromal cells in a 50 L single-use stirred tank bioreactor. *Biochem. Eng. J.* **120**:49–62.

Lennaertz A, Knowles S, Drugmand J-C, Castillo J. 2013. Viral vector production in the integrity® iCELLis® single-use fixed-bed bioreactor, from bench-scale to industrial scale. *BMC Proc.* **7**:P59.

Longley Jr R, Radzniak L, Santoro M, Tsao Y-S, Condon RGG, Lio P, Voloch M, Liu Z. 2005. Development of a Serum-free Suspension Process for the Production of a Conditionally Replicating Adenovirus using A549 Cells. *Cytotechnology* **49**:161–171. https://www.ncbi.nlm.nih.gov/pmc/articles/PMC3449904/.

Machiels JP, Salazar R, Rottey S, Duran I, Dirix L, Geboes K, Wilkinson-Blanc C, Pover G, Alvis S, Champion B, Fisher K, McElwaine-Johnn H, Beadle J, Calvo E. 2019. A phase 1 dose escalation study of the oncolytic adenovirus enadenotucirev, administered intravenously to patients with epithelial solid tumors (EVOLVE). *J. Immunother. Cancer* **7**:1–15.

Maranga L, Brazao TF, Carrondo MJTT. 2003. Virus-like particle production at low multiplicities of infection with the baculovirus insect cell system. *Biotechnol. Bioeng.* **84**:245–53.

Maranga L, Cunha A, Clemente J, Cruz P, Carrondo MJT. 2004. Scale-up of virus-like particles production: Effects of sparging, agitation and bioreactor scale on cell growth, infection kinetics and productivity. *J. Biotechnol.* **107**:55–64.

McManamey WJJ. 1979. Sauter mean and maximum drop diameters of liquid-liquid dispersions in turbulent agitated vessels at low dispersed phase hold-up. *Chem. Eng. Sci.* **34**:432–434. https://www.sciencedirect.com/science/article/pii/0009250979850812.

Muckelbauer J, Sack JS, Ahmed N, Burke J, Chang CY, Gao M, Tino J, Xie D, Tebben AJ. 2011. X-ray crystal structure of bone marrow kinase in the X chromosome: A Tec family kinase. *Chem. Biol. Drug Des.* **78**:739–748.

Murhammer DW, Goochee CF. 1990. Sparged Animal Cell Bioreactors: Mechanism of Cell Damage and Pluronic F-68 Protection. *Biotechnol. Prog.* **6**:391–397.

Neubauer P, Junne S. 2016. Scale-Up and Scale-Down Methodologies for Bioreactors. In: , pp. 323–354.

Nienow AW, Coopman K, Heathman TRJ, Rafiq QA, Hewitt CJ. 2016a. Bioreactor Engineering Fundamentals for Stem Cell Manufacturing. In: . *Stem Cell Manuf.*

Nienow AW. 1998. Hydrodynamics of Stirred Bioreactors. *Appl. Mech. Rev.* **51**:3–32.

Nienow AW. 2006. Reactor engineering in large scale animal cell culture. *Cytotechnology* **50**:9–33. https://pubmed.ncbi.nlm.nih.gov/19003068.

Nienow AW, Hewitt CJ, Heathman TRJ, Glyn VAM, Fonte GNGN, Hanga MP, Coopman K, Rafiq QA. 2016b. Agitation conditions for the culture and detachment of hMSCs from microcarriers in multiple bioreactor platforms. *Biochem. Eng. J.* **108**:24–29. https://www.sciencedirect.com/science/article/pii/S1369703X15300309.

Nienow AW, Rafiq QA, Coopman K, Hewitt CJ. 2014. A potentially scalable method for the harvesting of hMSCs from microcarriers. *Biochem. Eng. J.* **85**:79–88. https://www.sciencedirect.com/science/article/pii/S1369703X14000278.

De Oliveira Souza MC, Da Silva Freire M, Dos Reis Castilho L. 2005. Influence of culture conditions on vero cell propagation on non-porous microcarriers. *Brazilian Arch. Biol. Technol.* **48**:71–77.

Osiecki MJ, McElwain SDL, Lott WB. 2018. Modelling mesenchymal stromal cell growth in a packed bed bioreactor with a gas permeable wall. *PLoS One*

13:e0202079.

Pacek AWW, Chamsart S, Nienow AWW, Bakker A. 1999. The influence of impeller type on mean drop size and drop size distribution in an agitated vessel. *Chem. Eng. Sci.* **54**:4211–4222. https://www.sciencedirect.com/science/article/pii/S0009250999001566.

Patel R, Dasgupta D, Vernekar M. 2019. High-density culture of Vero cells in novel perfusion bioreactor system. *J Appl Biol Biotech* **7**:50–55.

Petiot E, El-Wajgali A, Esteban G, Gény C, Pinton H, Marc A. 2012. Real-time monitoring of adherent Vero cell density and apoptosis in bioreactor processes. *Cytotechnology* **64**:429–441.

Placek J, Tavlarides LL. 1985. Turbulent flow in stirred tanks. Part I: Turbulent flow in the turbine impeller region. *AIChE J.* **31**:1113–1120.

Rasey JS, Cornwall MM, Maurer BJ, Boyles DJS, Hofstrand P, Chin L, Cerveny C. 1996. Growth and radiation response of cells grown in macroporous gelatin microcarriers (CultiSpher-G®). *Br. J. Cancer* **27**:S78–S81.

Rourou S, van der Ark A, van der Velden T, Kallel H. 2007. A microcarrier cell culture process for propagating rabies virus in Vero cells grown in a stirred bioreactor under fully animal component free conditions. *Vaccine* **25**:3879–3889.

Scherzad A, Steber M, Gehrke T, Rak K, Froelich K, Schendzielorz P, Hagen R, Kleinsasser N, Hackenberg S. 2015. Human mesenchymal stem cells enhance cancer cell proliferation via IL-6 secretion and activation of ERK1/2. *Int J Oncol* **47**:391–397. https://doi.org/10.3892/ijo.2015.3009.

Seeliger MA, Young M, Henderson MN, Pellicena P, King DS, Falick AM, Kuriyan J. 2005. High yield bacterial expression of active c-Abl and c-Src tyrosine kinases. *Protein Sci.* **14**:3135–9.

Seixas JD, Sousa BB, Marques MC, Guerreiro A, Traquete R, Rodrigues T,

Albuquerque IS, Sousa M, Lemos AR, Sousa PMF, Bandeiras TM, Wu D, Doyle SK, Robinson C V, Koehler A, Corzana F, Matias P, Bernardes G. 2020. Rationally Designed Potent BMX Inhibitors Reveals Mode of Covalent Binding at the Atomic Level. https://chemrxiv.org/articles/preprint/Rationally_Designed_Potent_BMX_Inhibitors_Reveals_Mode_of_Covalent_Binding_at_the_Atomic_Level/11558310.

Sequeira DP, Correia R, Carrondo MJT, Roldão A, Teixeira AP, Alves PM. 2018. Combining stable insect cell lines with baculovirus-mediated expression for multi-HA influenza VLP production. *Vaccine* **36**:3112–3123. https://linkinghub.elsevier.com/retrieve/pii/S0264410X17302463.

Serra M, Cunha B, Peixoto C, Gomes-Alves P, Alves P. 2018. Advancing manufacture of human mesenchymal stem cells therapies: technological challenges in cell bioprocessing and characterization. *Curr. Opin. Chem. Eng.* **22**:226–235.

Silva AC, Carrondo MJT, Alves PM. 2011. Strategies for improved stability of Peste des Petits Ruminants Vaccine. *Vaccine* **29**:4983–4991. http://www.sciencedirect.com/science/article/pii/S0264410X11006578.

Silva AC, Delgado I, Sousa MFQQ, Carrondo MJTT, Alves PM. 2008. Scalable culture systems using different cell lines for the production of Peste des Petits ruminants vaccine. *Vaccine* **26**:3305–3311.

Stacey G, Hawkins R, Carter P, Hunt C, Young L. 2007. Replacement Seed Stocks for MRC-5 cells. *WHO* **WHO/BS/07.**:1–9.

Tescione L, Lambropoulos J, Paranandi MR, Makagiansar H, Ryll T. 2015. Application of bioreactor design principles and multivariate analysis for development of cell culture scale down models. *Biotechnol. Bioeng.* **112**:84–97.

Trabelsi K, Majoul S, Rourou S, Kallel H. 2012. Development of a measles vaccine production process in MRC-5 cells grown on Cytodex1 microcarriers and in a stirred bioreactor. *Appl. Microbiol. Biotechnol.* **93**:1031–1040.

https://doi.org/10.1007/s00253-011-3574-y.

Trabelsi K, Rourou S, Loukil H, Majoul S, Kallel H. 2005. Comparison of various culture modes for the production of rabies virus by Vero cells grown on microcarriers in a 2-l bioreactor. *Enzyme Microb. Technol.* **36**:514–519. http://www.sciencedirect.com/science/article/pii/S0141022904003539.

Tramper J, Williams JB, Joustra D, Vlak JM. 1986. Shear sensitivity of insect cells in suspension. *Enzyme Microb. Technol.* **8**:33–36.

Tripathi NK, Shrivastava A. 2019. Recent Developments in Bioprocessing of Recombinant Proteins: Expression Hosts and Process Development. *Front. Bioeng. Biotechnol.* **7**:420. https://pubmed.ncbi.nlm.nih.gov/31921823.

Wright B, Bruninghaus M, Vrabel M, Walther J, Shah N, Bae S-A, Johnson T, Yin J, Zhou W, Konstantinov K. 2015. A novel seed-train process: Using high-density cell banking, a disposable bioreactor, and perfusion technologies. *Bioprocess Int.* **13**.

ITQB-UNL | Av. da República, 2780-157 Oeiras, Portugal
Tel (+351) 214 469 100 | Fax (+351) 214 411 277

www.itqb.unl.pt